THE BEHAVIOR OF PRESTRESSED HIGH PERFORMANCE CONCRETE BRIDGE GIRDERS FOR US HIGHWAY 401 OVER THE NEUSE RIVER IN WAKE COUNTY, NC

By

Mervyn J. Kowalsky
Co-Principal Investigator

Paul Zia
Co-Principal Investigator

Hazim M. Dwairi
Graduate Research Assistant

Randall Wilson
Graduate Research Assistant

Final Report

In cooperation with the

North Carolina Department of Transportation

And

Federal Highway Administration
The United States Department of Transportation

Department of Civil Engineering
North Carolina State University
Raleigh, N.C. 27695-7908

August 2003

Technical Report Documentation Page

1. Report No. **FHWA/NC/2002-03**	2. Government Accession No.	3. Recipient's Catalog No.
4. Title and Subtitle **The behavior of prestressed high performance concrete bridge girders for US highway 401 over the Neuse River in Wake County, NC**		5. Report Date **August 15, 2003**
		6. Performing Organization Code
7. Author(s) Mervyn J. Kowalsky, Paul Zia, Matt C. Wagner, and Bruce A. Warren		8. Performing Organization Report No.
9. Performing Organization Name and Address **North Carolina State University, Box 7908, Raleigh, Wake, NC**		10. Work Unit No. (TRAIS)
		11. Contract or Grant No.
12. Sponsoring Agency Name and Address **North Carolina Department of Transportation 1 South Wilmington Street Raleigh, North Carolina 27611**		13. Type of Report and Period Covered **Final Report July 2001 - July 2003**
		14. Sponsoring Agency Code **2002-17**

15. Supplementary Notes

Funded by USDOT FHWA as high performance concrete showcase project.

16. Abstract

This report represents phase three of US 401 HPC Bridge research project. It includes a full description of the bridge instrumentation for the purposes of in-service monitoring, controlled load testing and long-term monitoring. Effects due to thermal and traffic loading, over a period of four months, are reported. Strains and deflection due to controlled load testing are also reported, with comprehensive analysis of the results.

17. Key Words **High performance concrete, bridges, prestressed, field monitoring.**	18. Distribution Statement		
19. Security Classif. (of this report)	20. Security Classif. (of this page)	21. No. of Pages **50**	22. Price

Form DOT F 1700.7 (8-72) **Reproduction of completed page authorized**

DISCLAIMER

The contents of this report reflect the views of the author(s) and not necessarily the view of the University. The author(s) are responsible for the facts and the accuracy of the data presented herein. The contents do not necessarily reflect the official views or policies of either the North Carolina Department of Transportation or the Federal Highway Administration at the time of publication. This report does not constitute a standard, specification, or regulation.

Table of Contents

List of Tables

List of Figures

1. INTRODUCTION AND OBJECTIVES

In October 1996, the Federal Highways Administration (FHWA) entered into a cooperative with the North Carolina Department of Transportation (NCDOT), through which funding was provided for a joint project between NCDOT and North Carolina State University (NCSU) to instrument and monitor the behavior of the High Performance Concrete (HPC) Bridge on US 401 over the Neuse River in Wake County of North Carolina. This bridge is one of the first HPC bridges constructed in North Carolina. The bridge is a set of dual (North Bound and South Bound) four-span bridges. The four spans of the bridge are 91.9 ft., 91.9 ft., 57.4 ft., and 57.4 ft. consisting of AASHTO Type IV prestressed concrete girders used for the longer spans, and Type III for the shorter spans. The entire bridge has a girder spacing of about 10 ft. 6 in. The concrete used for the bridge shall have a minimum 28-day compressive strength of 10,000 psi for the girders and 6,000 psi for the deck.

The joint project included the following four tasks:

(1) Specification of expected properties and associated quality control procedures for HPC concrete produced in typical plant and field conditions, including testing of specimens taken from "full scale" batches. Requirements regarding production and quality control of HPC materials are included in the special provisions for the project.

(2) Internal and external instrumentation of four girders at the plant will be installed, and monitoring of temperature and behavior of the girders at the plant will be conducted. Work will include the evaluation of transfer lengths of strands at both ends of at least two girders.

(3) External instrumentation is used on the same four girders after erection at the site, as well as internal instrumentation used in the cast in place connections between girders. Following instrumentation, performance of the bridge is to be assessed by performing a live load test on the bridge before opening to traffic, and a second live load test one year after the first live load test. Also, monitoring short-term behavior through a period immediately following opening of the bridge to traffic shall be conducted.

(4) Long-term evaluation of the structure.

Make note that previous research has been prepared for phase one and two of the joint project In phase one, Warren (2000) assembled a data acquisition system and developed the necessary computer code for the CR323X data logger (Campbell Scientific Inc.) to accumulate data. Phase two involved the use of the data acquisition system to monitor the short-term behavior of the girders during and after their casting along with the properties of the concrete used.

The work presented in this report represents phase three of the joint project between NCDOT and NCSU. It involves instrumenting the bridge with internal and external instruments for the use of the data acquisition system to collecting data during two live load tests and short-term monitoring of the girders.

2. RESEARCH OBJECTIVES AND METHODS FOR PHASE THREE OF THE JOINT PROJECT BETWEEN NCDOT AND NCSU

2.1. Overview

The objective of the research involved in phase three of the joint project is to investigate the performance of the US 401 HPC Bridge by validating analytical models assumed during design, with a specific emphasis on (1) girder stiffness and deflection calculations, (2) creep and shrinkage effects, and (3) thermal effects. In order to accomplish this objective, the US 401 Southbound Bridge of the dual set is to be instrumented internally and externally, and a live load test be conducted prior to its opening of traffic. After the bridge has been opened to traffic, the short-term monitoring for thermal and traffic load effects on the bridge may proceed. Additionally, after the bridge is opened for a full year, a second live load test is proposed to assess if there is any significant change in performance.

2.2. Report Objectives

The objective of this report will be to carry out the following tasks that will be performed to achieve the objective to phase three of the joint project:

(1) Give an account of the instrument locations, instrument identifications, and initial readings of the internal and external instrumentation of the US 401 Southbound Bridge.

(2) Report on the properties of the concrete specimens taken during the bridge deck casting.

(3) Describe the live load test setup and report the data collected during the live load test.

(4) Describe and analyze the results of short-term monitoring of the bridge

(5) Perform a structural analysis on the bridge for deflections and strains under identical loading conditions of the live load test to verify analytical models assumed during design emphasizing girder stiffness and deflection.

3. INTERNAL AND EXTERNAL INSTRUMENTATION OF THE US 401 SOUTHBOUND BRIDGE

3.1. Overview

The US 401 Southbound Bridge girders and deck were instrumented internally and externally only along Girder-line 4 and on each side adjacent to Girder-line 4. Girder-line 4 was the only portion of the southbound bridge instrumented due to the uneconomical cost associated with instrumenting the entire bridge. Also, the data collected along Girder-line 4 would be sufficient in achieving the objective of phase three and four of the joint project. A layout of the southbound bridge can be seen in Figure 1 to give a physical representation of the general location of where the instrumented girder of the bridge is located.

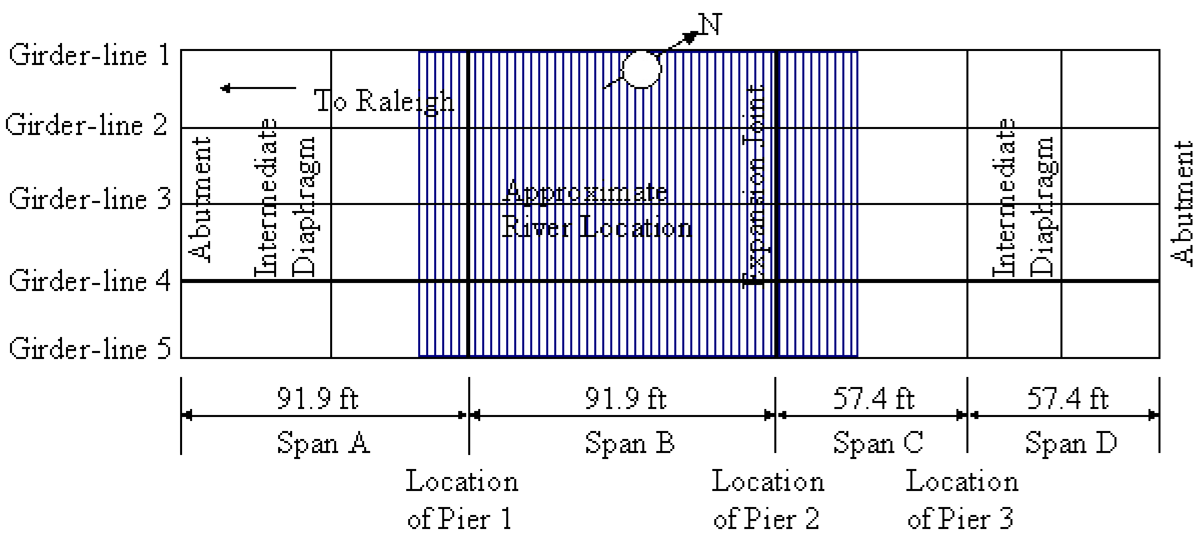

Figure 1. General Layout of The US 401 Southbound Bridge

The instruments that were installed internally and externally for the girders and deck along Girder-line 4 are as follows:

(1) Omega FF-K-24 thermocouples,

(2) Roctest EM-5 Vibrating Wire Gauges (VWGs),

(3) and Schaevitz DC-SE Series Linear Voltage Differential Transducers (LVDTs).

The thermocouples will be installed to monitor temperature changes for any environmental loadings and environmental effects throughout the life of the structure. The VWGs will be installed to monitor the shrinkage strains and to determine the behavior of the joints with continuity reinforcement. In addition, the LVDTs will be installed to measure longitudinal girder movements. These instruments will be connected to two data acquisition systems located at the intermediate diaphragms of Spans A and D underneath the bridge to record the measurements for the first and second live load test, and for short-term monitoring. The specifics on these instruments, such as instrument location and identification, will be explained in detail later in this section.

3.2. Internal Instrumentation Retained Inside Of Girders That Were Used During Girder Casting

In phase two of the joint project, instruments were cast into the girders of Spans A, B, C, and D of Girder-line 4 at the prestressing plant in Charlotte, NC. The instruments that were embedded into the girders were thermocouples, Electrical Resistance Strain Gages (ERSGs), and VWGs. These instruments were embedded into the girders to accomplish the objectives of phase two, described earlier in Section 1. However, only a portion of the thermocouples and none of the ERSGs were retained for phase three.

Figure 2 and Figure 3 show the cross-sections located at mid-span of each girder where the retained thermocouples are located in those cross-sections.

Identification labels were assigned to each of the thermocouples used in phase two during Matthew Wagner's research, but in phase three new identification labels were reassigned to the thermocouples retained. In Table 1, the corresponding identifications between the original assigned labels and new assigned labels are displayed.

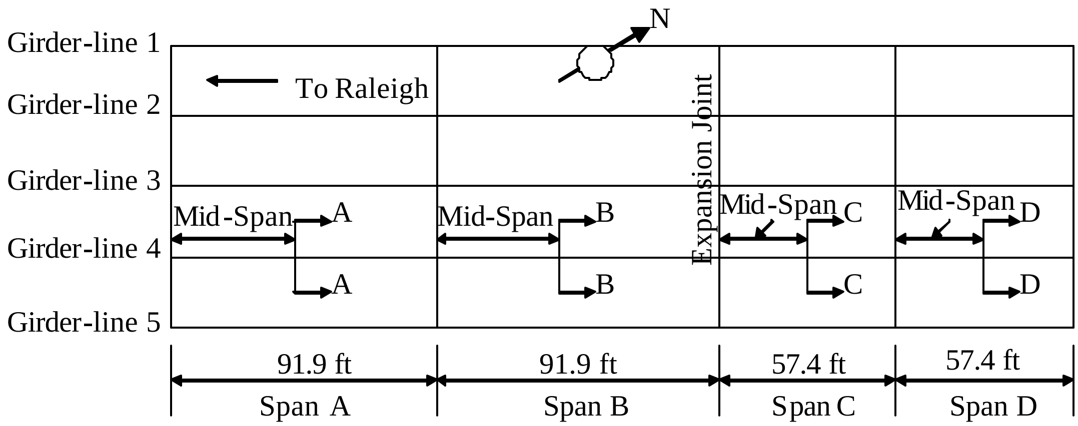

Figure 2 Retained Thermalcouple Locations In Each Girder Cross-Section

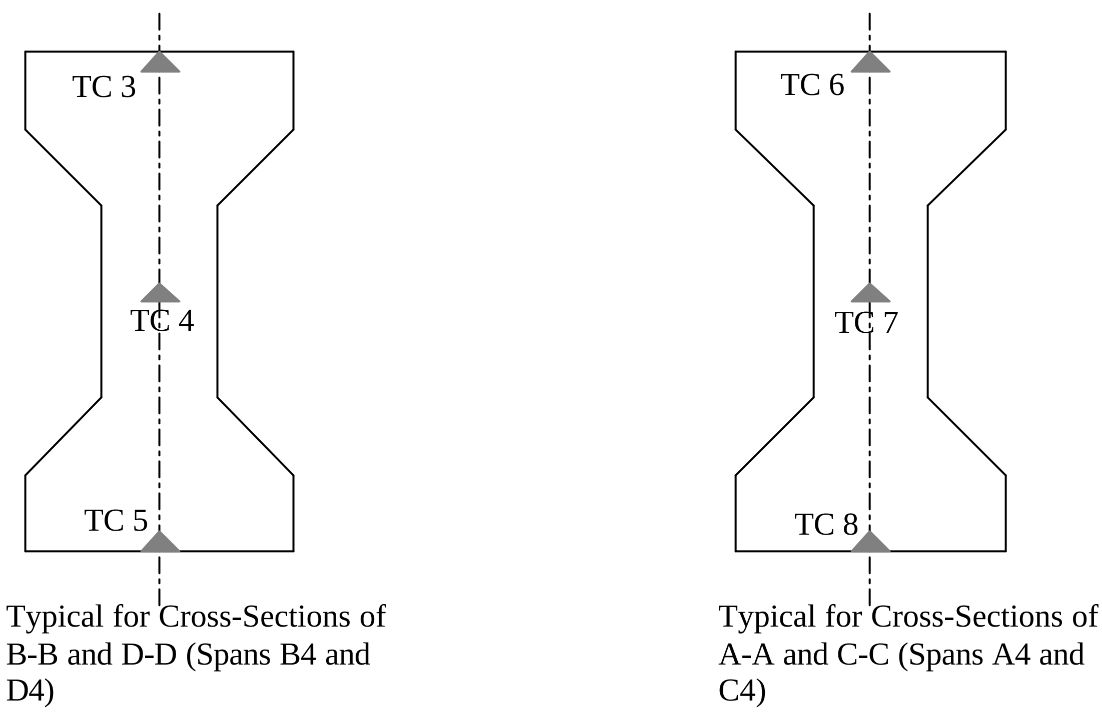

Figure 3 Retained Thermalcouples Of Girder Cross-Sections Along Girder-line 4

Table 1. Identification Labels of Thermocouples In Girders

Matthew Wagner's Identification Assignment = New Identification Assignment
Span A4:
TC 1 = TC 6
TC3 = TC 7
TC5 = TC 8
Span B4:
TC 1 = TC 3
TC3 = TC 4
TC5 = TC 5
Span C4:
TC 1 = TC 6
TC3 = TC 7
TC5 = TC 8
Span D4:
TC 1 = TC 3
TC3 = TC 4
TC5 = TC 5

VWG's are like the thermocouples that were retained in phase three from phase two. Unlike the thermocouples all the VWG's were retained, where only a portion were retained in phase three. Figure 4 shows a graphical representation where the retained VWG's are located in each of the girders with respect to Girder-line 4, and the VWG's cross-sectional placement at those girders locations too.

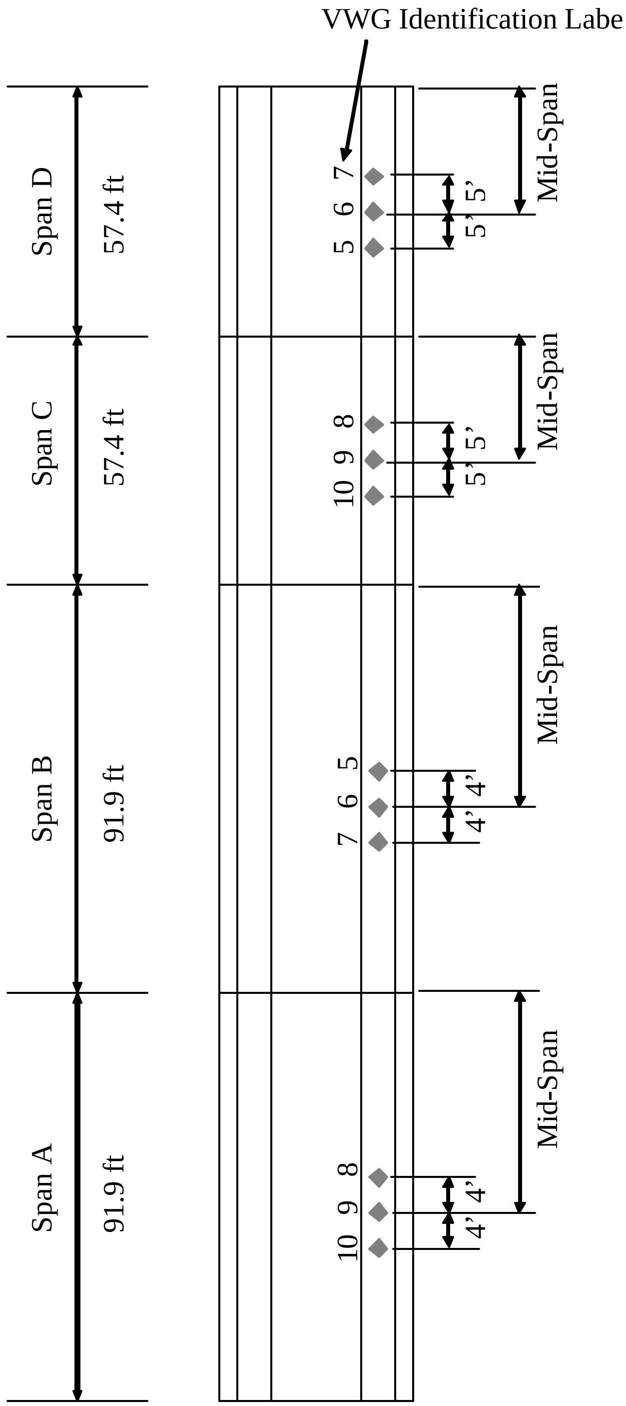

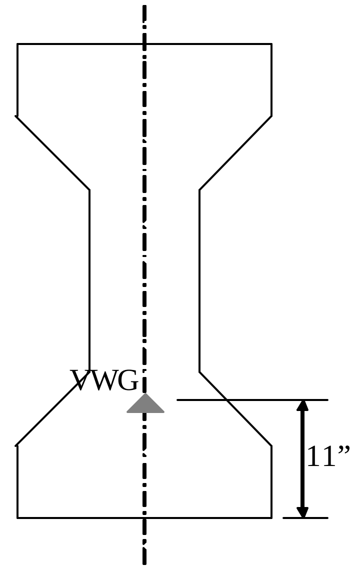

Typical for Cross-Sections of VWGs 5, 6, 7, 8, 9, and 10 for Spans C4 and D4

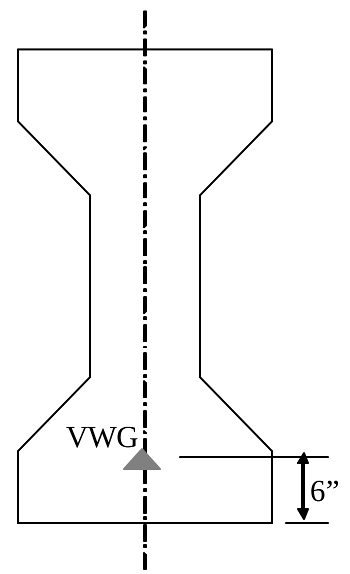

Typical for Cross-Sections of VWGs 5, 6, 7, 8, 9, and 10 for Spans A4 and B4

Figure 4. Retained Vibrating Wire Gauge Locations In The Girders Along The Entire Span Length Of Girder-line 4 And The VWG Cross-Sectional Placement at Those Locations

Identification labels were also assigned to each of the VWGs used in phase two during Matthew Wagner's research, but in phase three, new identification labels were reassigned to the VWGs retained. In Table 2, the corresponding identifications between the original assigned labels and new assigned labels are displayed.

Table 2. Identification Labels of VWG's In Girders

Matthew Wagners Identification Assignment = New Identification Assignment
Span A4:
VWG 1 = VWG 8
VWG 2 = VWG 9
VWG 3 = VWG 10
Span B4:
VWG 1 = VWG 5
VWG 2 = VWG 6
VWG 3 = VWG 7
Span C4:
VWG 1 = VWG 8
VWG 2 = VWG 9
VWG 3 = VWG 10
Span D4:
VWG 1 = VWG 5
VWG 2 = VWG 6
VWG 3 = VWG 7

To determine the total strain change in the concrete of the girders, initial readings were taken from the embedded VWGs. In Table 7, the Appendix displays initial readings taken from the embedded VWGs. These readings were taken at the beginning and end of the girder casting during phase two by Matthew Wagner on October 3, 2000 – October 6, 2000 and just over a year later on October 14, 2001 and October 28, 2001 before the deck of the bridge was cast.

3.3. Installation of the Internal Instruments Inside The Bridge Deck And The Cast In Place Connection Between The Girders

During phase three of the joint project additional internal instrumentation was installed along with the retained instruments from phase two to monitor the effected properties of the concrete described earlier in Section 3.1. The additional internal instruments used in phase three were placed into the bridge deck and bent diaphragms or continuous joints of the US 401 Southbound Bridge during its construction. The types of internal instruments cast into the bridge deck are thermocouples and VWGs, and the internal instruments cast into the bent diaphragms are VWGs.

Figure 5 shows the locations of the cross-sections where the thermocouples are located in the bridge deck, and Figure 6 shows the locations of where the thermocouples are located inside those cross-sections.

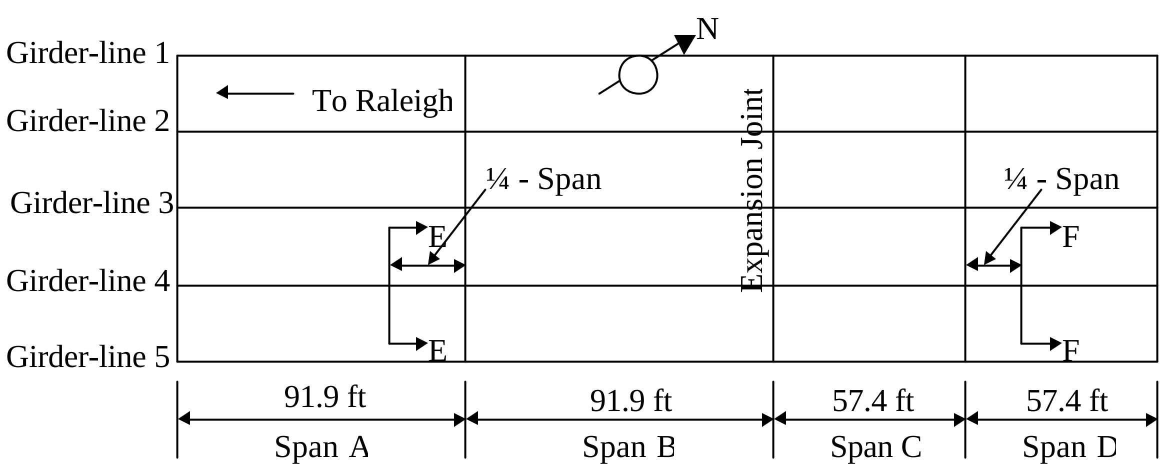

Figure 5 Installed Thermalcouples In Cross-Sectional Locations Along The Deck

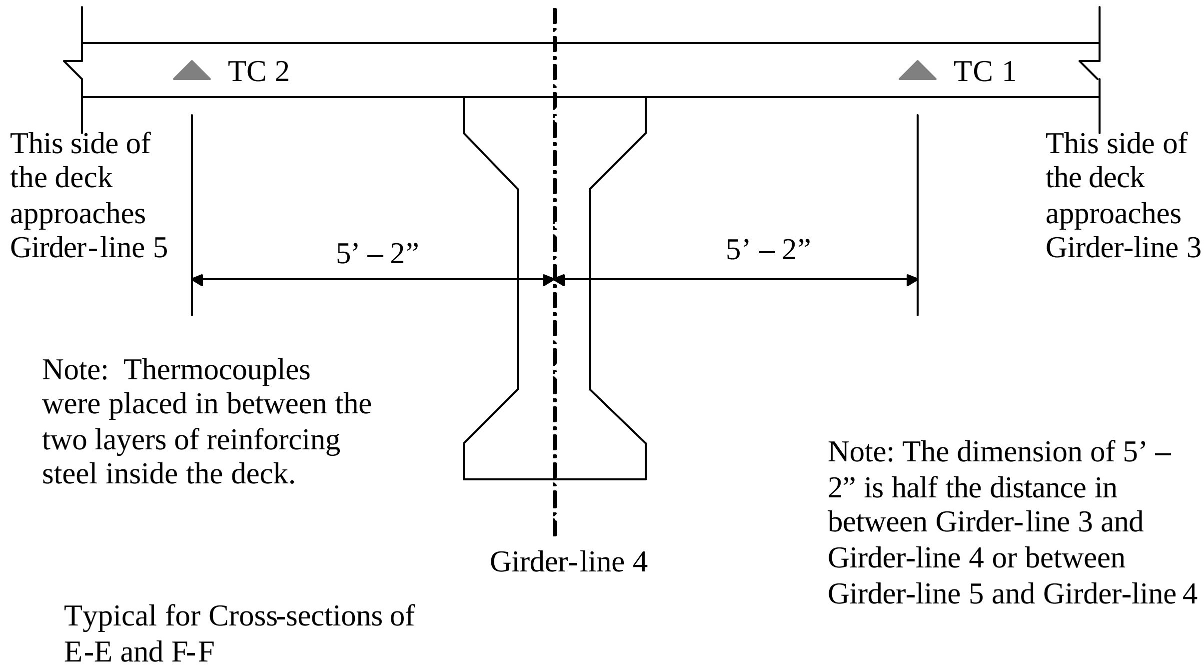

Figure 6 Installed Thermalcouples In Each Deck Cross-Sectional Location

Figure 7 shows the locations of the cross-sections where the VWGs are located in the bridge deck and bent diaphragm. Figure 8 shows the locations of where the VWGs are located inside those cross-sections.

As in Section 3.2, the total strain change in the concrete of the bridge deck and the bent diaphragms are determined from initial readings taken from the embedded VWGs. Table 8 in the Appendix displays initial readings taken from the embedded VWGs. These readings were taken on October 14, 2001 and October 28, 2001 before the deck of the bridge was cast.

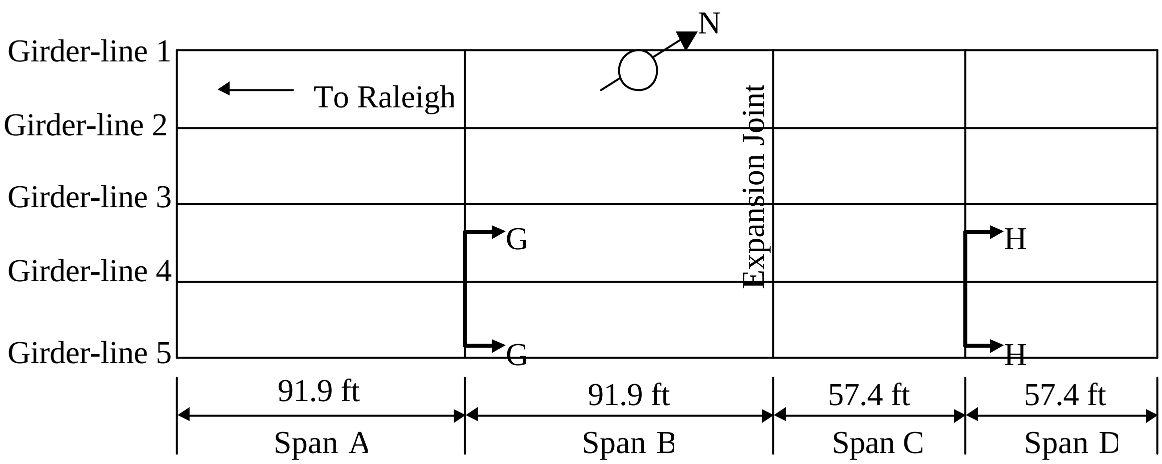

Figure 7. Installed Vibrating Wire Gauges In Cross-Sectional Locations In The Deck And Girder Of Bent Diaphragms

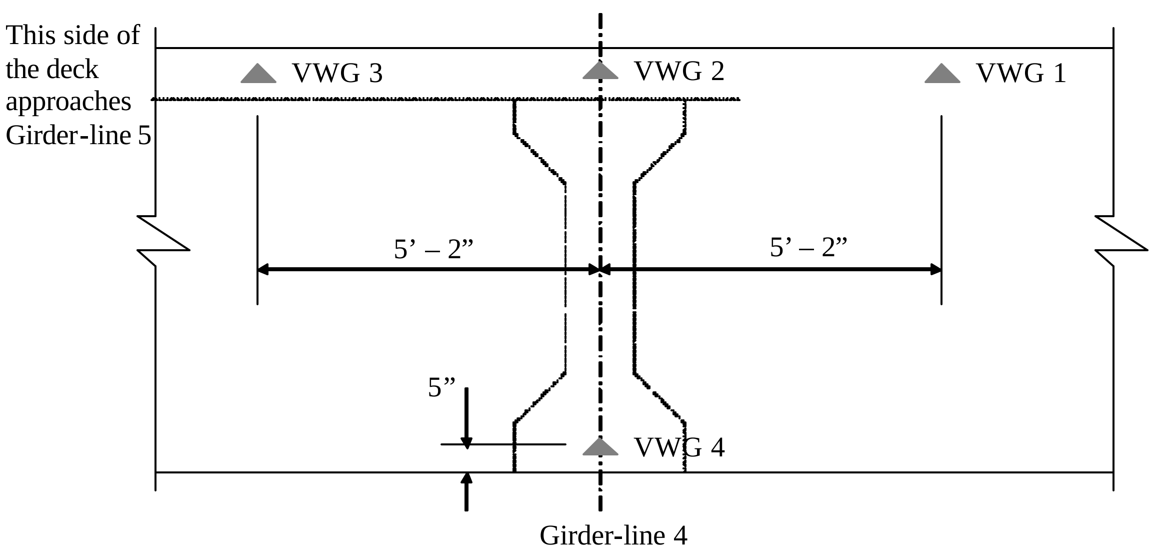

Typical for Cross-Sections of G-G and H-H

Note: VWGs inside the deck were placed in between the two layers of reinforcing steel

Note: The dimension of 5' – 2 is half the distance in between Girder-line 3 and Girder-line 4 or between Girder-line 5 and Girder-line 4

Figure 8. Installed Vibrating Wire Gauges In The Deck And Girder Of Each Bent Diaphragm Cross-Sectional Location

3.4. Installation of External Instrumentation On The Bridge

External instrumentation was installed on the bridge during phase three of the joint project to monitor the effected properties of the concrete described earlier in Section 3.1. The types of external instruments placed onto the bridge were LVDTs. The LVDTs used in phase three were placed at the two bridge abutments and Pier 2 along Girder-line 4, to locate these locations, refer to Figure 9. A target was placed on the two ends of each continuous span of girders underneath the bridge deck at the bridge locations. Each LVDT was connected to a post, and each post was attached to Pier 2 and the abutments. The LVDTs have a spring-loaded stroke that rests on the target. When there are longitudinal girder movements, the stroke is allowed to move back and forth with the girders, while the LVDT casing is secured into place where a measurement reading is recorded.

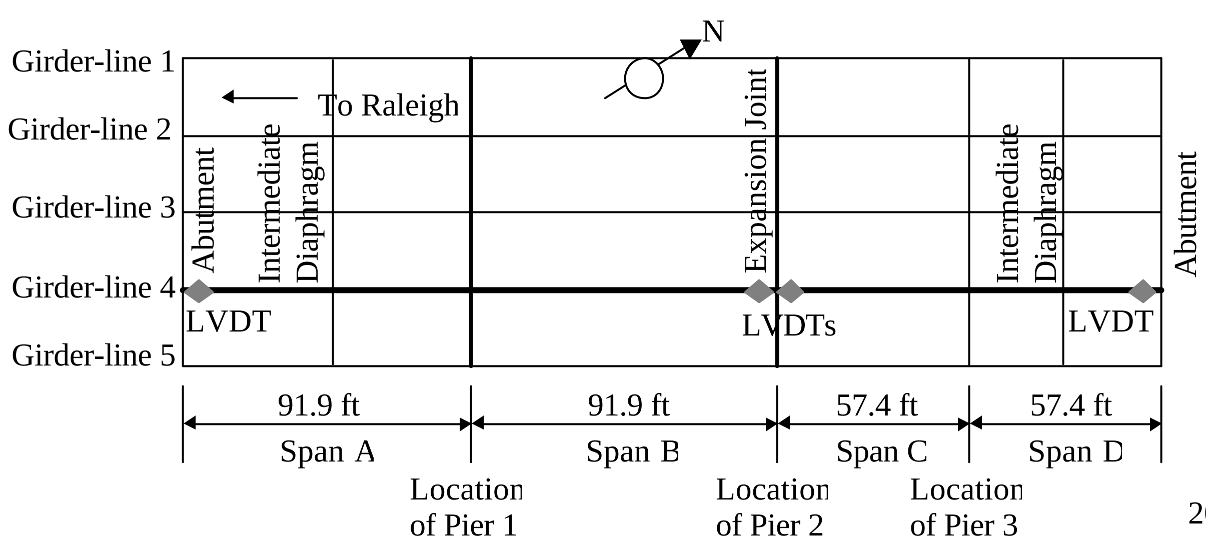

Figure 9. Locations of Installed LVDTs underneath the Bridge Deck along Girder-line 4

For a LVDT reading to be taken by the data acquisition system described in Section 1, the program that the data acquisition system executes must have a conversion factor written into it, to convert measured voltage into measured lengths. Table 3 displays the conversion factors for each LVDT used on the bridge along with its identification label.

Table 3. Identification Labels And Conversion Factors For The LVDTs Placed Along Girder-line 4

LVDT Location	LVDT Identification Label	Conversion Factor (volt/inch)
Span A4 at abutment	S/N 1729	9.9979
Span B4 at Pier 2	S/N 1728	10.0114
Span C4 at Pier 2	S/N 1701	20.0818
Span D4 at abutment	S/N 1700	20.0776

3.5. Instruments Connected To Data Acquisition System

The instruments that have been described in Sections 3.2, 3.3, and 3.4 were connected to the data acquisition system described in Section 1, where readings were taken for the first and second live load tests and short-term monitoring of phase three. The instruments of Spans A and B, which can be seen in Figure 1, are connected to the data acquisition system bolted to the intermediate diaphragm under Span A of the bridge; the instruments of Spans C and D are connected to the other data acquisition system bolted to the intermediate diaphragm under Span D.

A diagram of the general layout of the data acquisition system can be seen in Bruce Warren's thesis on page 37 in Figure 4.4 (Warren 2000). In Figure 4.4, there are three multiplexers to which the instruments are connected. The thermocouples are connected to the AM25T multiplexer, the LVDTs are connected to the AM416-A multiplexer, and the VWGs are connected to the AM416-B miltiplexers. Diagrams of components within the data acquisition system can also be seen in Bruce Warren's thesis on pages 38-42 in Figures 4.5-4.9. In Figures 4.5-4.9, aspects of the component characteristics, the interconnection between the components of the data acquisition system and the instrument connections can be seen as well.

Each multiplexer has channels where the instruments' wiring is connected, and the measurement readings are recorded by the datalogger. The instrument's identification label and the channel, which the instrument is connected, are tabulated in Table 4.

Table 4. Instruments Connected To The Channels Of Each Multplexer

Data Acquisition System Located Under Span A of the Bridge		Data Acquisition System Located Under Span D of the Bridge	
Multiplexer AM416-A - LVDTs		Multiplexer AM416-A – LVDTs	
Instrument Identification	Channel Identification	Instrument Identification	Channel Identification
Span A4 at abutment	Channel 1	Span D4 at abutment	Channel 1
		Span C4 at Pier 2	Channel 2
		Span B4 at Pier 2	Channel 3
Multiplexer AM416-B - VWGs		Multiplexer AM416-B – VWGs	
Instrument Identification	Channel Identification	Instrument Identification	Channel Identification
VWG 1	Channel 1	VWG 1	Channel 1
VWG 2	Channel 2	VWG 2	Channel 2
VWG 3	Channel 3	VWG 3	Channel 3
VWG 4	Channel 4	VWG 4	Channel 4
VWG 5	Channel 5	VWG 5	Channel 5
VWG 6	Channel 6	VWG 6	Channel 6
VWG 7	Channel 7	VWG 7	Channel 7
VWG 8	Channel 8	VWG 8	Channel 8
VWG 9	Channel 9	VWG 9	Channel 9
VWG 10	Channel 10	VWG 10	Channel 10
Multiplexer AM25T - Thermocouples		Multiplexer AM25T - Thermocouples	
Instrument Identification	Channel Identification	Instrument Identification	Channel Identification
TC 1	Channel 1	TC 1	Channel 1
TC 2	Channel 2	TC 2	Channel 2
TC 3	Channel 3	TC 3	Channel 3
TC 4	Channel 4	TC 4	Channel 4
TC 5	Channel 5	TC 5	Channel 5
TC 6	Channel 6	TC 6	Channel 6
TC 7	Channel 7	TC 7	Channel 7
TC 8	Channel 8	TC 8	Channel 8

4. CONCRETE CASTING OF THE US 401 SOUTHBOUND BRIDGE DECK

4.1. Overview

During phase three of the joint project between the NCDOT and NCSU, the HPC bridge deck of the US 401 Southbound Bridge was cast into place. The bridge deck was cast into two segments on two different days. The first segment was cast onto the girders of Spans C and D on October 26, 2001, and the second segment of the bridge deck was cast onto the girders of Spans A and B on October 31, 2001. Referring back to Figure 1 in Section 3.1, one can see the general location of the spans where the bridge deck segments were cast into place.

When each of the bridge deck segments was cast, 4” x 8” concrete cylinder specimens were taken for samples to determine the compressive strength and elastic modulus of the HPC. Also, a 6” x 12” concrete cylinder specimen with a VWG embedded into the cast cylinder was taken from each bridge deck segment casting to monitor the shrinkage of the HPC. Finally, a 3’ x 3’ slab specimen with two VWGs embedded into the specimen was cast when the second segment of the bridge deck was cast into place. The slab was cast to monitor shrinkage in the specimen resulting in simulated shrinkage conditions that the bridge deck would experience when in place.

4.2. 4”x 8” Concrete Cylinder Specimens

There were a total of twelve 4” x 8” cylinder specimens sampled or six specimens for each bridge deck segment. The specimens were cured for a week, before taken back to the lab, by covering and placing them in a region close to the cast bridge deck simulating the conditions that the bridge deck would have cured under for that period.

Four specimens from the twelve were tested for compressive strength on December 18, 2001. The two specimens taken from the October 26, 2001 casting produced compressive strengths of 6,650 psi and 6,745 psi, and the two specimens taken from the October 31, 2001 casting produced compressive strengths of 5,410 psi and 5,205 psi.

Two specimens from the twelve were tested for compressive strength and modulus of elasticity on January 8, 2002. A specimen taken from the October 26, 2001 casting produced a compressive strength of 7,018 psi and a modulus of elasticity of 4,250 ksi, and a specimen taken from the October 31, 2001 casting produced a compressive strength of 5,904 psi and a modulus of elasticity of 4,370 ksi.

Four other specimens from the twelve were tested for 90-day compressive strength and modulus of elasticity on January 24, 2002 for the samples taken from the October 26, 2001 casting and on January 31, 2002 for the October 31, 2001 casting. The two specimens taken from the October 26, 2001 casting produced compressive strengths of 7,510 psi and 6,523 psi and a modulus of elasticity of 4,060 ksi and 4,130 ksi. The two specimens taken from the October 31, 2001 casting produced compressive strengths of 5,789 psi and 5,787 psi and a modulus of elasticity of 4,750 ksi and 3,330 ksi.

The last two specimens of the twelve were never tested and still intact for any future testing of the HPC strength properties. In addition, the modulus of elasticity for each cylinder specimen was extracted from the tested stress vs. strain relationship that can be seen in Graphs 47-50 in the Appendix C.

4.3. 3’ x 3’ Slab Specimen And 6” x 12” Cylinder Specimen

The 6” x 12” cylinder specimens sampled for each bridge deck segment were cured, in the same manner as the 4” x 8” cylinder specimens, for a week before the specimens were taken back to the lab. The embedded VWGs in each of the 6” x 12” cylinder specimens recorded the strain due to any shrinkage effects in HPC specimen. As discussed in Section 3.2 and 3.3, an initial strain measurement must be recorded to determine the total strain change in the specimen. The initial strain measurements were recorded for each of the cylinders and tabulated in Table 9 in the Appendix, along with readings recorded on other following dates.

The 3’ x 3’ slap specimen’s formwork and reinforcement was constructed by the NCDOT. Once the slab specimen’s formwork and reinforcement was constructed, the two VWGs were installed between the two layers of reinforcement in the form before the specimen was cast. The layout of the reinforcement and the locations of the VWGs in the slab specimen can be seen in Figure 10.

The VWGs embedded into the specimen recorded the strains due to any shrinkage effects in the HPC specimen, which were used to determine total strain change. The initial strain measurements were recorded for the slab and tabulated in Table 8 in the Appendix, along with readings recorded on other following dates.

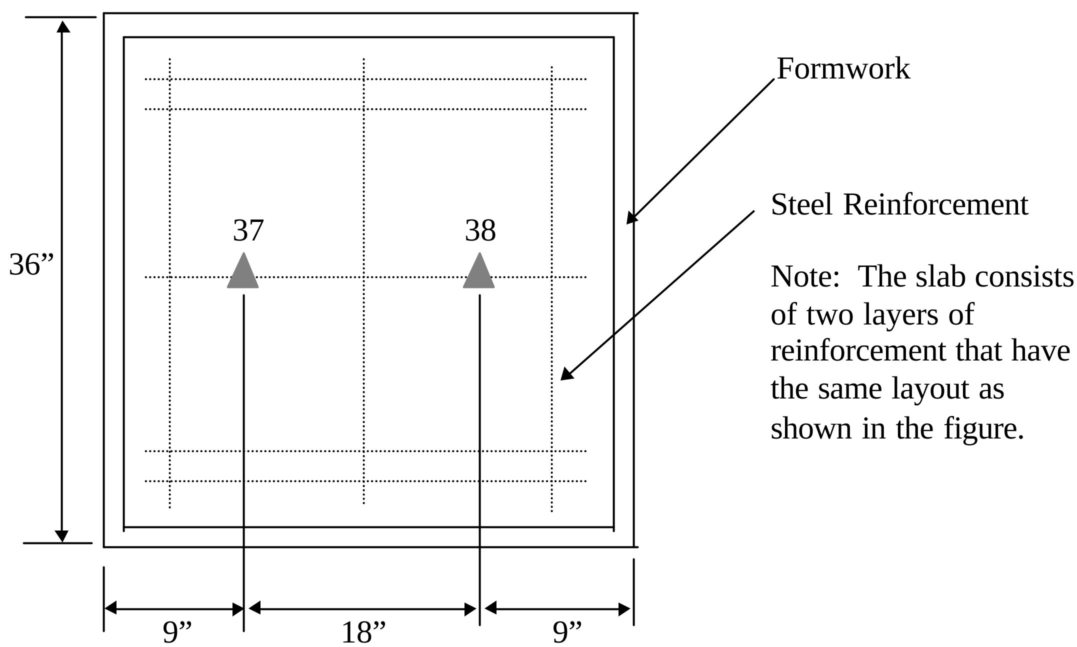

Figure 10 3’ x 3’ x 8 ½” Slab Specimen

5. FIRST LIVE LOAD TEST

5.1. Overview

On May 21, 2002, the first live load test was performed on the US 401 Southbound Bridge to achieve the objectives of phase three for the joint project between the NCDOT and NCSU. The live load test was performed by placing a five-axle truck and trailer loaded with rock at certain positions along the bridge over Girder-lines 2, 3, and 4. When the truck and trailer was at a given position, the internal and external instruments recorded strains and deflections that the girders and bridge deck were subjected too. The live load test performed had two test runs; the first and second run were carried out when the truck and trailer were loaded to roughly half and full truck and trailer weight capacity, respectively.

The instruments that were utilized for the live load test were VWGs, LVDTs, string potentiometers and accelerometers. The VWG and LVDT locations and applications are described earlier in Sections 3.2, 3.3, and 3.4. The string potentiometers and accelerometers are additional external instruments that were temporarily installed on the bridge for the period that the live load test was implemented. The string potentiometer and accelerometer locations are described in more detail in Section 5.2. The string potentiometers recorded the deflections of the bridge girders relative to the ground as the truck and trailer was positioned at different points along the bridge. The accelerometers recorded the accelerations of the vibrations of the bridge as the truck and trailer drove across it.

The string potentiometers and accelerometers were not connected to the Campbell Scientific data acquisition system described in Sections 1.1 and 3.5; they were connected to an Optim data acquisition system. The reason these instruments were connected to the

Optim system instead of the Campbell Scientific system was do to the fact, that the Optim system could generate a massive number of readings in a short amount of time that the Campbell system could not. To accurately represent acceleration from the vibration of the bridge as the truck and trailer move across it, a large number of accelerometer readings are necessary in minute time intervals to be recorded.

Once the live load test was carried out, there was a large amount of data collected. This information was sorted through and displayed in the form of plots and tables that describe the behavior of the bridge during the live load test in a meaningful manner. These results generated will be expanded on later in Section 5.5. These results are then compared to the structural analysis results of the bridge in Section 6, where conclusions are drawn in Section 7.

5.2. String Potentiometer And Accelerometer Locations

As described in Section 5.1, the string potentiometers record girder displacement and the accelerometers record accelerations due to bridge vibrations. Also, these instruments were temporarily installed on the bridge the day of the live load test. There were two string potentiometers that were installed underneath the bridge deck on the girders at mid-span of Spans A and D, which can be seen in Figure 11. The string potentiometer was attached to a concrete block with a line tied to a spring-loaded cable in the instrument. This line led up to an eyebolt that was screwed into a wooden block glued to the girder where the line was tied off at the eyebolt. Also, there were two accelerometers that were installed on the bridge deck at mid-span of Spans A and D, which can be seen in Figure 11. The accelerometers were attacked on the sidewalk of the bridge deck with epoxy. This kept the instrument isolated from the activities going on during the live load test on the rest of bridge deck.

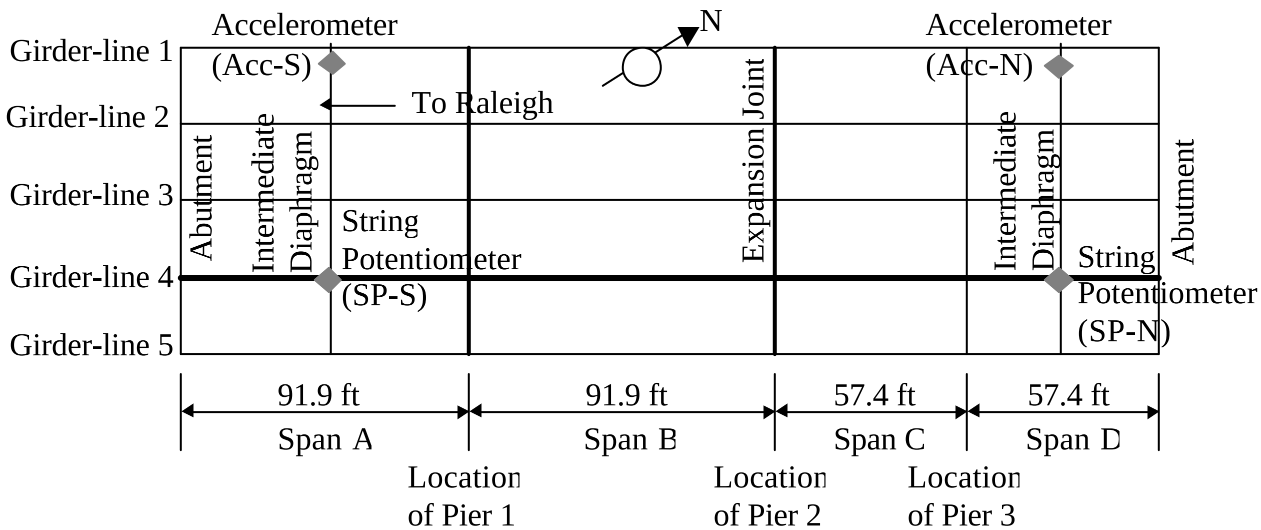

Figure 11. Locations Of String Potentiometers And Accelerometers Installed On The Bridge

5.3. Truck And Trailer

The five-axle truck and trailer was loaded to the desired weights for each of the test runs performed to accomplish the live load test objectives. The truck and trailer was loaded at the NCDOT Road Maintenance Yard in Bunn, NC. When the truck was loaded to the desired weight at the maintenance yard, the axles of the truck and trailer were weighed to establish the wheel loads. The axles were weighed with portable scales provided by the DMV. Finally, the loaded truck and trailer was sent to the bridge site to perform one of the two test runs of the live load test.

The first test run was performed with the truck and trailer loaded to a desired middleweight and the second run was performed with the truck and trailer loaded to a gross weight of roughly around 80,000 pounds. Therefore, the truck and trailer was loaded to excessive weights that violate roadway weight restrictions. Therefore, the NCDOT had to obtain a permit from the DMV to travel the highway from the maintenance yard to the bridge site and the truck and trailer had to be escorted by a state highway patrol car to ensure safety on the highway.

Once the truck and trailer was loaded and weighed, the wheel load information was used to calculate the center of gravity of the truck and trailer. The center of gravity was used in the determination of where the truck was to be positioned along each of the bridge spans. Also, the wheel loads are a detrimental peace of information that is used in the structural analysis of the bridge for validating assumptions made in the design process. The wheel loads for each test run of the loaded truck can be seen in Table 5. The dimensions of the truck and trailer axle space lengths and the location of the center of gravity for each of the loadings can be seen in Figure 12.

Table 5. Wheel Load Weights In pounds

	Test Run 1		Test Run 2	
	Driver Side	Passenger Side	Driver Side	Passenger Side
Axle 1	4,400	4,880	4,700	4,500
Axle 2	5,700	7,160	9,000	8,700
Axle 3	5,500	6,520	9,000	7,900
Axle 4	4,400	6,900	9,000	9,900
Axle 5	4,400	6,200	9,300	10,500
Total	56,060		82,500	

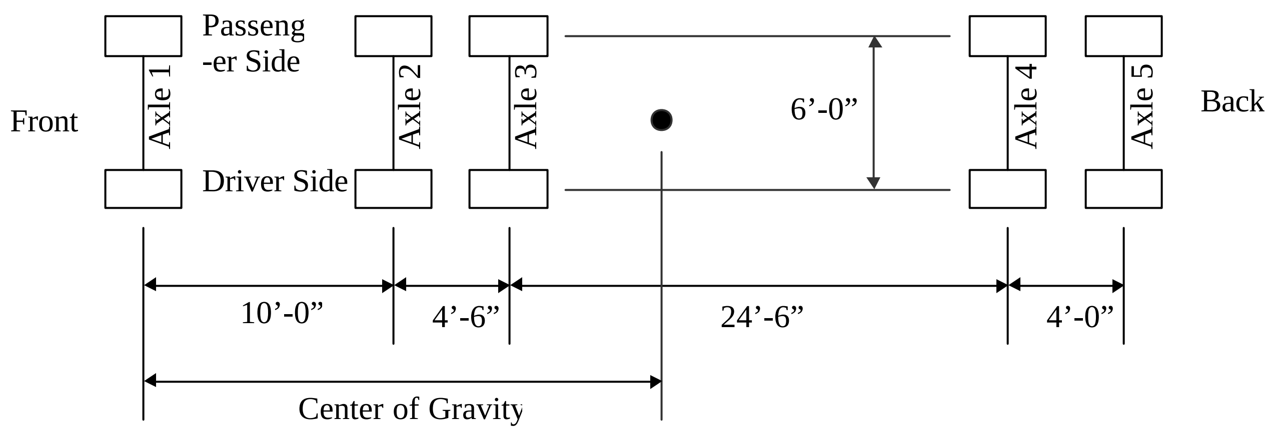

Center of Gravity Distance for Test Run 1 =21' 6"
Center of Gravity Distance for Test Run 2 = 25' 9"

Figure 12. Axle Spacing Dimensions And Center Of Gravity Location

5.4. Locations Where The Truck And Trailer Were Positioned For The Live Load Test

The live load test was simulated by positioning the heavily loaded five-axle truck and trailer at locations with the driver side or the passenger side wheel-line over Girder-lines 3 and 4 for each of the spans. This would produce the maximum girder deflections and strains necessary for reliable measurements to be taken along Girder-line 4. The positions where determined by calculating the center of gravity of the truck and trailer and lining its location up with the mid-span location of each span and each continuity joint. There were a total of fourteen positions that the truck and trailer were placed at for each of the two test runs. These truck and trailer positions for the live load test can be seen in Figure 13.

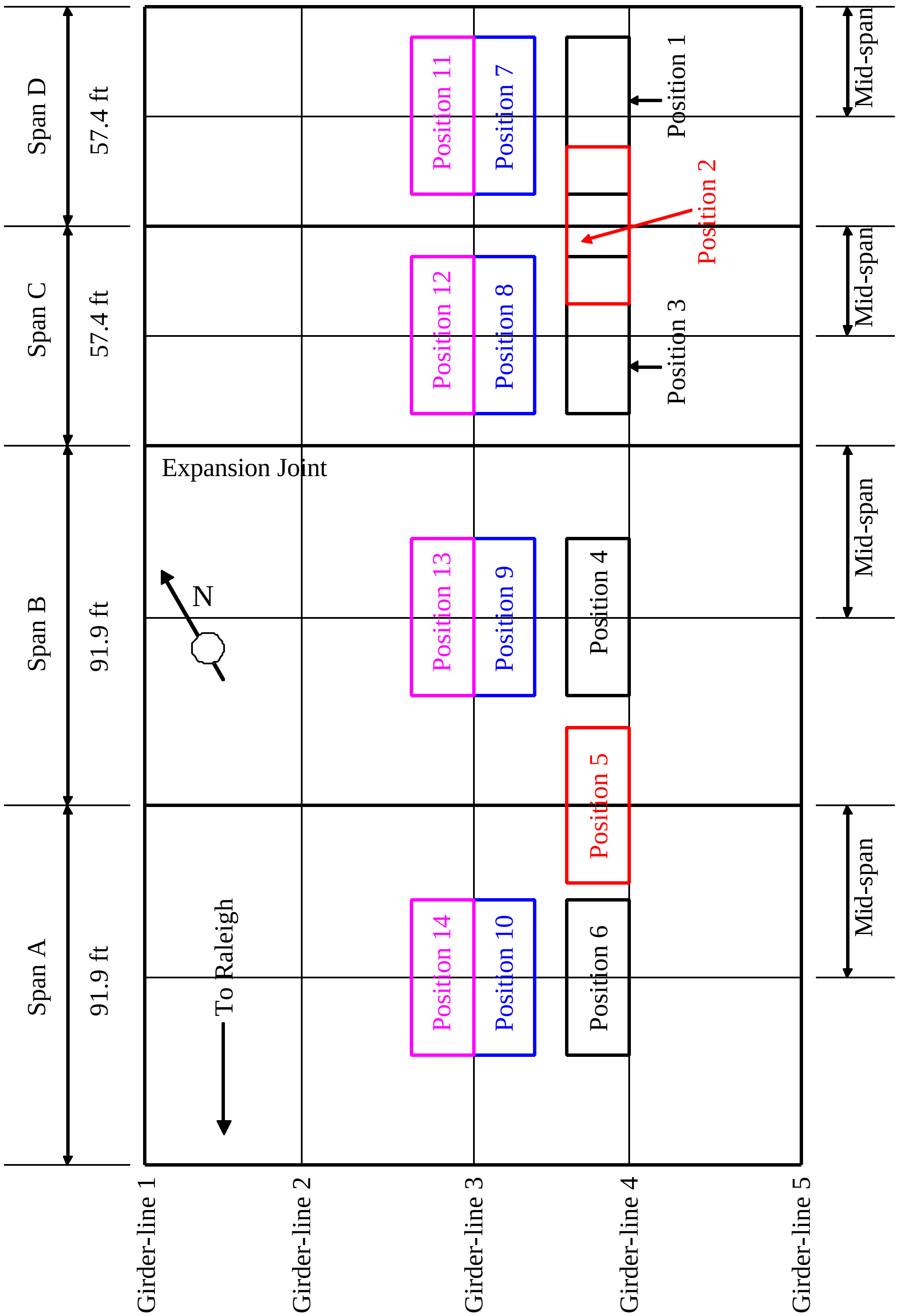

Figure 13. Truck and Trailer Positions For The Live Load Test

5.5. Live Load Test Data

The live load test performed on the US 401 Southbound Bridge over the Neuse River in Wake County, NC was accomplished with two test runs, as described earlier in Section 5.1. The first test run was conducted with the five-axle truck and trailer loaded to a total weight of 56,060 lbs, and the second test run was conducted with the five-axle truck and trailer loaded to a total weight of 82,500 lbs. The first and second test runs were carried out by placing the five-axle truck and trailer at Positions 1 through 14. When the truck and trailer came to rest at the designated positions, instrument readings were taken for strains and deflections that the girders and deck were subjected too during the loading. Before each test run was conducted, initial readings were taken for the VWGs and LVDTs to determine the total strain change and longitudinal girder movements in the girders and deck only due the loading caused by the truck and trailer.

The Campbell Scientific data acquisition system took readings of both the VWGs and LVDTs, and stored the data in output files for each position that the truck and trailer was placed for each test run. The readings were sorted through and the strain readings from the VWGs and longitudinal girder movement deflection readings from the LVDTs were extracted from these output files. Once the strain and longitudinal girder movement deflection readings from the test runs were determined, the initial readings were subtracted from the test run readings to calculate the total strain changes and longitudinal girder movement deflections in the girders and deck due to the various truck and trailer loading positions.

The girder deflection readings in the string potentiometers were taken by the Optim data acquisition system, which stored the data in output files for each position that the truck and trailer was placed for each test run. The girder deflection readings were output in the files in the form of deflection vs. time. This is because the Optim data acquisition system takes enormous amounts of readings in a brief amount of time. Therefore, the string potentiometers were allowed to take readings for around thirty seconds to allow the truck and trailer to move into the designated position and come to rest.

Although, the stain changes and deflections are summarized in table form, the field data gained by the live load test can be displayed graphically in appendix A to show relationships in a much more meaningful manner. Just note that to interpret these graphs properly, one should refer back to Sections 3.2-3.3 for instrument locations in the girders and deck and to Section 5.4 in Figure 13 for truck and trailer positions.

Therefore, the strains in the girders can be viewed in Graphs 1- 8 and the strains in the continuity joints can be viewed in Graphs 9-12 for the various truck and trailer positions of each test run performed. In addition, the strains vs. girder depth in the continuity joints can be viewed in Graphs 13-15 for the various truck and trailer positions of each test run performed. Finally, the girder deflections in Spans A and D can be seen in Graphs 16 and 17 for the various truck and trailer positions for each test run performed.

Lastly, accelerometers were implemented in the live load test; the purpose of using the accelerometers is to demonstrate any stiffness changes in the bridge system between the first and second live load tests. There is a relationship between system vibrations and system stiffness, therefore, the acceleration readings taken during each live load test when the loaded truck and trailer move across the bridge will signal any system stiffness degradation over time. The acceleration readings were taken at the end of the second test run when the truck and trailer was loaded to a total weight of 82,500 lbs, and it was drove over the bridge. The accelerometers took readings at the mid-spans of both Spans A and D of the bridge. These acceleration readings can be viewed in Graphs 18 and 19 with respect to time.

6. Structural Analysis Performed On The US 401 Southbound Bridge Simulating Truck and Trailer Loading Conditions At Various Positions On The Bridge

6.1. Overview

After the first live load test was carried out on the US 401 Southbound Bridge for phase three of the joint project between the NCDOT and NCSU, a structural analysis was performed on an analysis model of the US 401 Southbound Bridge under identical truck and trailer loading conditions at various positions on the bridge. The analysis model took into account the physical dimensions and properties of the bridge, such as the span lengths, member cross-sectional dimensions, and the modulus of elasticity of the girders and deck. The analysis took into account the truck and trailer wheel loads, axle distances between one another, and the location of where the truck and trailer were positioned on the bridge to simulate the loading condition that the bridge was subjected too. These known aspects of the analysis were input into spreadsheets and a structural analysis program to calculate moments, deflections, and strains at instruments locations to compare the actual field data to the results of the structural analysis.

The structural analysis of the bridge under the simulated loading conditions is a very important part of phase three. The structural analysis verifies any assumptions made during the design process of the bridge. One such assumption made during the design process of the bridge was how a load is distributed from the deck to the girders caused by a design truck and trailer loading. In this section of the report, the structural analysis was performed to determine if the results from the wheel load distribution factors assumed in design compare accurately with the actual field data results.

6.2. Assumptions made during the Structural Analysis

First, the structural analysis performed only simulated the truck and trailer loading conditions at Positions 1, 3, 4, 6, 7, 8, 9, and 10, these truck and trailer positions can be viewed in Section 5.4 in Figure 13. This was because Girder-line 4 was the only girder-line of the bridge to be instrumented for the project. Therefore, the truck and trailer positioned at locations along the bridge in between Girder-lines 3 and 4 would result in a majority of the wheel loads to translate into Girder-line 4 when the truck and trailer was positioned at 1, 3, 4, and 6 and a portion of the wheel loads to translate into Girder-line 4 when the truck and trailer was positioned at 7, 8, 9, and 10. The effects of Positions 2 and 5 were neglected in the analysis because the truck and trailer was not positioned at the continuity joints with the truck and trailer wheel-line directly over Girder-line 3, this results inconclusively of how the wheel loads are distributed when the truck and trailer are positioned at continuity joints. Finally, it was assumed that when the truck and trailer was positioned at Positions 11-14 the wheel loads translated to Girder-line 4 could be neglected because the truck and trailer were positioned in between Girder-lines 2 and 3.

Next, the structural analysis did not take into account the self-weight of the girder and deck composite section and prestress effects. The reason for this was because when the live load test was performed, initial readings were taken before each test run, and subtracted from the data taken during each test run. This would negate any loads caused by the section self-weight and prestress effects from the field data results due to the truck and trailer loading.

Therefore, the only loads considered in the structural analysis were due to the truck and trailer.

Finally, AASHTO Standard Specifications for Highway Bridges Sixteenth Edition 1996 as amended by the 1997, 1998, 1999 Interim Revisions were used as guidelines for the effective flange width for the deck and wheel load distribution factors. Specification 10.38.3, Effective Flange Width was referred to as guidance for the determination of the effective flange width for the girder and deck composite section. Table 3.23.1 Distribution of Wheel Loads in Longitudinal Beams was referred to for the wheel load distribution factor for Girder-line 4. The distribution factor was found to be S/5.5 for a concrete bridge made of prestressed concrete girders for a bridge designed for two or more traffic lanes where S is the average stringer spacing in feet.

However, the guideline for the wheel load distribution factors was not utilized in the structural analysis because this guideline took into account the wheel loads from a truck and trailer placed at a position on the deck so that the truck and trailer's wheel-lines would be straddling the girder. The positions that the truck and trailer were positioned at on the bridge during the live load test was with one of the truck and trailer's wheel lines directly over the girder. Therefore, the truck and trailer's wheel loads were distributed in the following manner based on a basic statics shown in Figure 14.

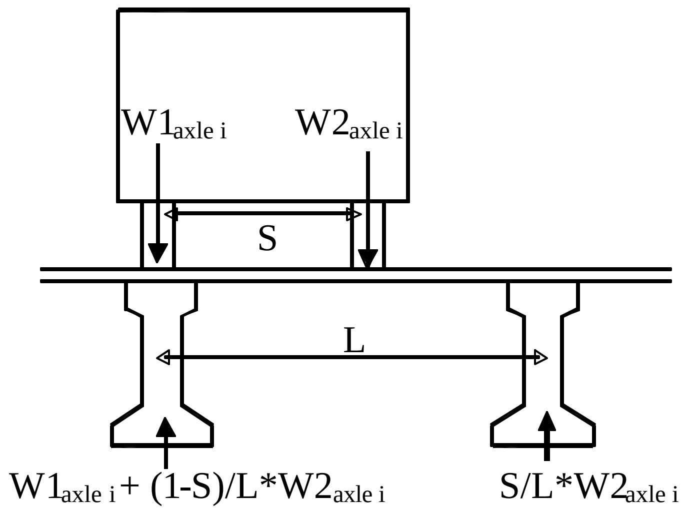

Figure 14. Axle Load Distribution

6.3. Structural Analysis Results and Field Data Comparison

The resulting strains, moments, and deflections due to the truck and trailer placed at Positions 1, 3, 4, 6, 7, 8, 9, and 10 for each test run were obtained from structural analysis. The structural analysis was performed based on the information and assumptions already described in Section 5.1 and 5.2. The analysis methods and programs used to calculate the strains, moments, and deflections are described in the Appendix along with the program output results and spreadsheet calculations.

The field data and resulting structural analysis data are compared and displayed graphically to show relationships in a much more meaningful manner. Just note that to interpret these graphs properly, one should refer back to Sections 3.2-3.3 for instrument locations in the girders and deck and to Section 5.4 in Figure 13 for truck and trailer positions.

Therefore, the strains in the girders can be viewed in Graphs 20-30 and the strains in the continuity joints can be viewed in Graphs 31-34 for the various truck and trailer positions of each test run performed. Also, the strains vs. girder depth in the continuity joints can be viewed in Graphs 35-42 for the various truck and trailer positions of each test run performed. Finally, the girder deflections in Spans A and D can be seen in Graphs 43 and 46 for the various truck and trailer positions for each test run performed.

7. SECOND LIVE LOAD TEST

On June 10, 2003, the second live load test was performed on the US 401 Bridge in the same manner the first test was conducted. The second live load test took place more than a year after the first test was conducted and eight months after the bridge was opened for traffic. The same truck was used with two runs, fully loaded and half-full loaded; the axle loads are shown in table 6. The researchers decided to omit loading positions 11-14 shown in figure 13, and the use of the accelerometers in the second test. This decision was taken due to the insignificance of the results obtained after analyzing the first live load test data.

Table 6. Wheel Load Weights In pounds

	Test Run 1		Test Run 2	
	Driver Side	Passenger Side	Driver Side	Passenger Side
Axle 1	4,880	4,500	5,020	4,460
Axle 2	6,380	6,240	9,320	7,960
Axle 3	6,140	5,780	9,360	7,480
Axle 4	4,620	5,420	7,900	8,380
Axle 5	4,060	4,440	9,000	8,000
Total	52,460		76,880	

The Optim data acquisition system was not used in the second live load test due to that fact that we are only interested in the maximum deflection when the truck comes to rest. Therefore, since the enormous number of data recorded by the Optim system is not needed, an electrical panel was assembled where the string potentiometers were connected to it through long wires; input voltage was given to the panel and string potentiometers through alkaline battery. High accuracy voltmeter was used to read the input and output voltages when the truck and trailer came to rest. The string potentiometers with the long wires were calibrated before the test in the laboratory to get the correct conversion factors. Figure 15 shows the maximum deflection recorded at mid-span A and D due to different loading positions for half-full truck (52,460 lb).

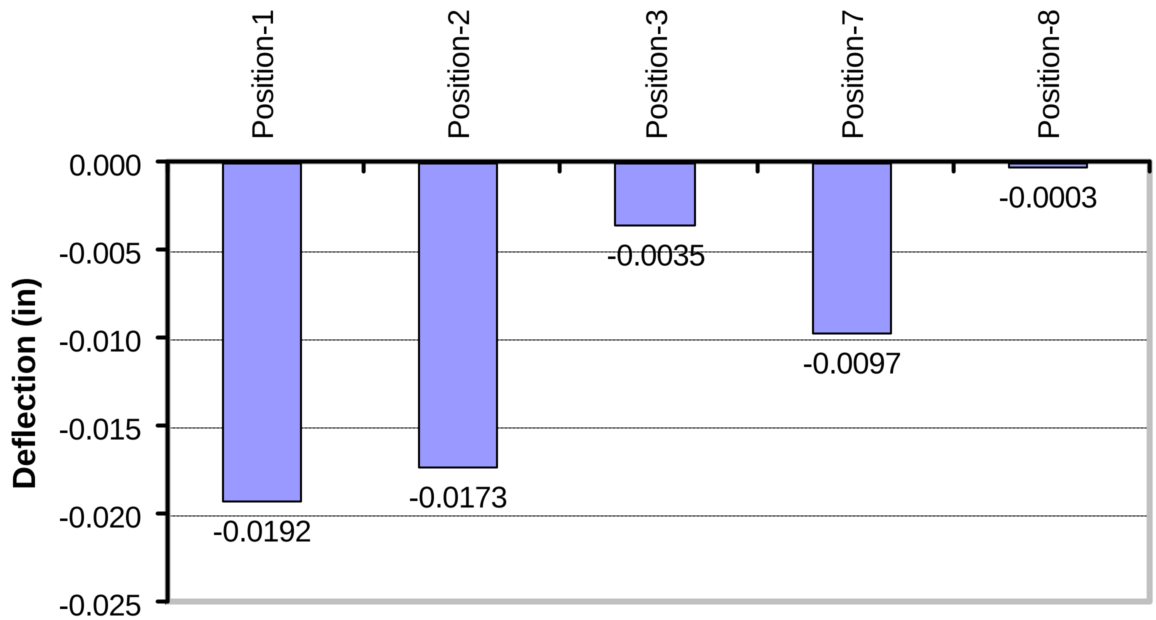

(a) Mid-Span D Deflection (52,460 lb)

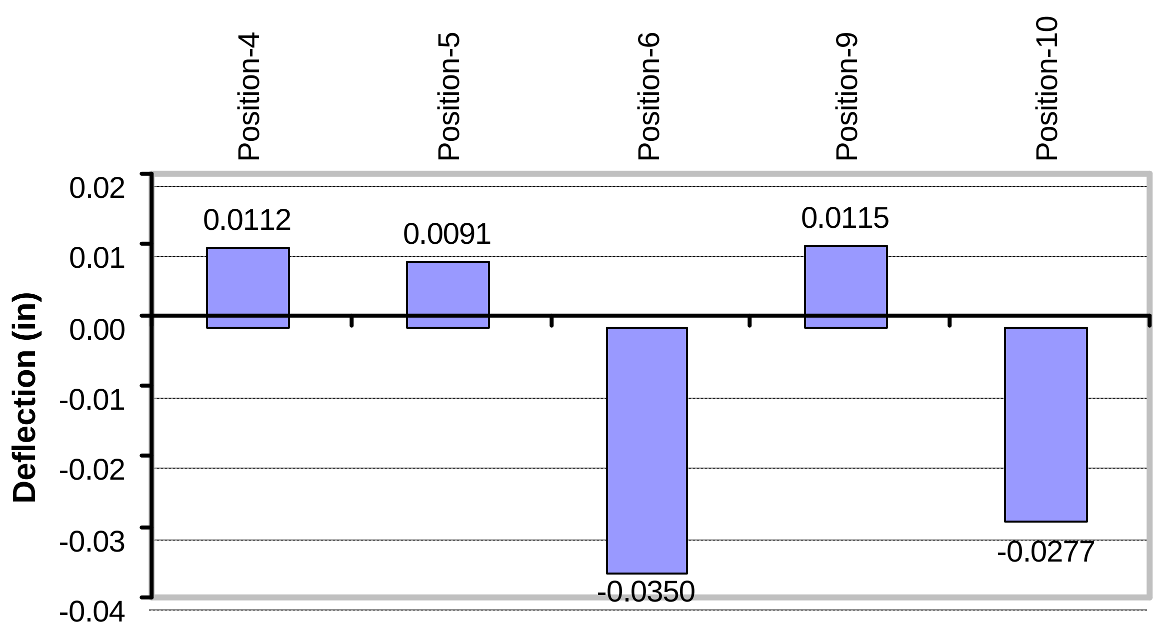

(b) Mid-Span A Deflection (52,460 lb)

Figure 15. Mid-Spans Deflection Due to Half-Full Truck

A comparison between actual and calculated strains is shown in figures 16 and 17. A simplified model was used for strain calculations; every two spans were assumed a continuous beam, although, joints constructed between spans do not guarantee full rigidity. Load distribution factors were obtained according to AASHTO provisions and axle loads were distributed accordingly. Figures 16(a) and 16(b) shows actual and calculated strains at mid-spans D and A, respectively. Calculated strains were higher than actual strains for both spans and different loading values and positions, it is clear that distribution factors given by AASHTO are higher than the actual values. Figure 17 shows strain distribution along cross-section depth at middle support between span A and B.

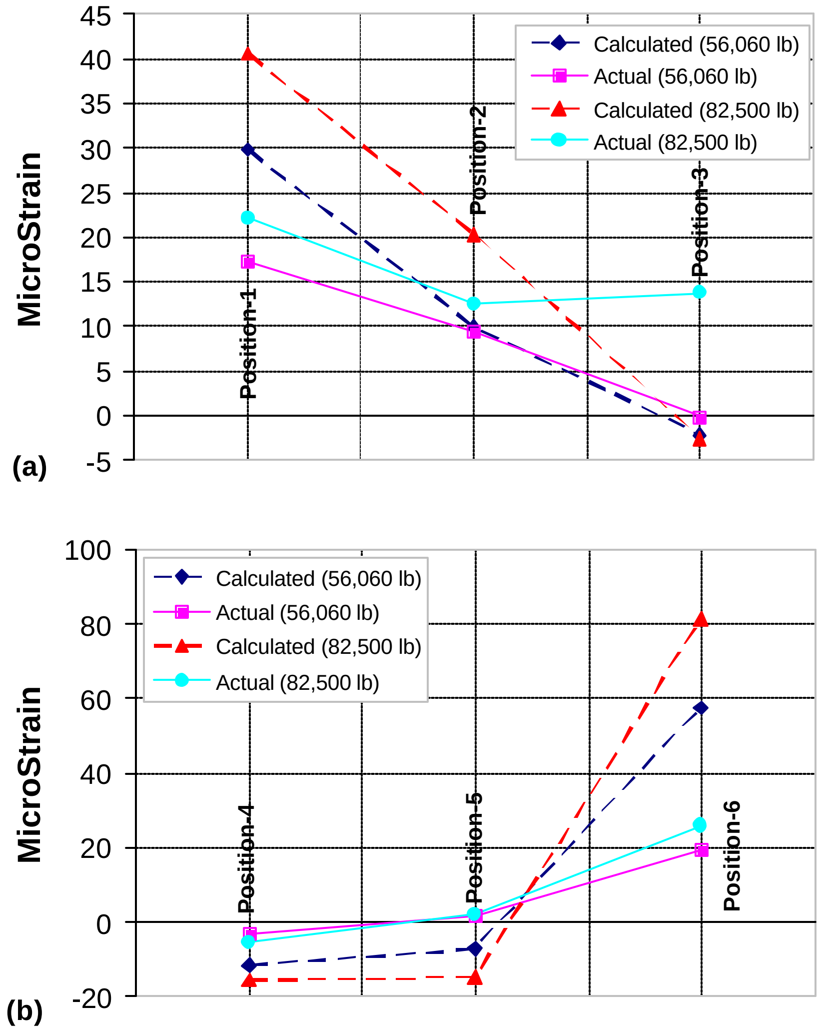

Figure 16. (a) VWG #6 Actual and Calculated Strains at Middle Span D (b) VWG #9 Actual and Calculated Strains at Middle Span A

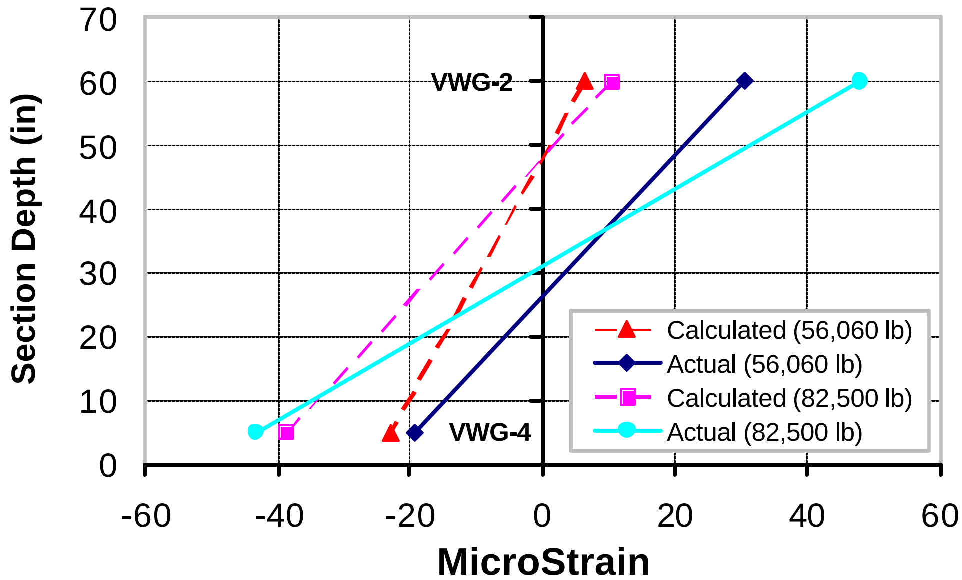

Figure 17. Actual and Calculated Strain Distribution along Girder Type IV Cross-Section at Middle Support between Spans A And B Due to Loading Position 5

8. IN-SERVICE BRIDGE BEHAVIOR

In order to study the bridge behavior under service loading some of the instruments used during casting were retained and additional instruments were used during construction to accommodate the needs of this phase.

Three types of instruments were utilized in this phase, twelve Omega FF-K-24 thermocouples were retained from the first phase and additional two thermocouples were placed in the deck at L/4 distance from support in spans A and D, as shown in figures 3, 5 and 6. Twelve EM-5 Vibrating Wire Gauges (VWGs) were retained and additional VWG's were placed at supports as shown in figures 4, 7 and 8. Finally, four LVDT's were used at each abutment and at the expansion joint to measure the longitudinal movement of the girders. All previous instruments were connected to Campbell scientific dataloggers, placed at bent diaphragms under the bridge.

The bridge was opened for traffic on October 2002 while the monitoring of the bridge started two months later. Data were recorded every 4 hours, 24 hours a day for four months under normal traffic loading. Figures 18 and 19 shows spans C and D end displacements due to thermal effects in addition to LVDTs differential displacement during the four months period, respectively. Thermal effects were calculated in reference to the lowest temperature, while LVDTs differential displacements represent the difference between LVDT reading at anytime and its reading when the lowest temperature was recorded. The LVDTs show additional end displacement due to traffic loading, however, maximum girder end displacement due to thermal effects and traffic loading was less than a quarter an inch. Girders end displacement caused by end rotations due to temperature gradient along the depth of the girder cross-section was found to be minimal and have no considerable effect on total end displacements.

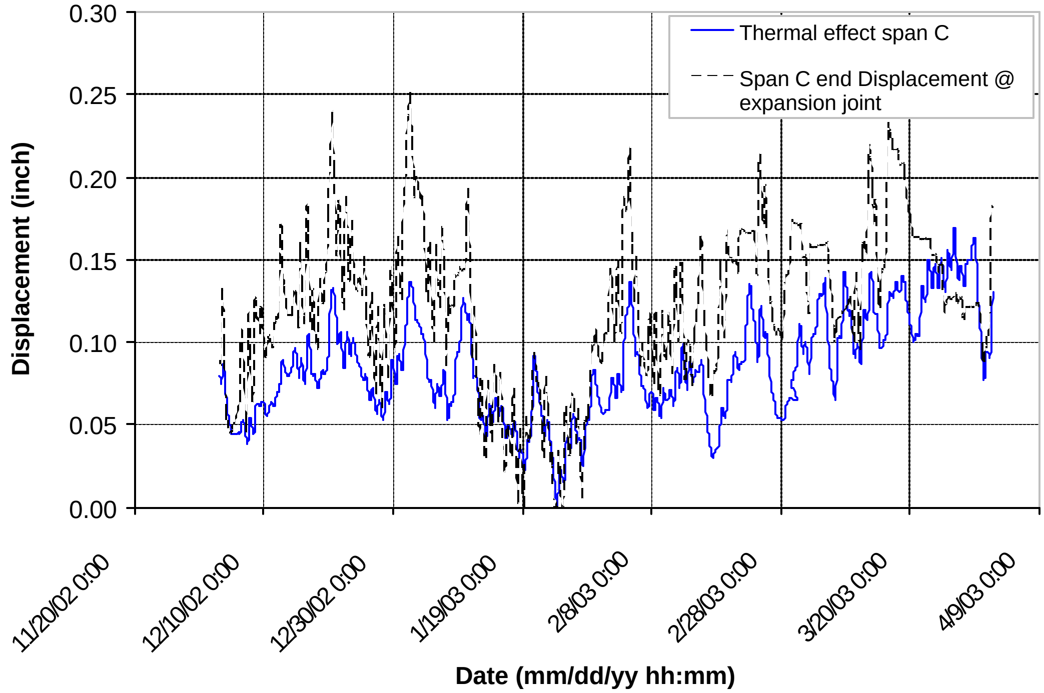

Figure 18. Girder C End Displacements Due To Thermal Effect And Traffic Loading

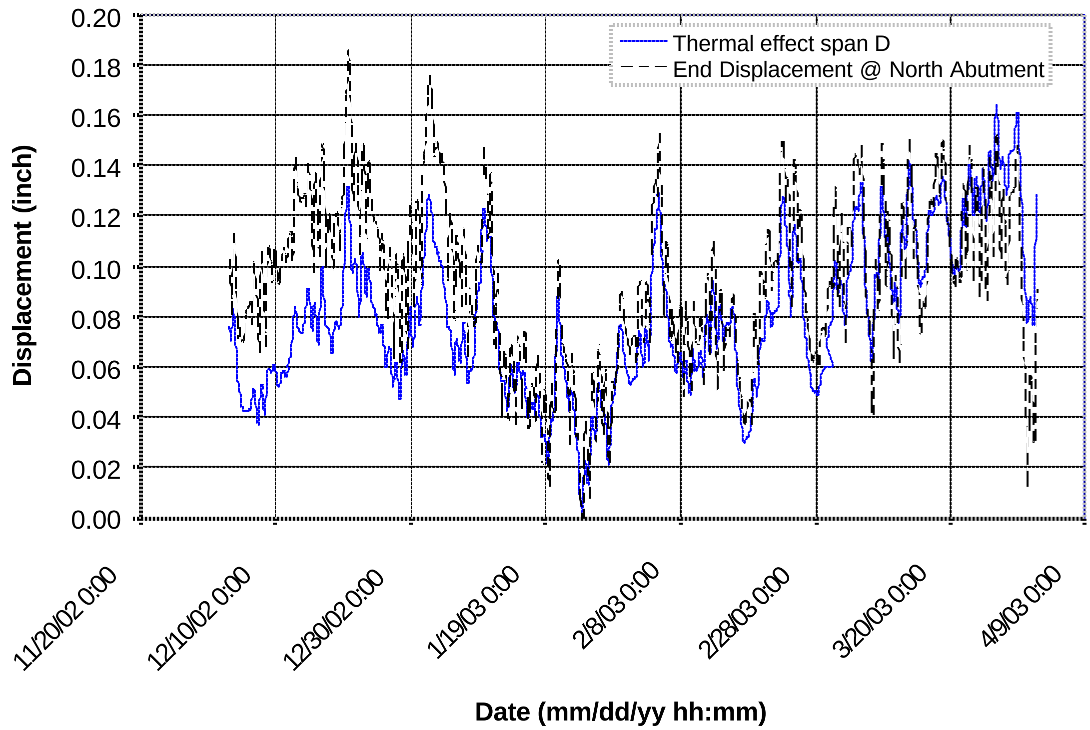

Figure 19. Girder D End Displacements Due To Thermal Effect And Traffic Loading

For additional information on thermocouples recorded temperatures and LVDT's readings, refer to graphs 51-68 in appendix D.

9. CONCLUSIONS AND RECOMMENDATIONS

This phase of the joint research project examined the in-service behavior and controlled load testing for four prestressed HPC girders. Based on this research the following conclusion and recommendation can be drawn:

(1) The instrument locations, instrument identifications, and initial readings of the internal and external instruments of the US 401 Southbound Bridge are summarized in Section 3 along with any other additional information about the instrumentation and data acquisition system.

(2) Section 4 describes the reason for each type of concrete specimen collected on October 26, 2001 and October 31, 2001 for the US 401 Southbound Bridge deck casting along with their corresponding mechanical properties.

(3) Section 5 describes the test setup and reports the data collected during the first live load test performed on the US 401 Southbound Bridge on May 21, 2002. In this section, a description of the locations and data collected for the string potentiometers and accelerometers that were temporarily installed on the day of the live load test are reported.

(4) Section 6 describes the structural analysis performed on the US 401 Southbound Bridge simulating the first live load test. The structural analysis was conducted in CAL-91 for moments and deflections at the location where instruments were

located in the live load test. Once the moments were determined, strains were calculated from those corresponding moments. The resulting strains and deflections from the structural analysis were tabulated and compared graphically with the field data collected in the first live load test.

(5) It can be seen based on the field data and structural analysis comparison graphs for Spans A and B that the loads transferred to a girder from the other loaded girder through the continuity joint is minimal. This can be seen in Graphs 28-30 and Graphs 45-46 that when the loaded truck and trailer is positioned at Position 4 and 9 on Span B that the load transferred to Span A is minimal based on the strain and deflection field data when compared to the structural analysis data. Also in Graphs 25-27 the loaded truck and trailer is positioned at Position 6 and 10 on Span A and the load transferred to Span B is minimal based on the strain field data when compared to the structural analysis data. It is concluded that either the girder stiffness is great enough to resist the load transferred or the continuity joint does not fully fix the two girders so that they act as a continuous span.

(6) It can be seen in the field data and structural analysis comparison graphs for Spans A and B and the continuity joint between Spans A and B that the structural analysis performed on the bridge model under identical live load conditions based on the bridge section properties produces data of the same trend but of larger magnitudes for strains and deflections when compared to the field data. Therefore, the analytical models assumed during design emphasizing girder stiffness and deflection result in a conservative HPC bridge design.

(7) The calculated strains and deflections for the second live load test, based on AASHTO load distribution factors and assumed model, were found to be higher than actual recorded data. Although, the assumed model is stiffer than the actual structure, the results could be attributed to the fact that AASHTO load distribution factors produces higher loading on the girder than the actual loading.

(8) After conducting the second live load test, it was found that a large number of the imbedded VWGs were not working; which, leads to suggest using different type of VWGs with longer lifetime in future projects.

(9) Mainly thermal effects with small effect due to traffic loading caused girder end displacements, over four months period of monitoring. Displacements due to end rotations caused by temperature gradient along cross-section depth could be neglected; however, maximum total girder end displacement was less than a quarter an inch.

(10) In general, the data collected through the controlled load testing were small and within instruments noise range in some cases, so it is recommended to consider using higher load for future testing.

REFERENCES

Warren, Bruce, Development of a Data Acquisition System for an Instrumented Highway Structure, MSCE Thesis, North Carolina State University, 2000.

Wagner, Matthew C. The Bahavior of Prestressed High Performance Concrete Bridge Girders for US Highway 401 Over the Neuse River in Raleigh, NC. MSCE Thesis, North Carolina State University, 2001.

American Association of State Highway and Transportation Official, Inc. Standard Specifications for Highway Bridges, Sixteenth Edition 1996, as Amended by the 1997, 1998, and 1999 Interim Revisions. 1999.

Appendix A: First Live Load Test Results

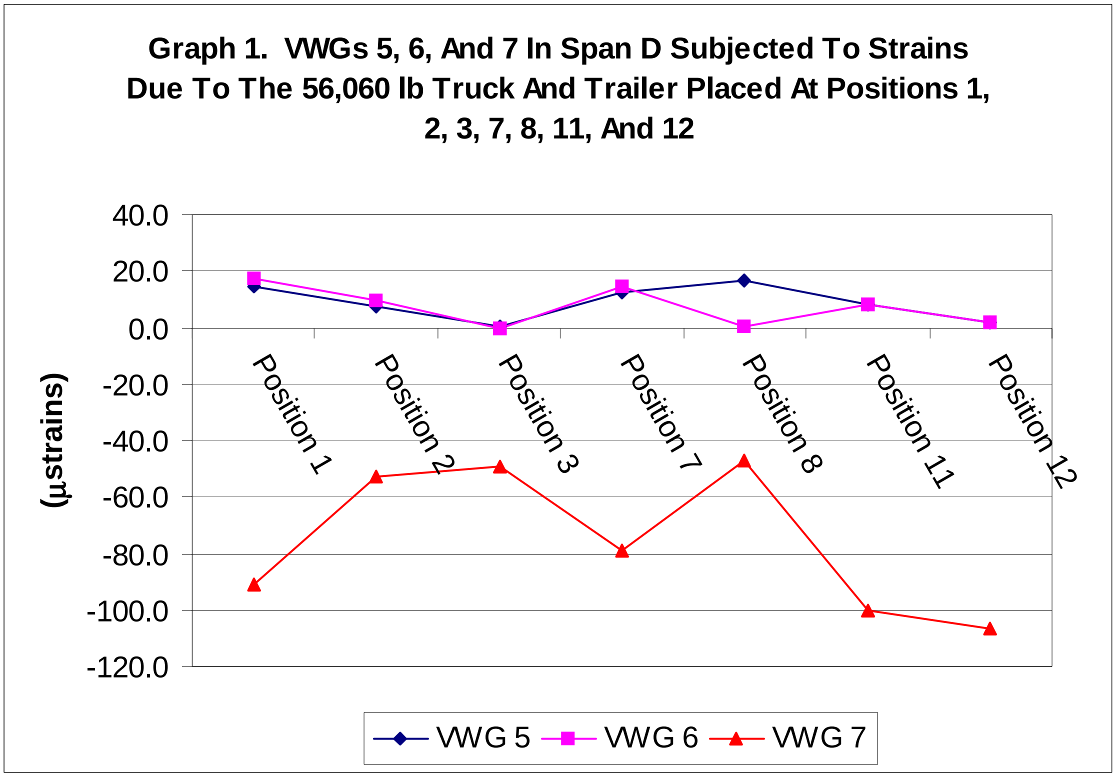
Graph 1. VWGs 5, 6, And 7 In Span D Subjected To Strains Due To The 56,060 lb Truck And Trailer Placed At Positions 1, 2, 3, 7, 8, 11, And 12
(µstrains)
40.0
20.0
0.0
-20.0
-40.0
-60.0
-80.0
-100.0
-120.0
Position 1
Position 2
Position 3
Position 7
Position 8
Position 11
Position 12
VWG 5
VWG 6
VWG 7

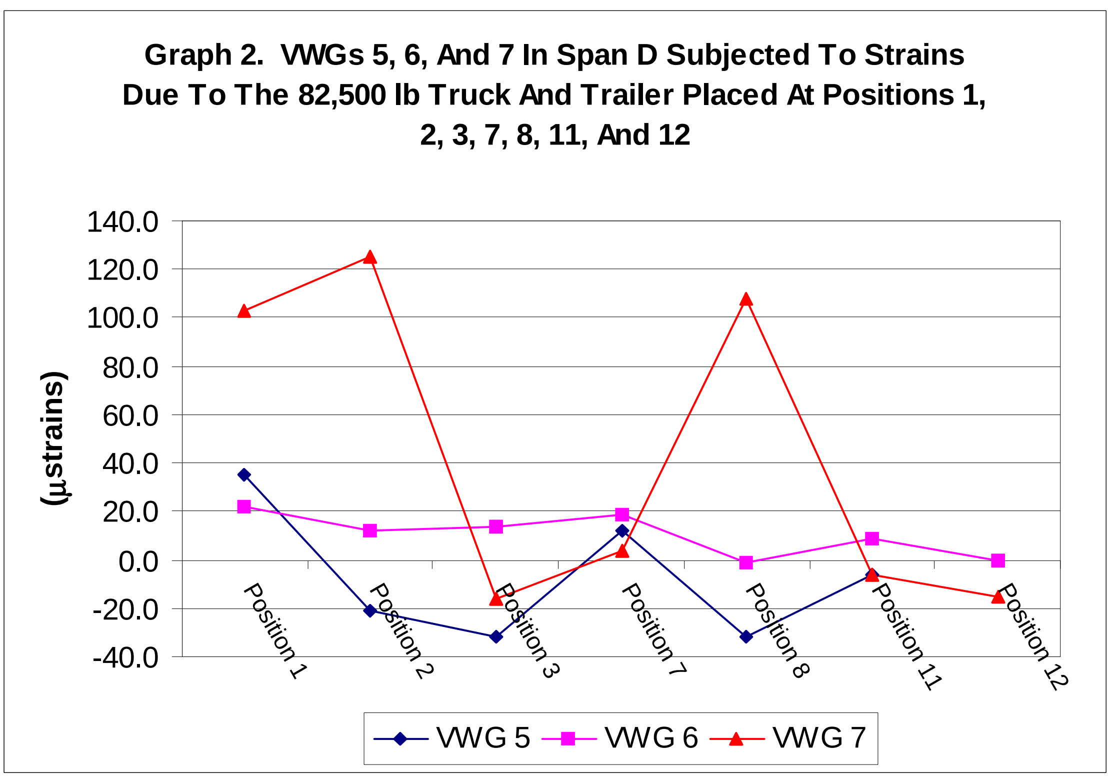
Graph 2. VWGs 5, 6, And 7 In Span D Subjected To Strains Due To The 82,500 lb Truck And Trailer Placed At Positions 1, 2, 3, 7, 8, 11, And 12
(µstrains)
140.0
120.0
100.0
80.0
60.0
40.0
20.0
0.0
-20.0
-40.0
Position 1
Position 2
Position 3
Position 7
Position 8
Position 11
Position 12
VWG 5
VWG 6
VWG 7

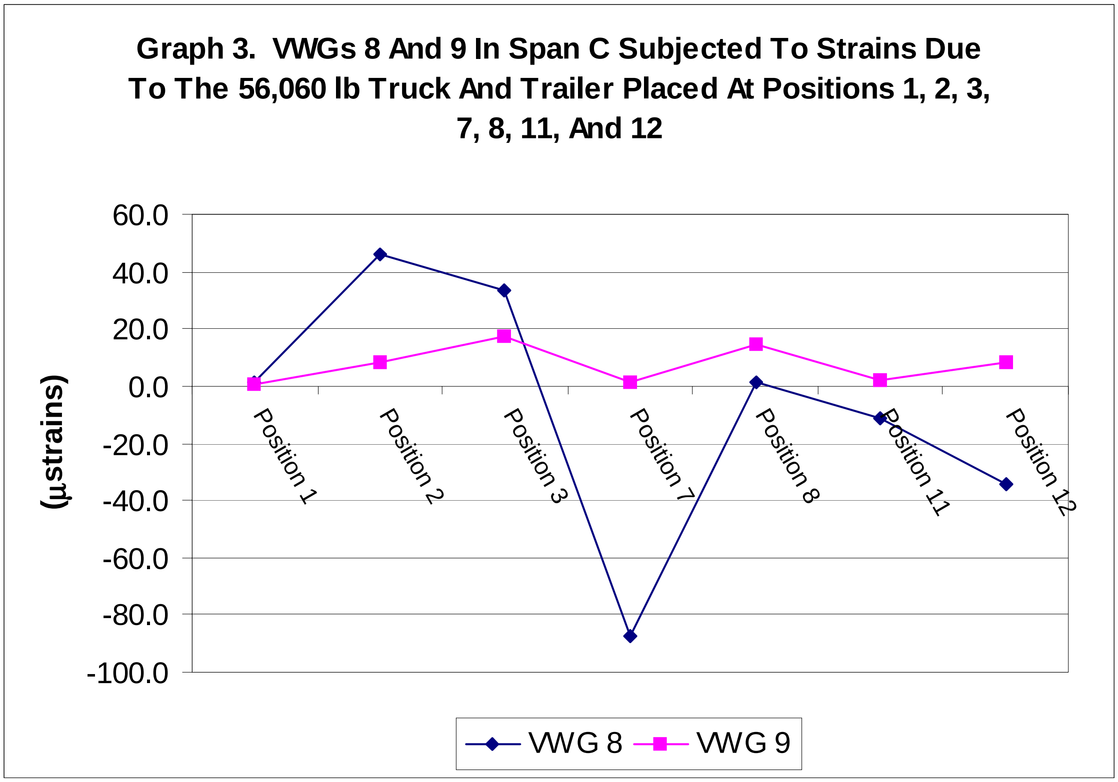
Graph 3. VWGs 8 And 9 In Span C Subjected To Strains Due To The 56,060 lb Truck And Trailer Placed At Positions 1, 2, 3, 7, 8, 11, And 12
60.0
40.0
20.0
0.0
-20.0
-40.0
-60.0
-80.0
-100.0
(µstrains)
Position 1
Position 2
Position 3
Position 7
Position 8
Position 11
Position 12
VWG 8
VWG 9

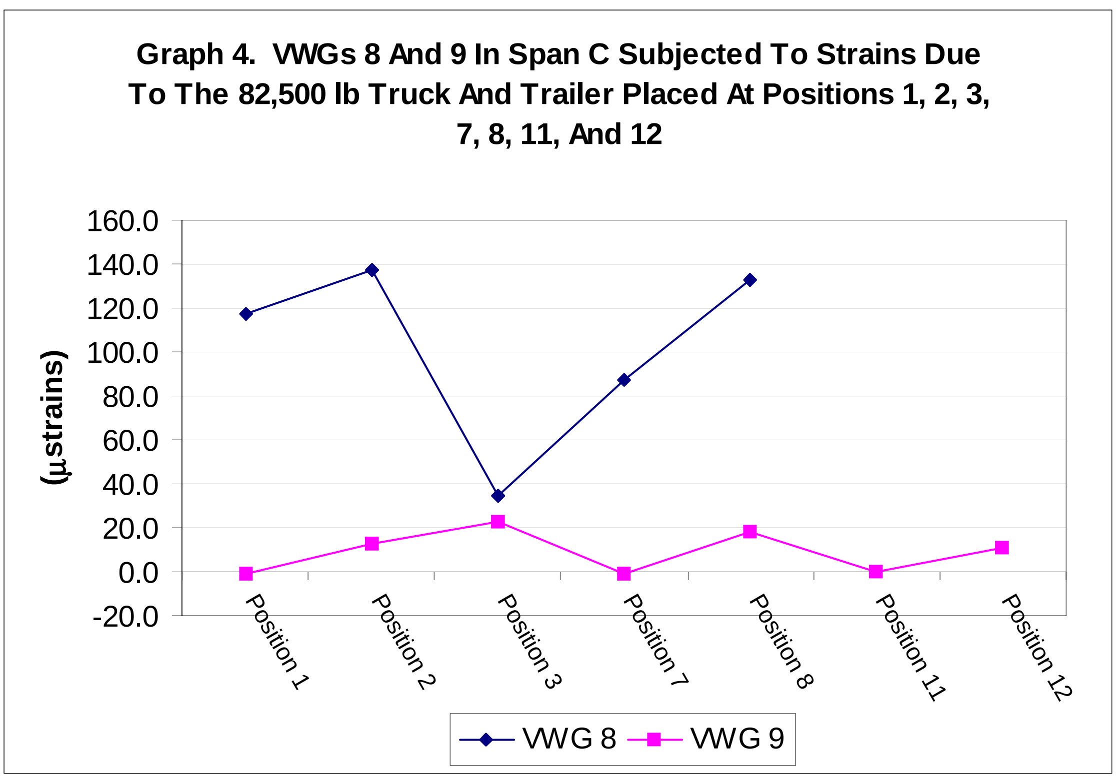
Graph 4. VWGs 8 And 9 In Span C Subjected To Strains Due To The 82,500 lb Truck And Trailer Placed At Positions 1, 2, 3, 7, 8, 11, And 12
160.0
140.0
120.0
100.0
80.0
60.0
40.0
20.0
0.0
-20.0
(µstrains)
Position 1
Position 2
Position 3
Position 7
Position 8
Position 11
Position 12
VWG 8
VWG 9

Graph 5. VWGs 5, 6 And 7 In Span B Subjected To Strains Due To The 56,060 lb Truck And Trailer Placed At Positions 4, 5, 6, 9, 10, 13, And 14

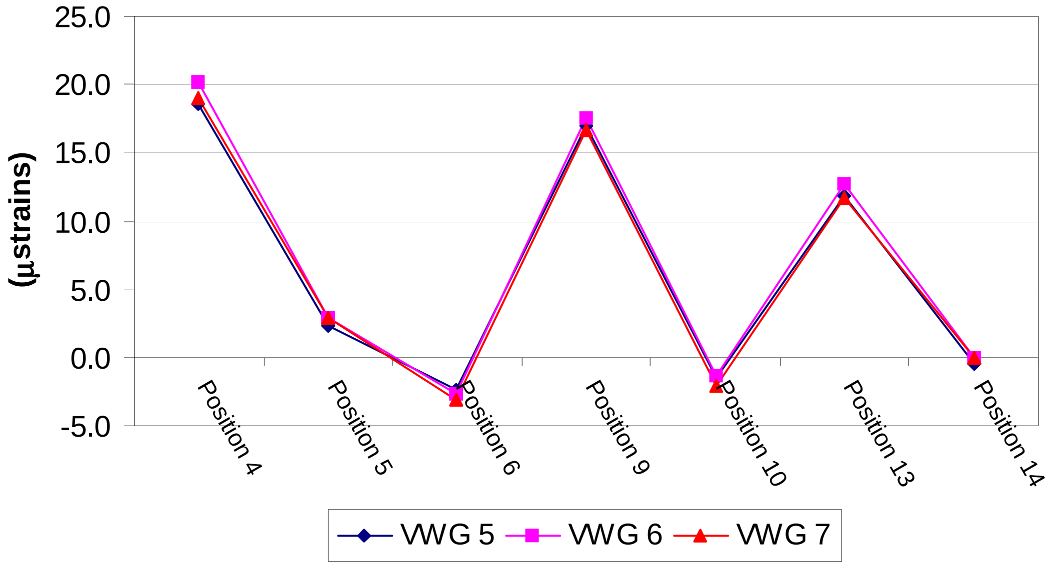

Graph 6. VWGs 5, 6 And 7 In Span B Subjected To Strains Due To The 82,500 lb Truck And Trailer Placed At Positions 4, 5, 6, 9, 10, 13, And 14

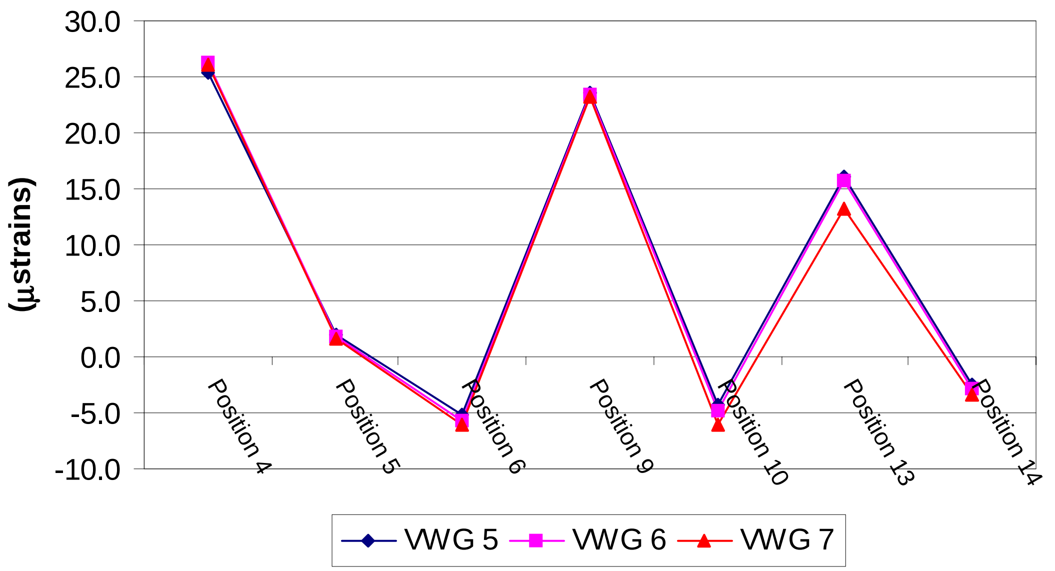

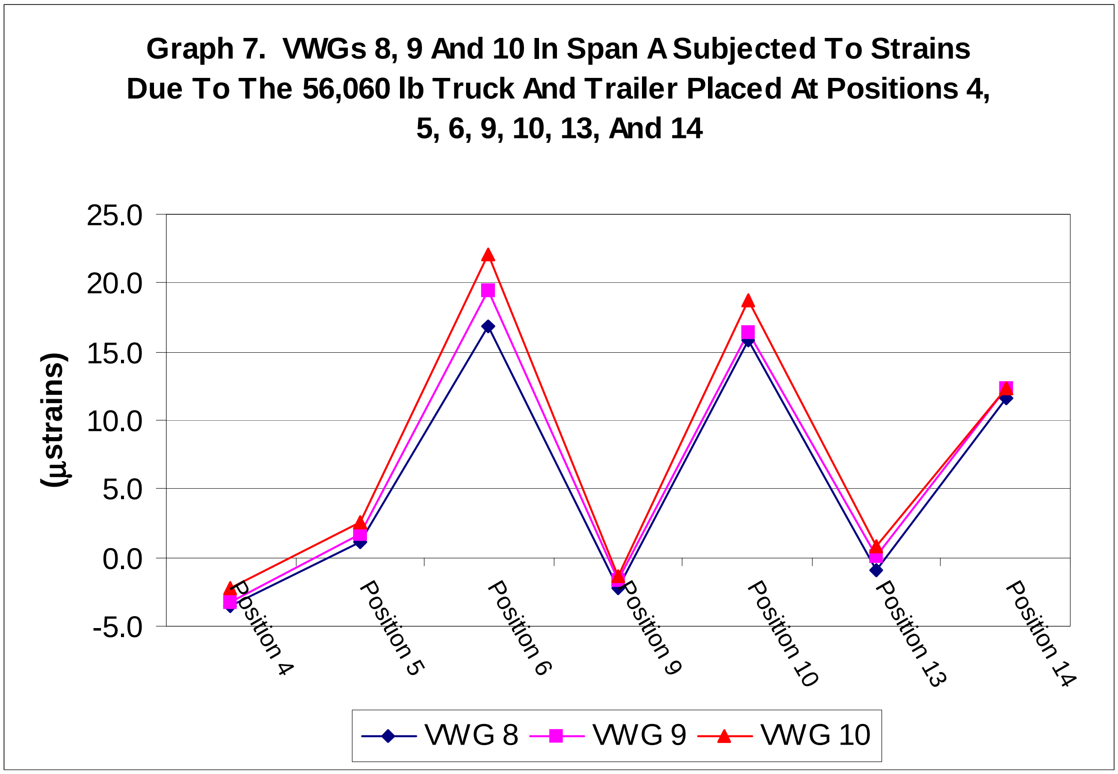
Graph 7. VWGs 8, 9 And 10 In Span A Subjected To Strains Due To The 56,060 lb Truck And Trailer Placed At Positions 4, 5, 6, 9, 10, 13, And 14
(µstrains)
25.0
20.0
15.0
10.0
5.0
0.0
-5.0
Position 4
Position 5
Position 6
Position 9
Position 10
Position 13
Position 14
VWG 8
VWG 9
VWG 10

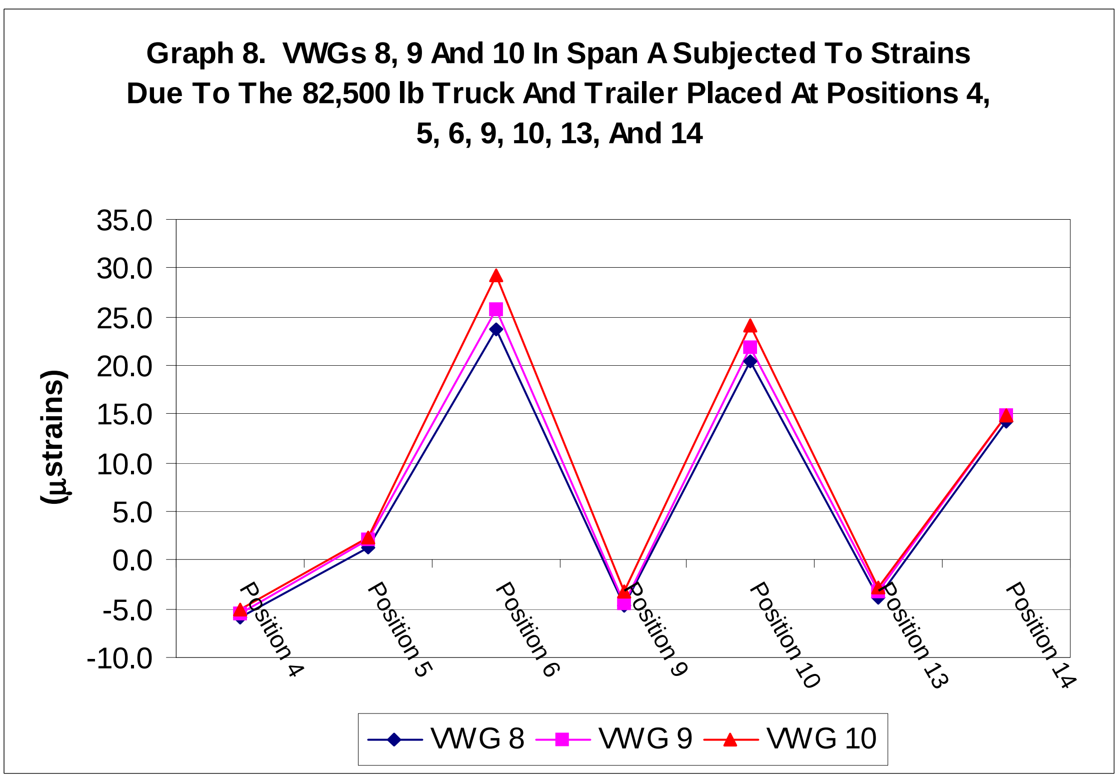
Graph 8. VWGs 8, 9 And 10 In Span A Subjected To Strains Due To The 82,500 lb Truck And Trailer Placed At Positions 4, 5, 6, 9, 10, 13, And 14
(µstrains)
35.0
30.0
25.0
20.0
15.0
10.0
5.0
0.0
-5.0
-10.0
Position 4
Position 5
Position 6
Position 9
Position 10
Position 13
Position 14
VWG 8
VWG 9
VWG 10

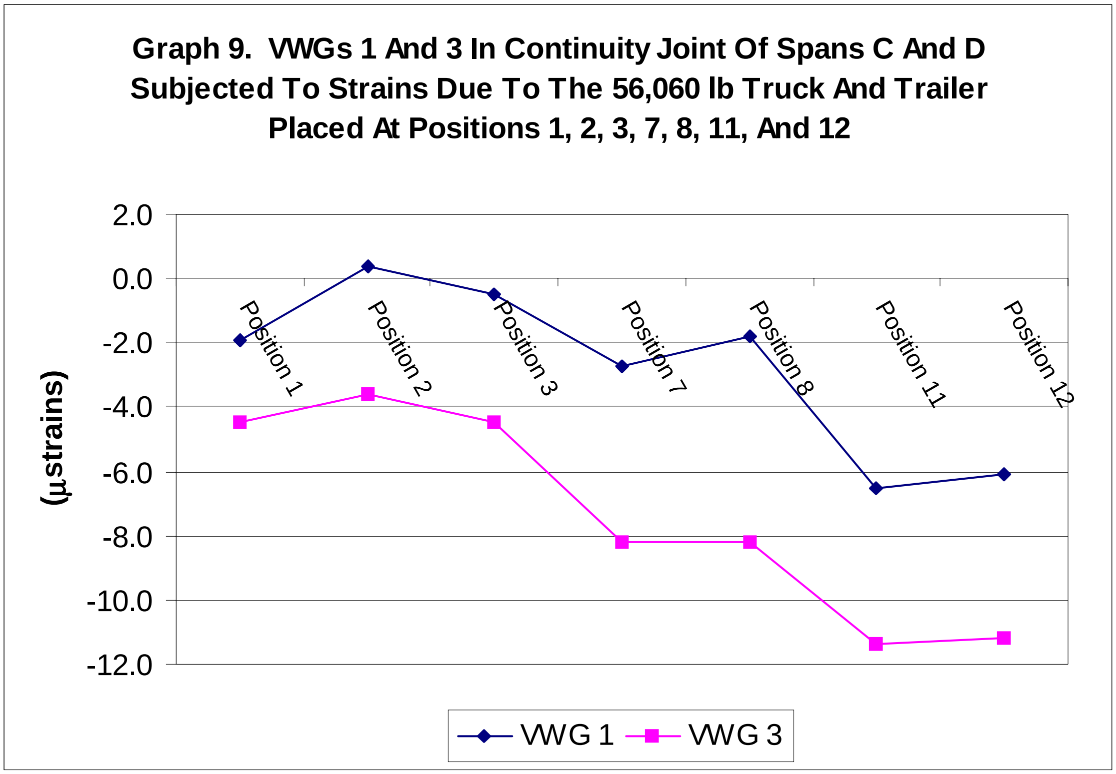

Graph 9. VWGs 1 And 3 In Continuity Joint Of Spans C And D Subjected To Strains Due To The 56,060 lb Truck And Trailer Placed At Positions 1, 2, 3, 7, 8, 11, And 12
2.0
0.0
-2.0
-4.0
-6.0
-8.0
-10.0
-12.0
(µstrains)
Position 1
Position 2
Position 3
Position 7
Position 8
Position 11
Position 12
VWG 1
VWG 3

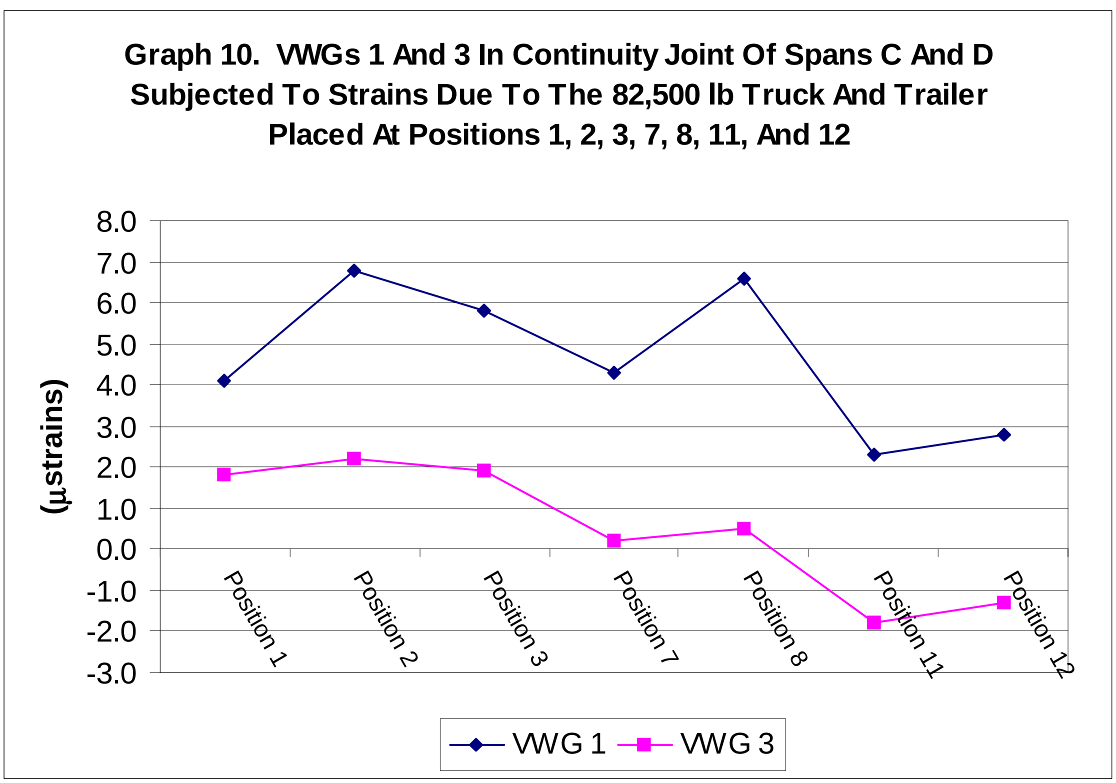

Graph 10. VWGs 1 And 3 In Continuity Joint Of Spans C And D Subjected To Strains Due To The 82,500 lb Truck And Trailer Placed At Positions 1, 2, 3, 7, 8, 11, And 12
8.0
7.0
6.0
5.0
4.0
3.0
2.0
1.0
0.0
-1.0
-2.0
-3.0
(µstrains)
Position 1
Position 2
Position 3
Position 7
Position 8
Position 11
Position 12
VWG 1
VWG 3

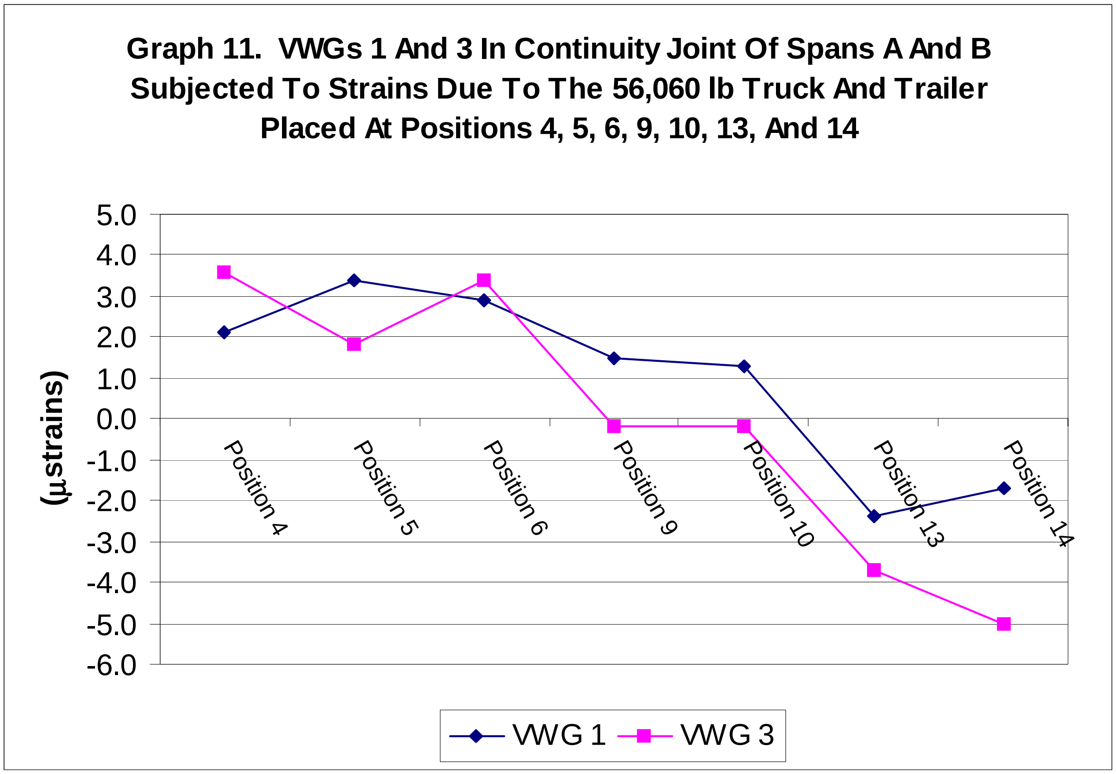
Graph 11. VWGs 1 And 3 In Continuity Joint Of Spans A And B Subjected To Strains Due To The 56,060 lb Truck And Trailer Placed At Positions 4, 5, 6, 9, 10, 13, And 14
(µstrains)
5.0
4.0
3.0
2.0
1.0
0.0
-1.0
-2.0
-3.0
-4.0
-5.0
-6.0
Position 4
Position 5
Position 6
Position 9
Position 10
Position 13
Position 14
VWG 1
VWG 3

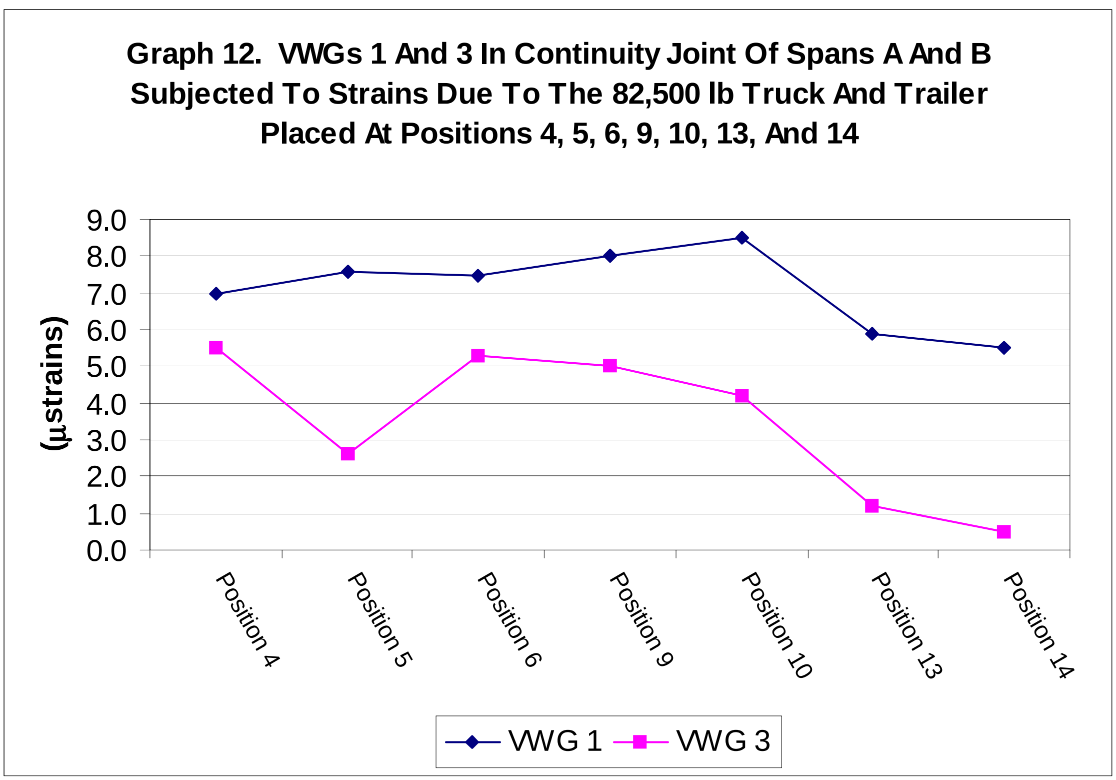
Graph 12. VWGs 1 And 3 In Continuity Joint Of Spans A And B Subjected To Strains Due To The 82,500 lb Truck And Trailer Placed At Positions 4, 5, 6, 9, 10, 13, And 14
(µstrains)
9.0
8.0
7.0
6.0
5.0
4.0
3.0
2.0
1.0
0.0
Position 4
Position 5
Position 6
Position 9
Position 10
Position 13
Position 14
VWG 1
VWG 3

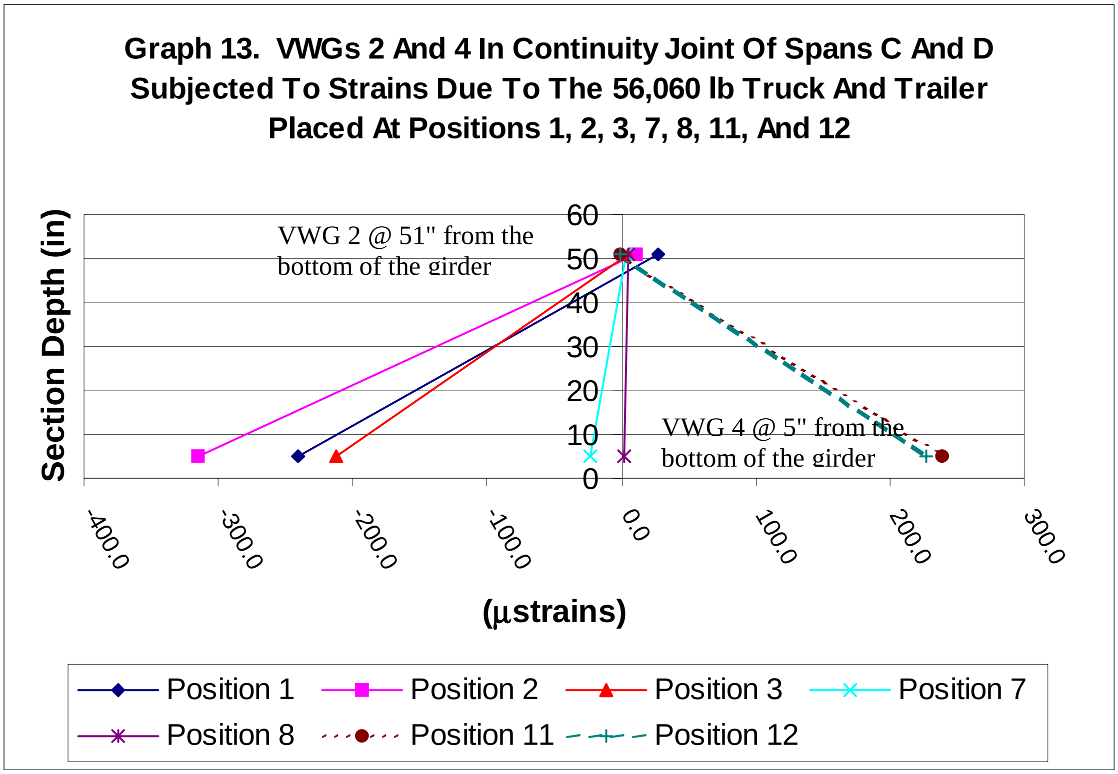
Graph 13. VWGs 2 And 4 In Continuity Joint Of Spans C And D Subjected To Strains Due To The 56,060 lb Truck And Trailer Placed At Positions 1, 2, 3, 7, 8, 11, And 12
VWG 2 @ 51" from the bottom of the girder
VWG 4 @ 5" from the bottom of the girder
Section Depth (in)
(µstrains)
Position 1
Position 2
Position 3
Position 7
Position 8
Position 11
Position 12

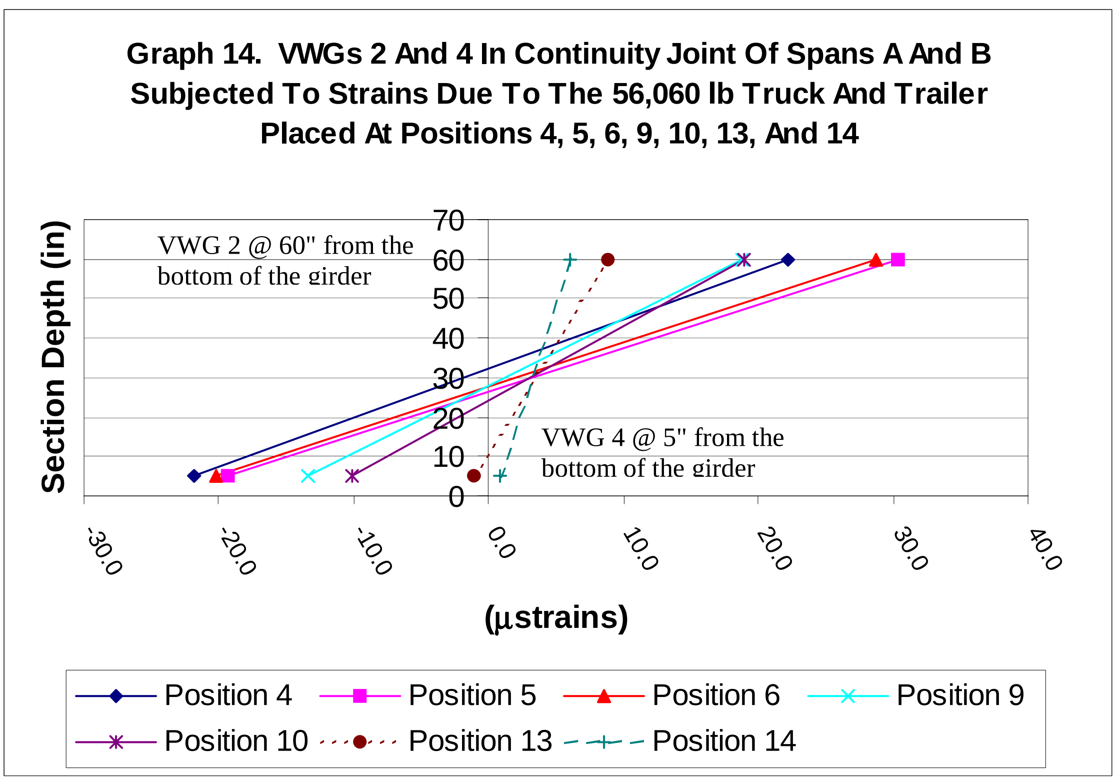
Graph 14. VWGs 2 And 4 In Continuity Joint Of Spans A And B Subjected To Strains Due To The 56,060 lb Truck And Trailer Placed At Positions 4, 5, 6, 9, 10, 13, And 14
VWG 2 @ 60" from the bottom of the girder
VWG 4 @ 5" from the bottom of the girder
Section Depth (in)
(µstrains)
Position 4
Position 5
Position 6
Position 9
Position 10
Position 13
Position 14

Graph 15. VWGs 2 And 4 In Continuity Joint Of Spans A And B Subjected To Strains Due To The 82,500 lb Truck And Trailer Placed At Positions 4, 5, 6, 9, 10, 13, And 14

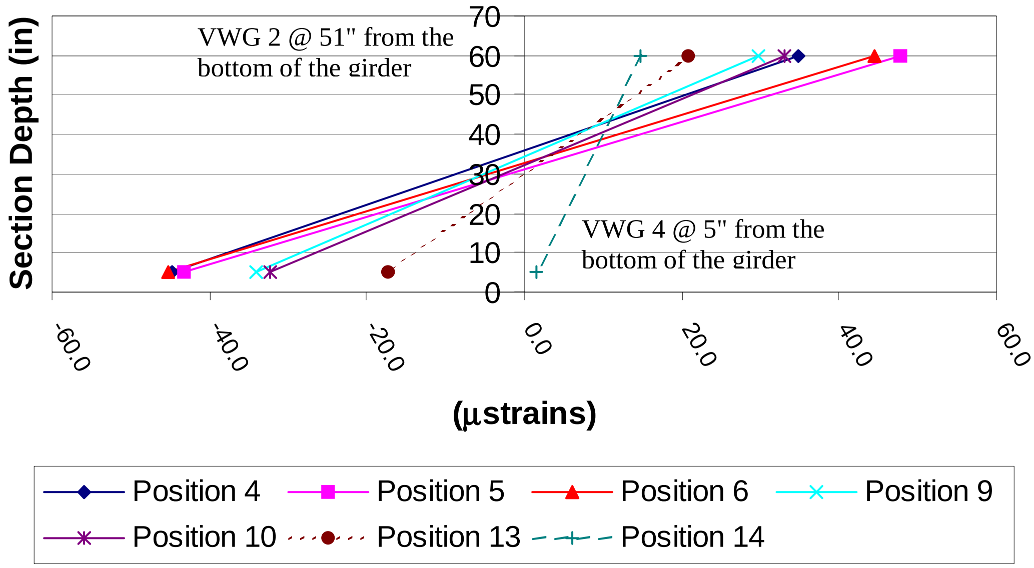

Graph 16. String Potentiometer Attached At Mid-Span Of Span D Subjected To Deflections Due To The 56,060 lb And 82,500 lb Truck And Trailer Placed At Positions 1, 2, 3, 7, 8, 11, And 12

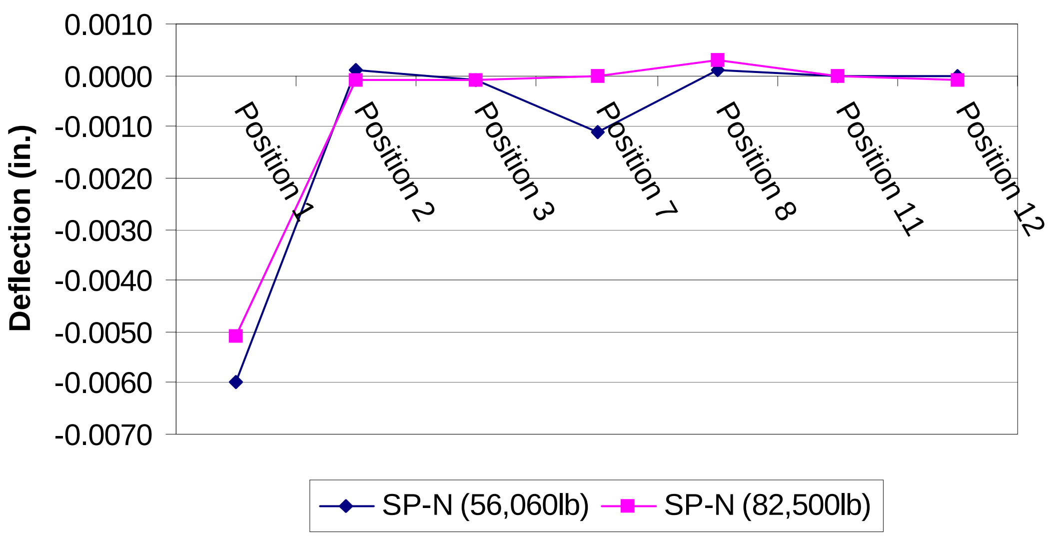

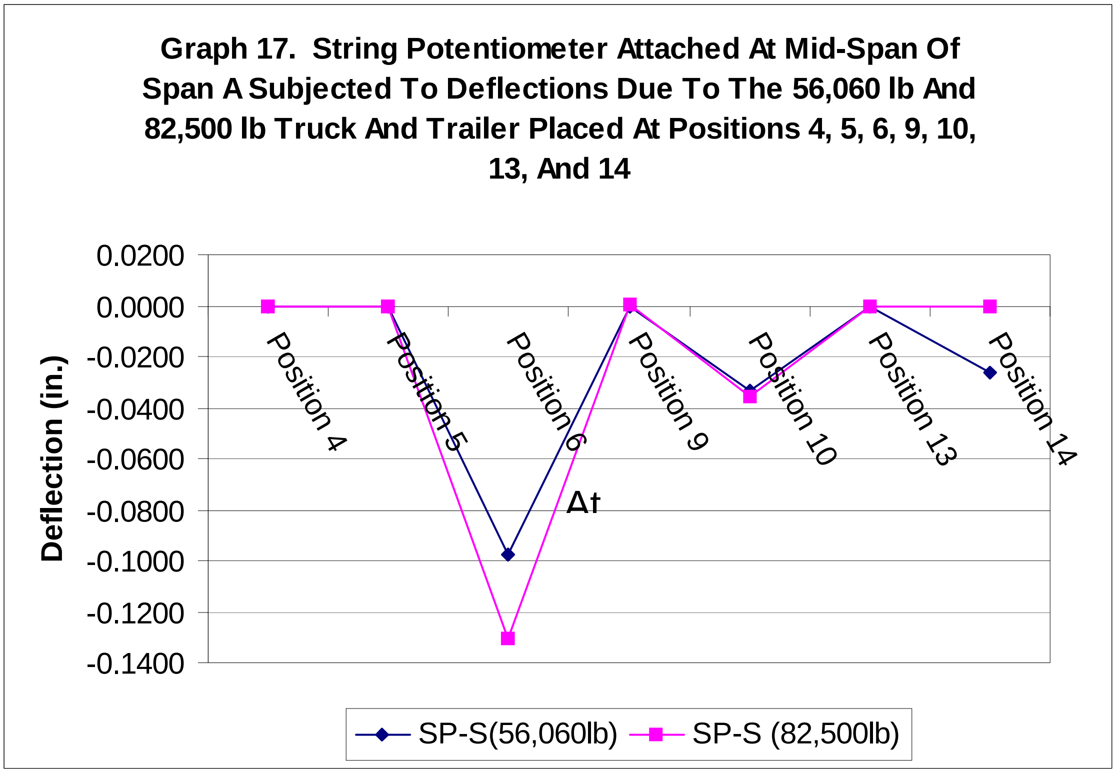
Graph 17. String Potentiometer Attached At Mid-Span Of Span A Subjected To Deflections Due To The 56,060 lb And 82,500 lb Truck And Trailer Placed At Positions 4, 5, 6, 9, 10, 13, And 14
Deflection (in.)
0.0200
0.0000
-0.0200
-0.0400
-0.0600
-0.0800
-0.1000
-0.1200
-0.1400
Position 4
Position 5
Position 6
Position 9
Position 10
Position 13
Position 14
Δt
SP-S(56,060lb)
SP-S (82,500lb)

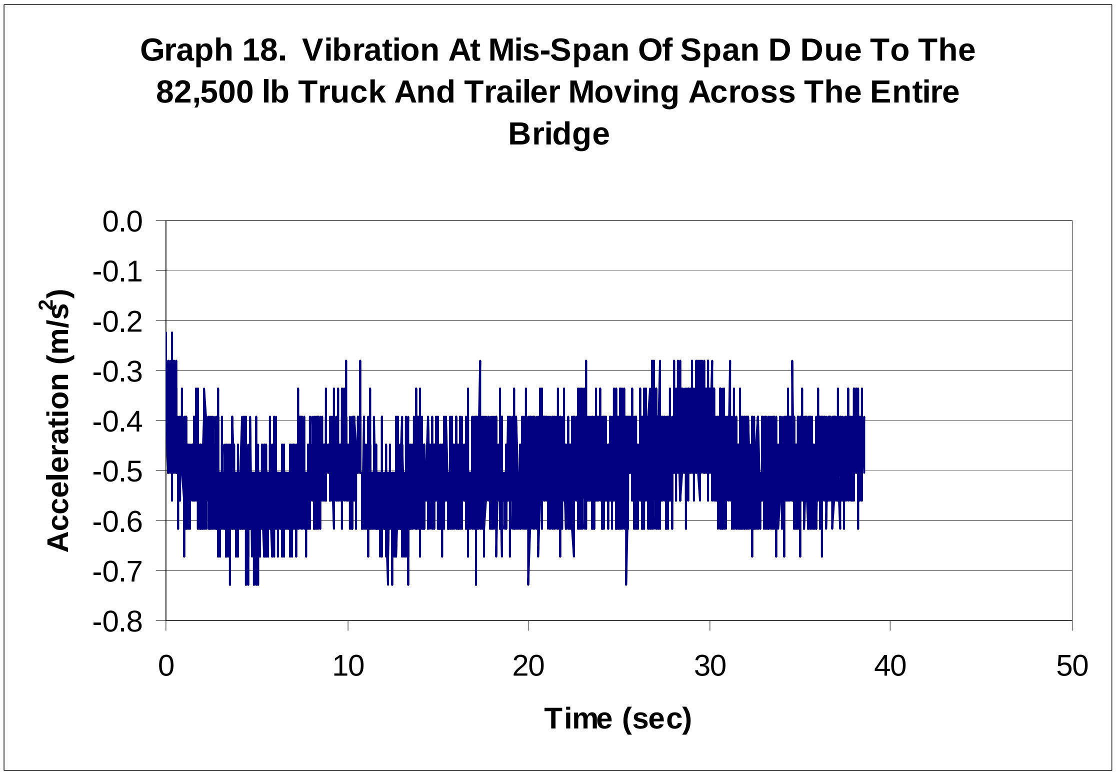
Graph 18. Vibration At Mis-Span Of Span D Due To The 82,500 lb Truck And Trailer Moving Across The Entire Bridge
Acceleration (m/s2)
0.0
-0.1
-0.2
-0.3
-0.4
-0.5
-0.6
-0.7
-0.8
0
10
20
30
40
50
Time (sec)

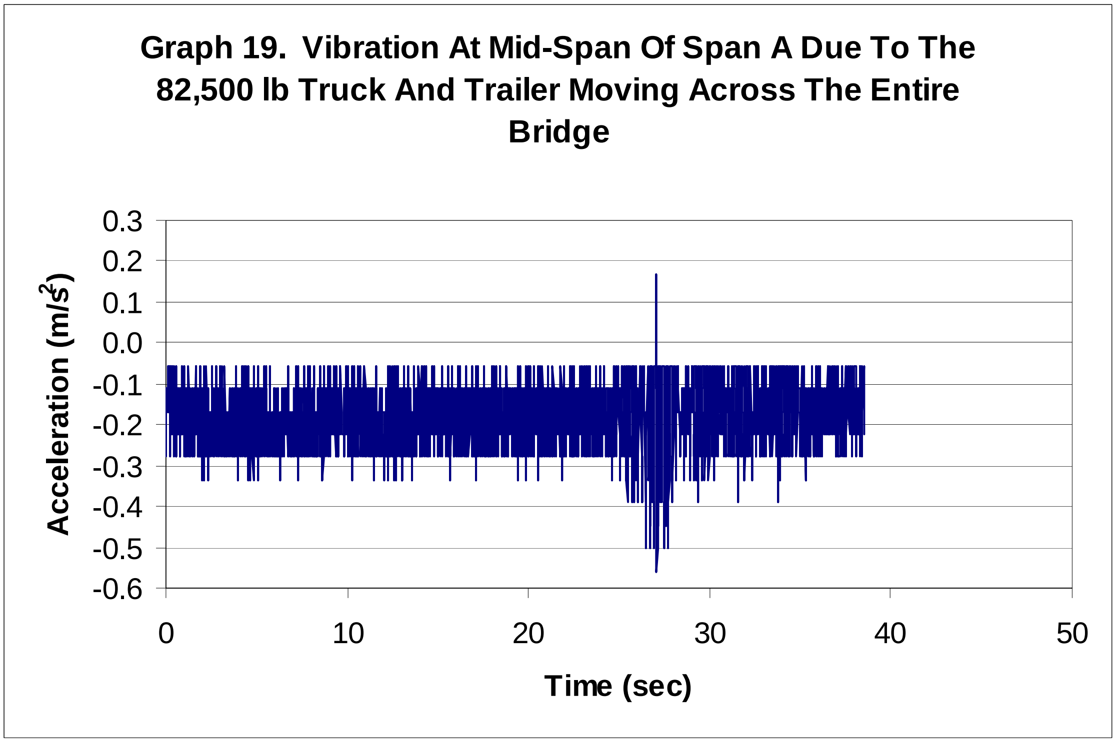
Graph 19. Vibration At Mid-Span Of Span A Due To The 82,500 lb Truck And Trailer Moving Across The Entire Bridge
Acceleration (m/s²)
0.3
0.2
0.1
0.0
-0.1
-0.2
-0.3
-0.4
-0.5
-0.6
0
10
20
30
40
50
Time (sec)

Appendix B: First Live Load Test Actual and Calculated Results

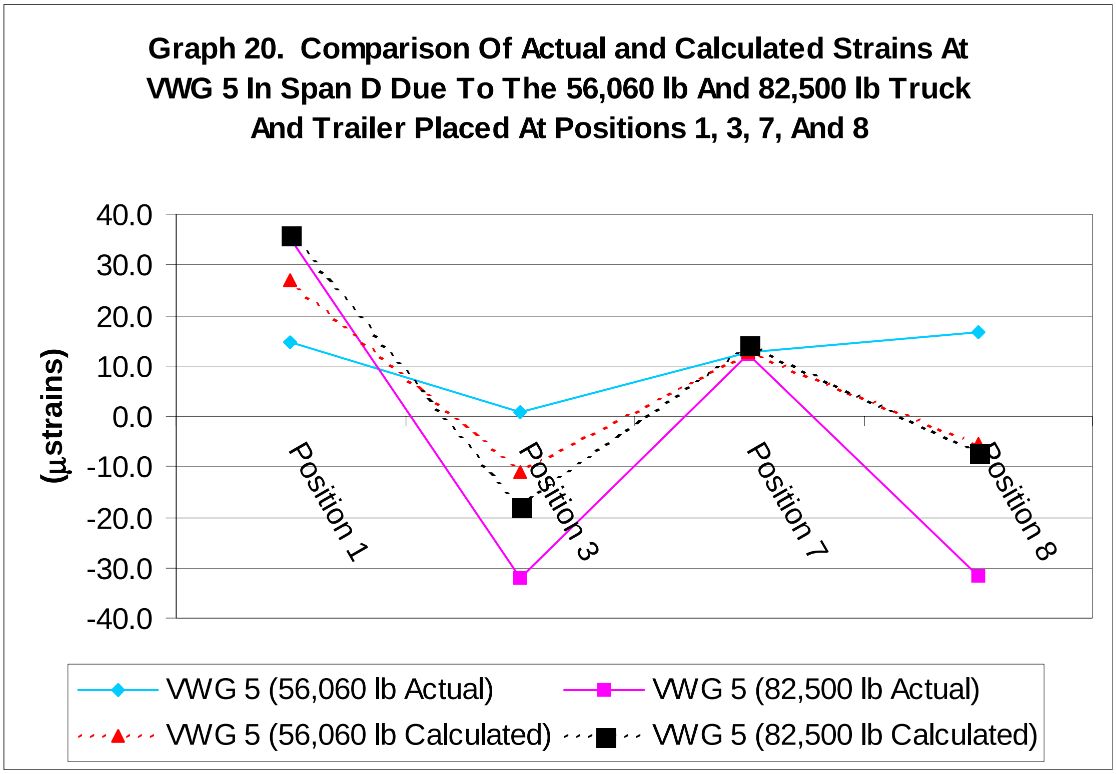
Graph 20. Comparison Of Actual and Calculated Strains At VWG 5 In Span D Due To The 56,060 lb And 82,500 lb Truck And Trailer Placed At Positions 1, 3, 7, And 8
40.0
30.0
20.0
10.0
0.0
-10.0
-20.0
-30.0
-40.0
(µstrains)
Position 1
Position 3
Position 7
Position 8
VWG 5 (56,060 lb Actual)
VWG 5 (82,500 lb Actual)
VWG 5 (56,060 lb Calculated)
VWG 5 (82,500 lb Calculated)

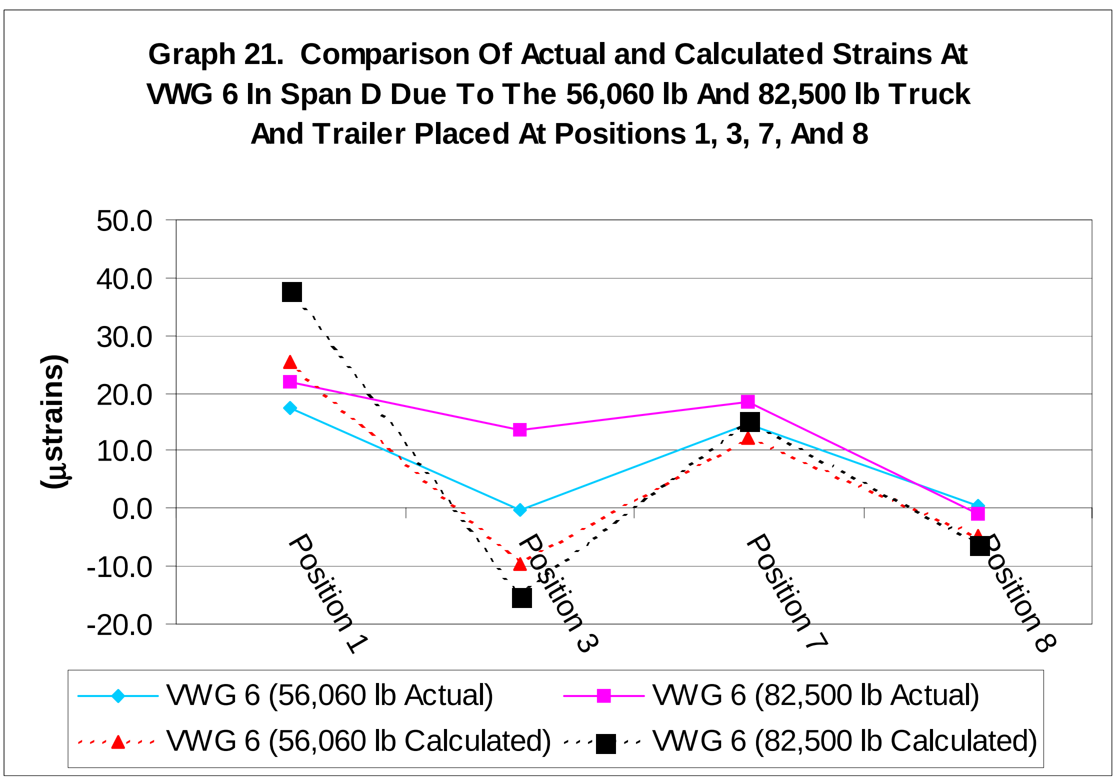
Graph 21. Comparison Of Actual and Calculated Strains At VWG 6 In Span D Due To The 56,060 lb And 82,500 lb Truck And Trailer Placed At Positions 1, 3, 7, And 8
50.0
40.0
30.0
20.0
10.0
0.0
-10.0
-20.0
(µstrains)
Position 1
Position 3
Position 7
Position 8
VWG 6 (56,060 lb Actual)
VWG 6 (82,500 lb Actual)
VWG 6 (56,060 lb Calculated)
VWG 6 (82,500 lb Calculated)

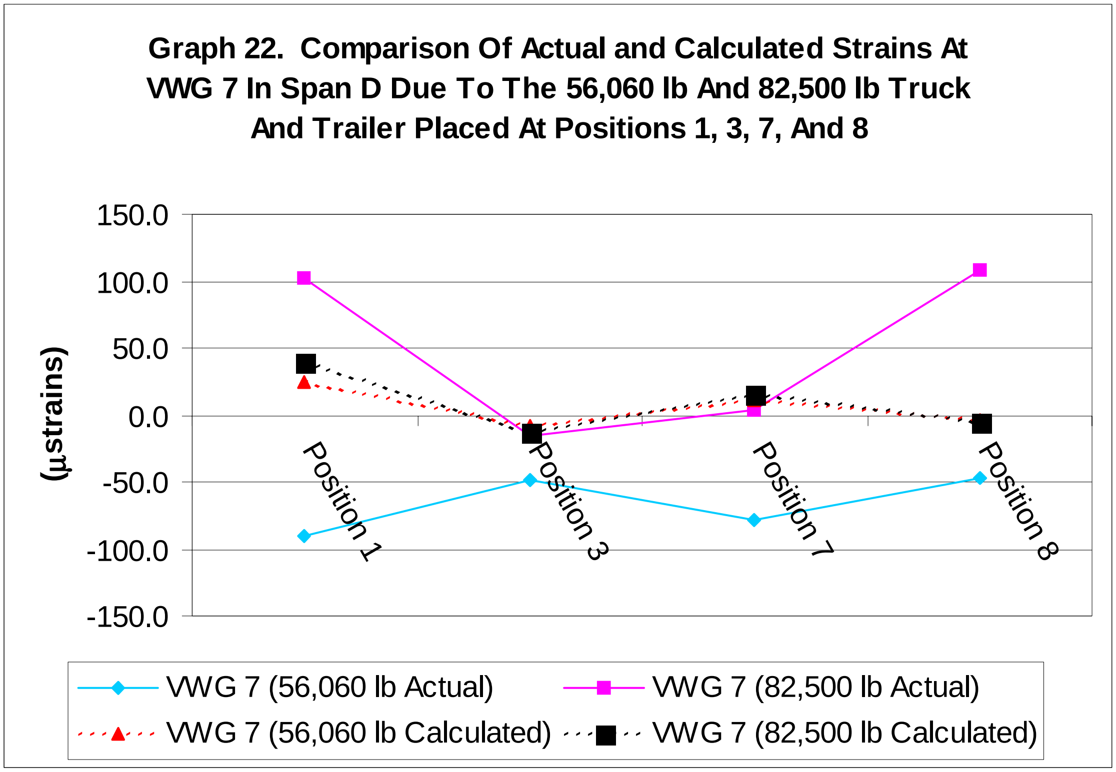
Graph 22. Comparison Of Actual and Calculated Strains At VWG 7 In Span D Due To The 56,060 lb And 82,500 lb Truck And Trailer Placed At Positions 1, 3, 7, And 8
150.0
100.0
50.0
0.0
-50.0
-100.0
-150.0
(µstrains)
Position 1
Position 3
Position 7
Position 8
VWG 7 (56,060 lb Actual)
VWG 7 (82,500 lb Actual)
VWG 7 (56,060 lb Calculated)
VWG 7 (82,500 lb Calculated)

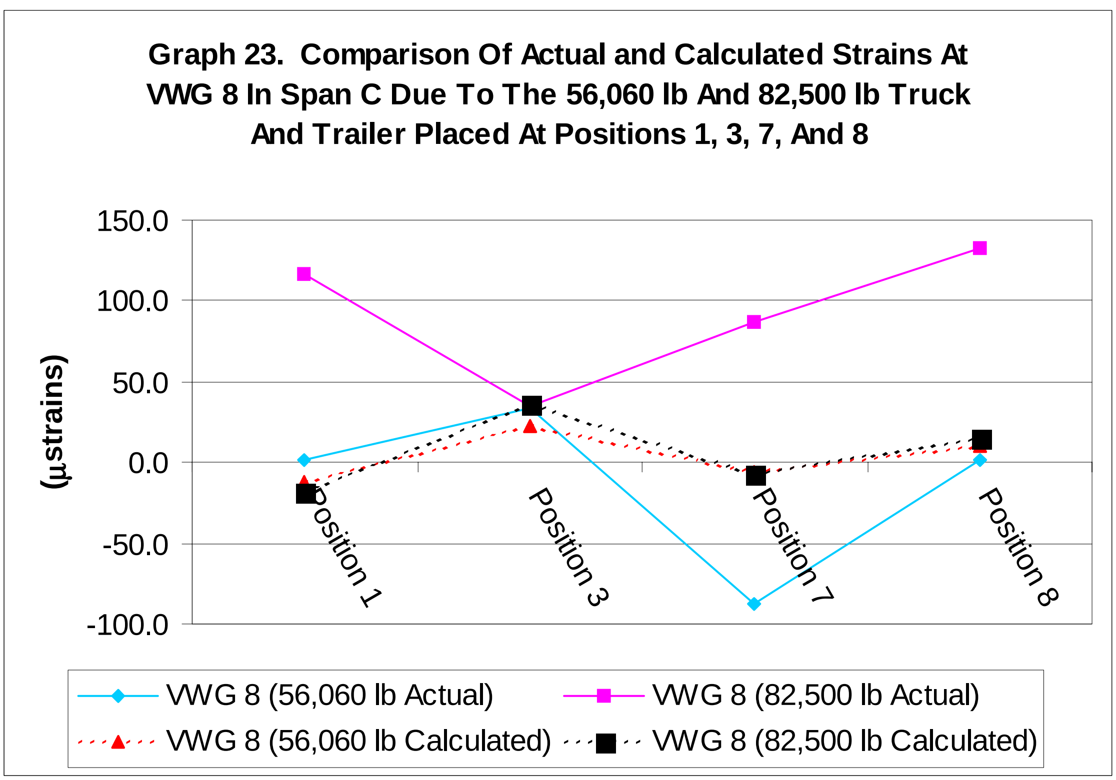
Graph 23. Comparison Of Actual and Calculated Strains At VWG 8 In Span C Due To The 56,060 lb And 82,500 lb Truck And Trailer Placed At Positions 1, 3, 7, And 8
150.0
100.0
50.0
0.0
-50.0
-100.0
(µstrains)
Position 1
Position 3
Position 7
Position 8
VWG 8 (56,060 lb Actual)
VWG 8 (82,500 lb Actual)
VWG 8 (56,060 lb Calculated)
VWG 8 (82,500 lb Calculated)

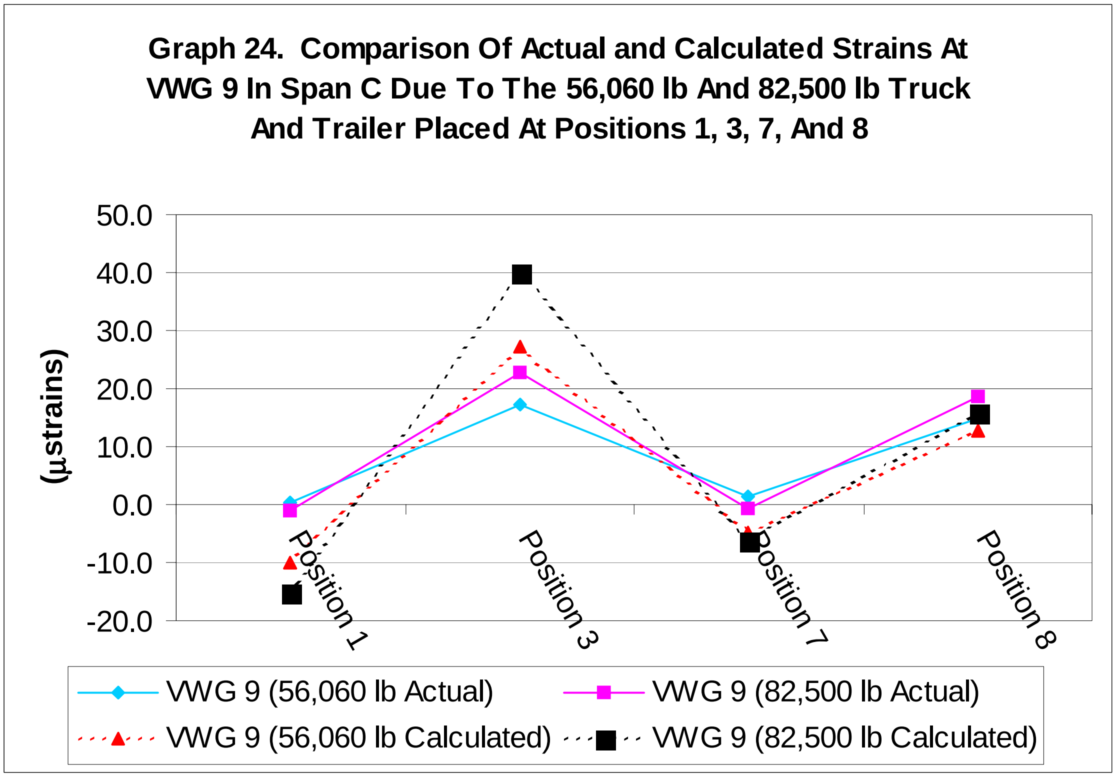
Graph 24. Comparison Of Actual and Calculated Strains At VWG 9 In Span C Due To The 56,060 lb And 82,500 lb Truck And Trailer Placed At Positions 1, 3, 7, And 8
50.0
40.0
30.0
20.0
10.0
0.0
-10.0
-20.0
(µstrains)
Position 1
Position 3
Position 7
Position 8
VWG 9 (56,060 lb Actual)
VWG 9 (82,500 lb Actual)
VWG 9 (56,060 lb Calculated)
VWG 9 (82,500 lb Calculated)

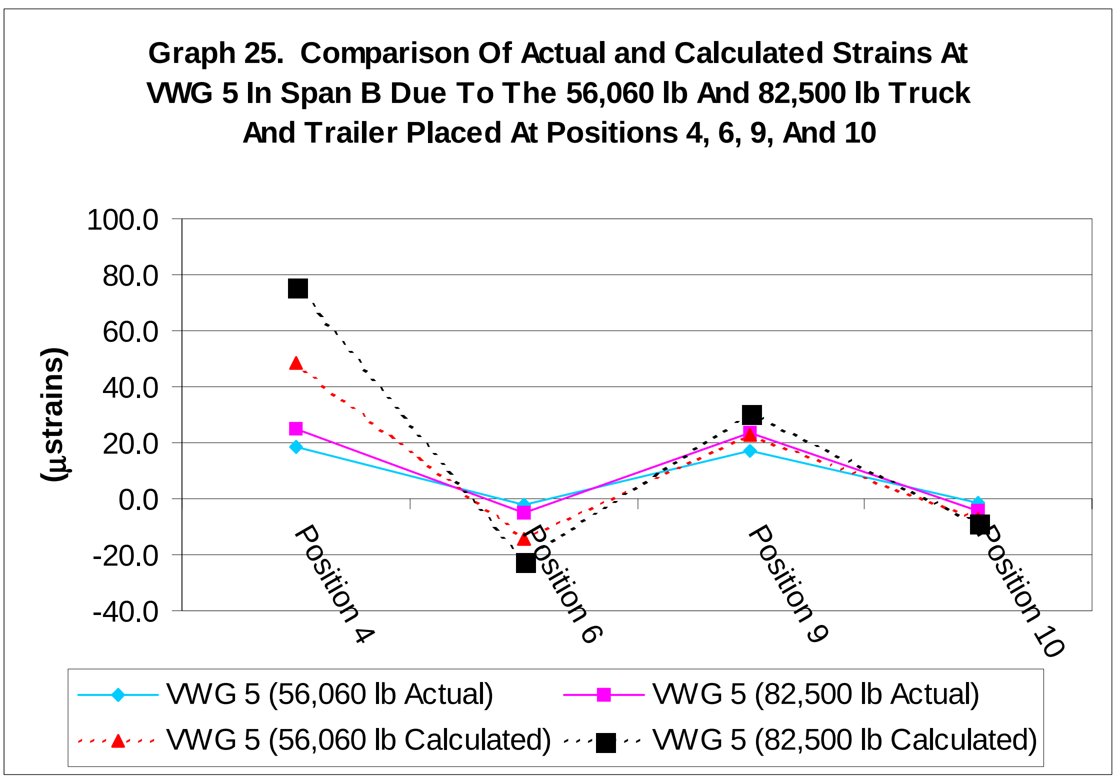
Graph 25. Comparison Of Actual and Calculated Strains At VWG 5 In Span B Due To The 56,060 lb And 82,500 lb Truck And Trailer Placed At Positions 4, 6, 9, And 10
100.0
80.0
60.0
40.0
20.0
0.0
-20.0
-40.0
(µstrains)
Position 4
Position 6
Position 9
Position 10
VWG 5 (56,060 lb Actual)
VWG 5 (82,500 lb Actual)
VWG 5 (56,060 lb Calculated)
VWG 5 (82,500 lb Calculated)

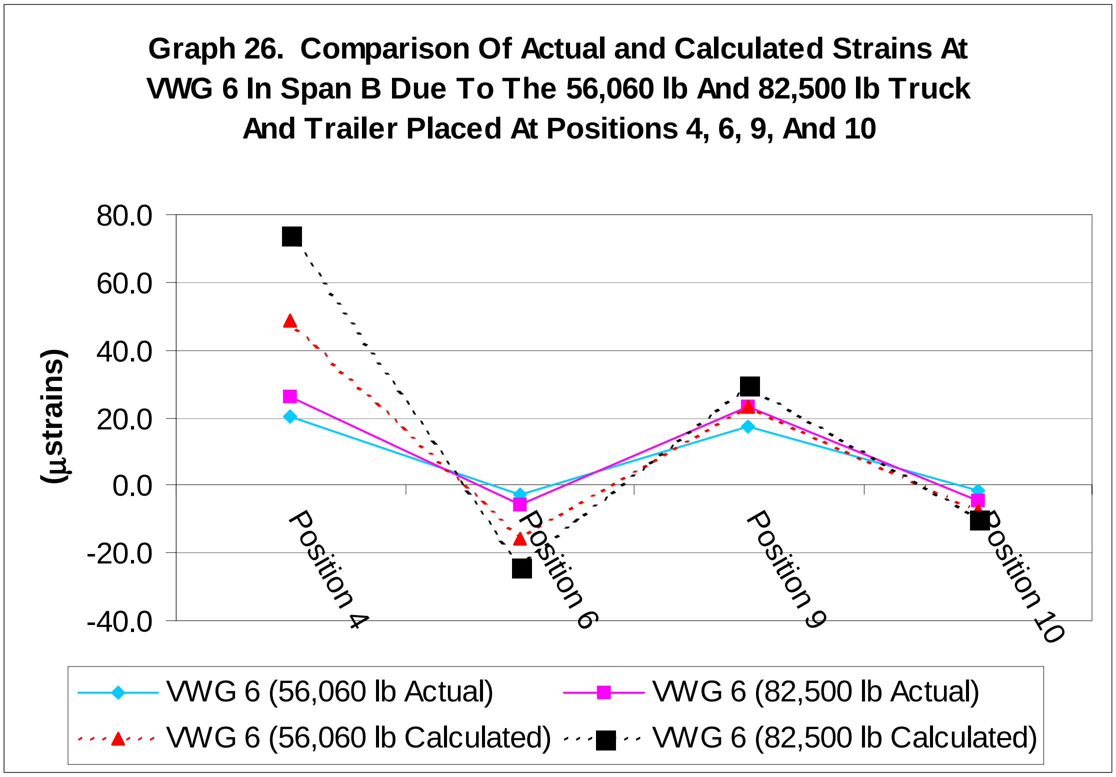
Graph 26. Comparison Of Actual and Calculated Strains At
VWG 6 In Span B Due To The 56,060 lb And 82,500 lb Truck
And Trailer Placed At Positions 4, 6, 9, And 10
80.0
60.0
40.0
20.0
0.0
-20.0
-40.0
(µstrains)
Position 4
Position 6
Position 9
Position 10
VWG 6 (56,060 lb Actual)
VWG 6 (82,500 lb Actual)
VWG 6 (56,060 lb Calculated)
VWG 6 (82,500 lb Calculated)

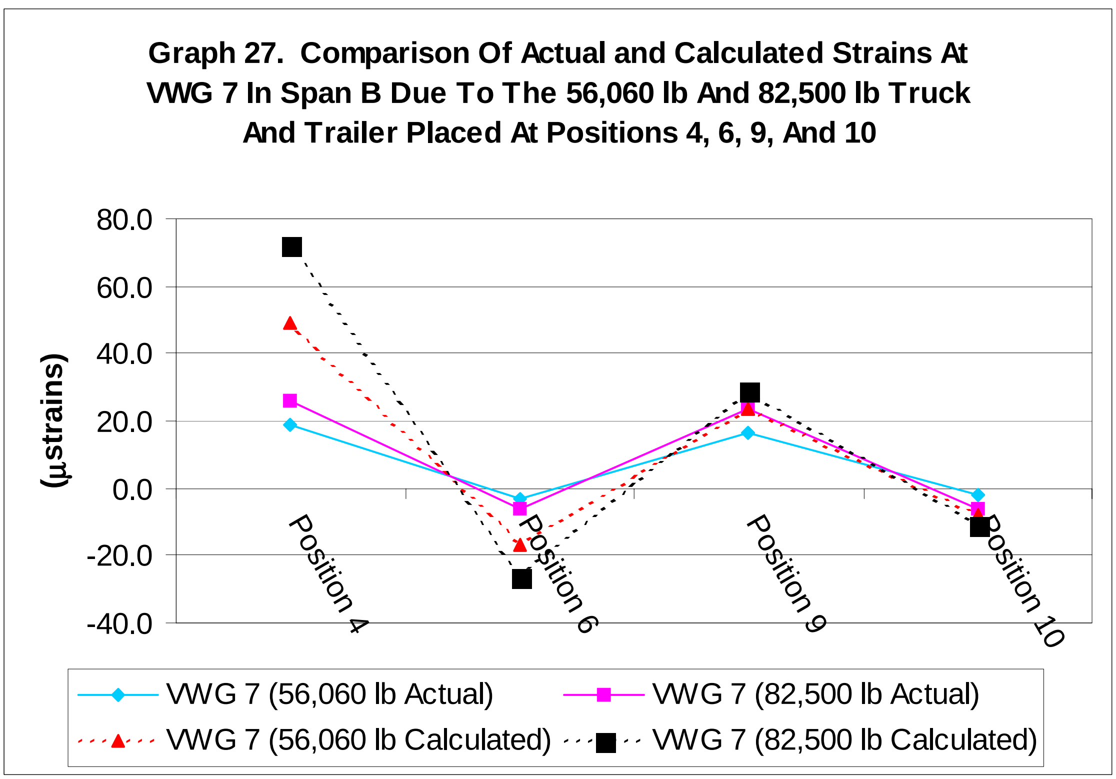
Graph 27. Comparison Of Actual and Calculated Strains At
VWG 7 In Span B Due To The 56,060 lb And 82,500 lb Truck
And Trailer Placed At Positions 4, 6, 9, And 10
80.0
60.0
40.0
20.0
0.0
-20.0
-40.0
(µstrains)
Position 4
Position 6
Position 9
Position 10
VWG 7 (56,060 lb Actual)
VWG 7 (82,500 lb Actual)
VWG 7 (56,060 lb Calculated)
VWG 7 (82,500 lb Calculated)

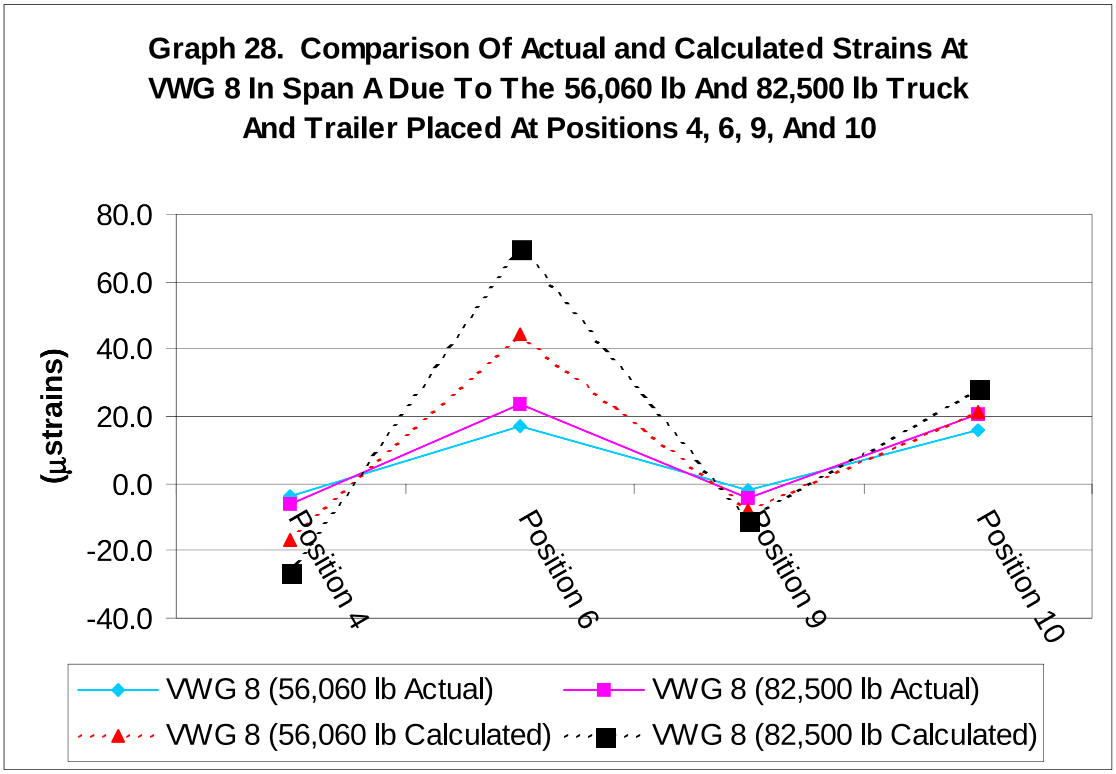
Graph 28. Comparison Of Actual and Calculated Strains At VWG 8 In Span A Due To The 56,060 lb And 82,500 lb Truck And Trailer Placed At Positions 4, 6, 9, And 10
(µstrains)
80.0
60.0
40.0
20.0
0.0
-20.0
-40.0
Position 4
Position 6
Position 9
Position 10
VWG 8 (56,060 lb Actual)
VWG 8 (82,500 lb Actual)
VWG 8 (56,060 lb Calculated)
VWG 8 (82,500 lb Calculated)

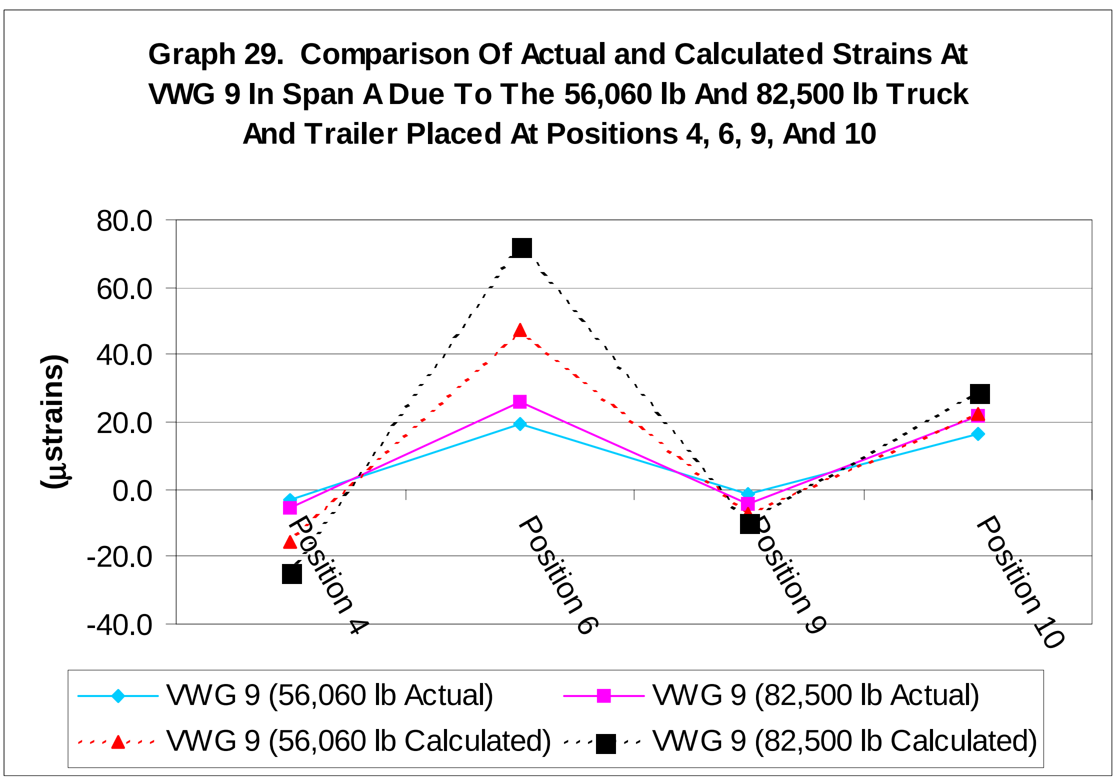
Graph 29. Comparison Of Actual and Calculated Strains At VWG 9 In Span A Due To The 56,060 lb And 82,500 lb Truck And Trailer Placed At Positions 4, 6, 9, And 10
(µstrains)
80.0
60.0
40.0
20.0
0.0
-20.0
-40.0
Position 4
Position 6
Position 9
Position 10
VWG 9 (56,060 lb Actual)
VWG 9 (82,500 lb Actual)
VWG 9 (56,060 lb Calculated)
VWG 9 (82,500 lb Calculated)

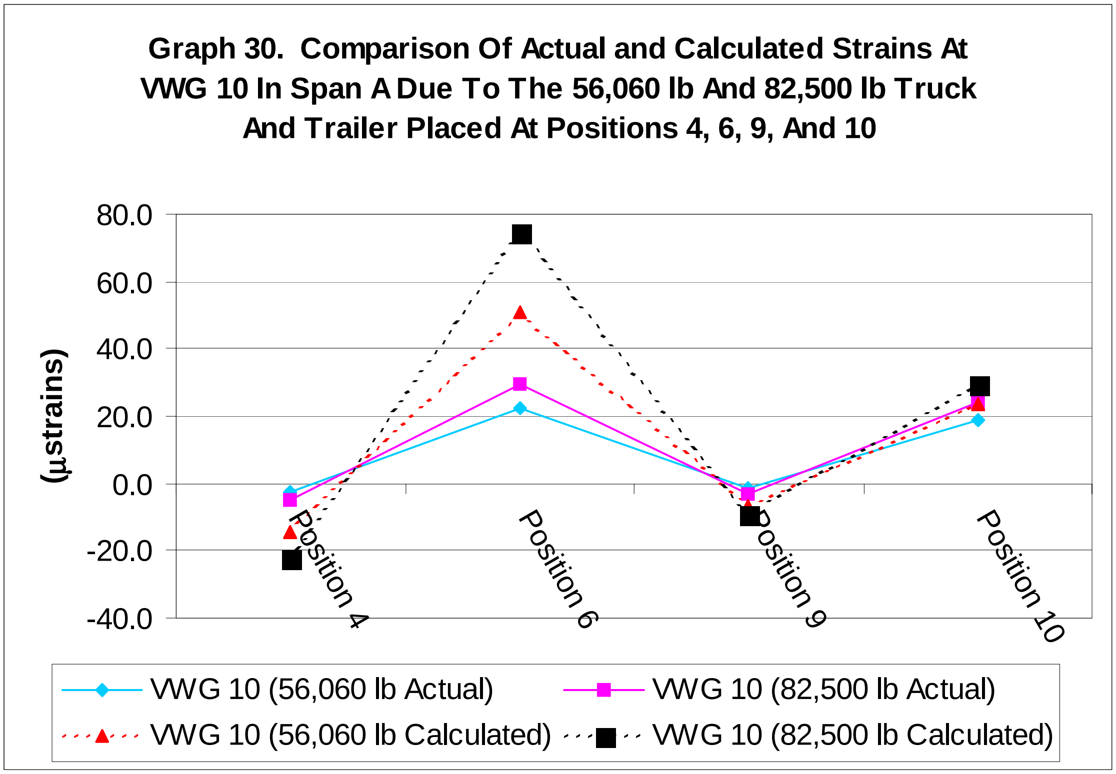
Graph 30. Comparison Of Actual and Calculated Strains At VWG 10 In Span A Due To The 56,060 lb And 82,500 lb Truck And Trailer Placed At Positions 4, 6, 9, And 10
(µstrains)
80.0
60.0
40.0
20.0
0.0
-20.0
-40.0
Position 4
Position 6
Position 9
Position 10
VWG 10 (56,060 lb Actual)
VWG 10 (82,500 lb Actual)
VWG 10 (56,060 lb Calculated)
VWG 10 (82,500 lb Calculated)

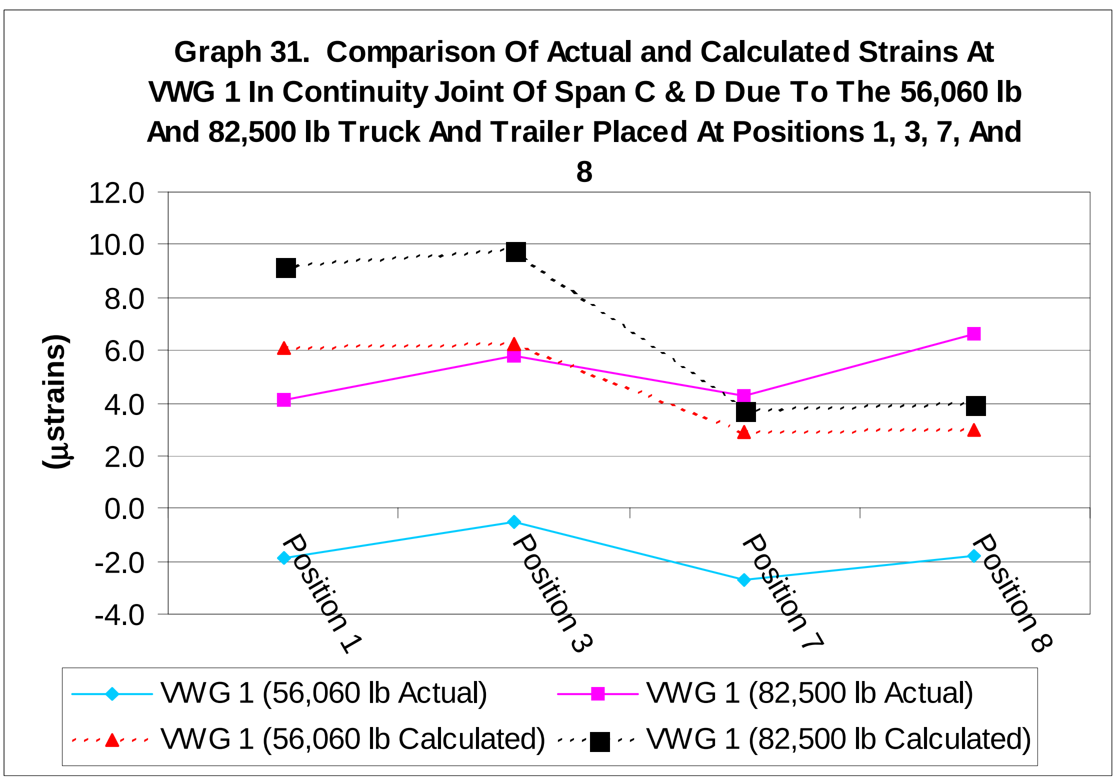
Graph 31. Comparison Of Actual and Calculated Strains At VWG 1 In Continuity Joint Of Span C & D Due To The 56,060 lb And 82,500 lb Truck And Trailer Placed At Positions 1, 3, 7, And 8
(µstrains)
12.0
10.0
8.0
6.0
4.0
2.0
0.0
-2.0
-4.0
Position 1
Position 3
Position 7
Position 8
VWG 1 (56,060 lb Actual)
VWG 1 (82,500 lb Actual)
VWG 1 (56,060 lb Calculated)
VWG 1 (82,500 lb Calculated)

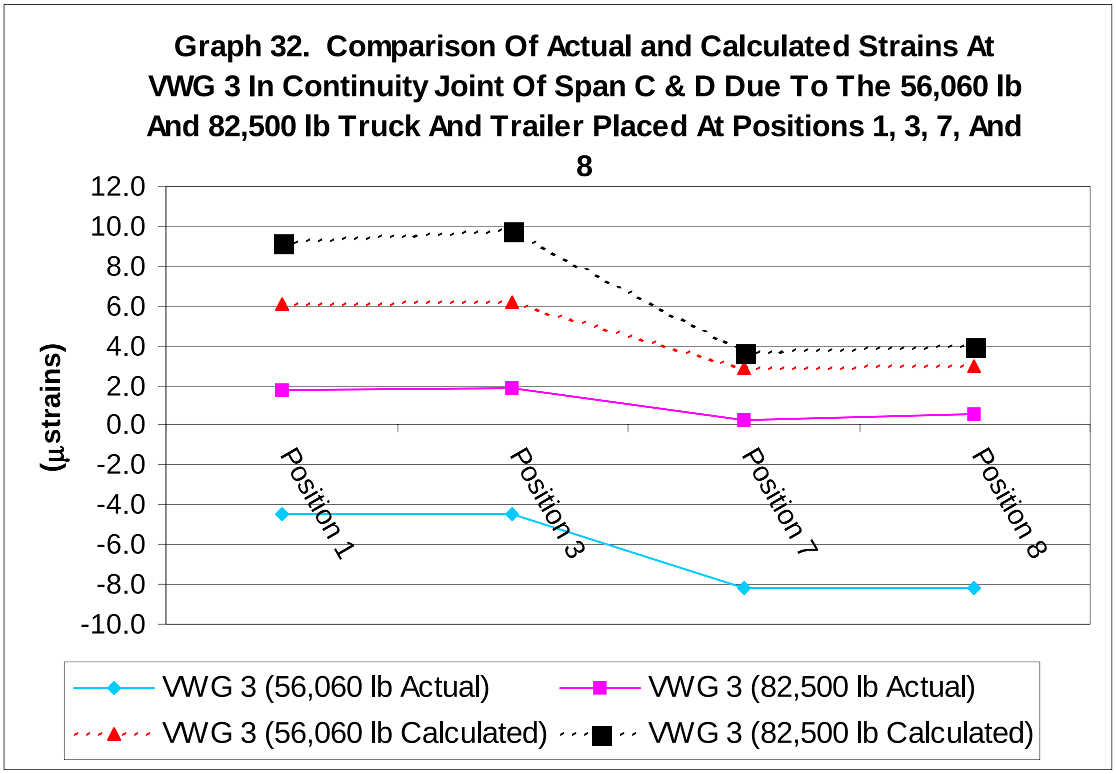
Graph 32. Comparison Of Actual and Calculated Strains At VWG 3 In Continuity Joint Of Span C & D Due To The 56,060 lb And 82,500 lb Truck And Trailer Placed At Positions 1, 3, 7, And 8
(µstrains)
12.0
10.0
8.0
6.0
4.0
2.0
0.0
-2.0
-4.0
-6.0
-8.0
-10.0
Position 1
Position 3
Position 7
Position 8
VWG 3 (56,060 lb Actual)
VWG 3 (82,500 lb Actual)
VWG 3 (56,060 lb Calculated)
VWG 3 (82,500 lb Calculated)

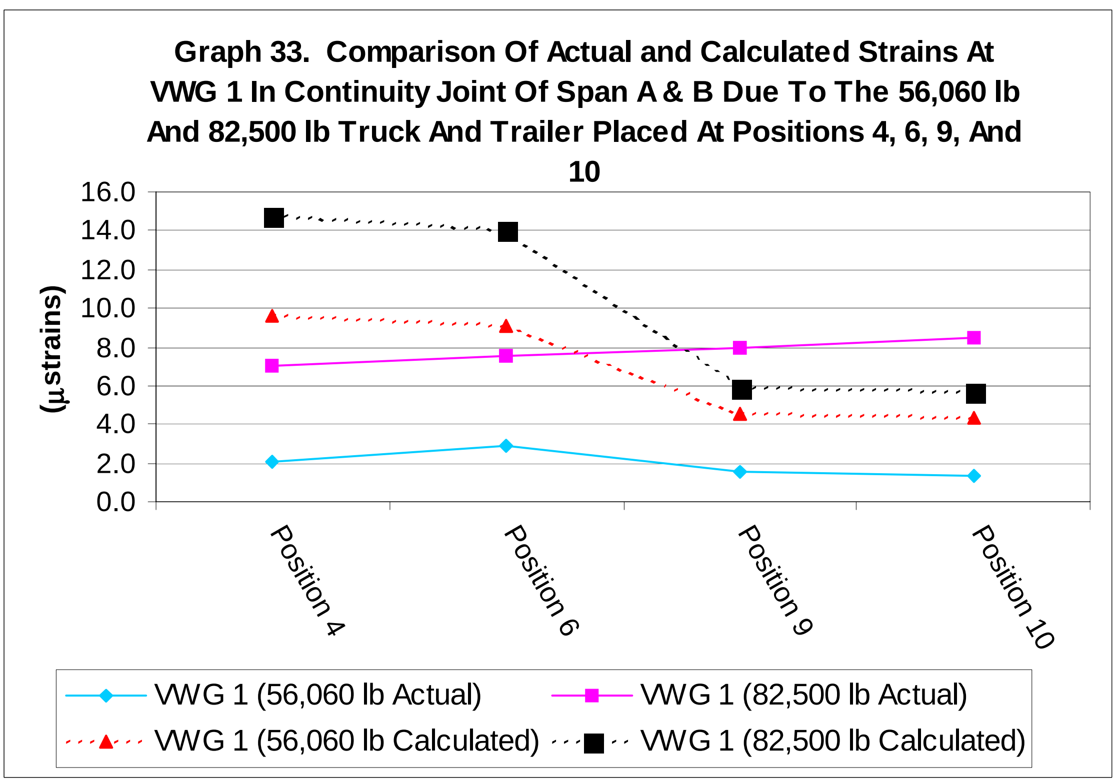
Graph 33. Comparison Of Actual and Calculated Strains At VWG 1 In Continuity Joint Of Span A & B Due To The 56,060 lb And 82,500 lb Truck And Trailer Placed At Positions 4, 6, 9, And 10
(µstrains)
16.0
14.0
12.0
10.0
8.0
6.0
4.0
2.0
0.0
Position 4
Position 6
Position 9
Position 10
VWG 1 (56,060 lb Actual)
VWG 1 (82,500 lb Actual)
VWG 1 (56,060 lb Calculated)
VWG 1 (82,500 lb Calculated)

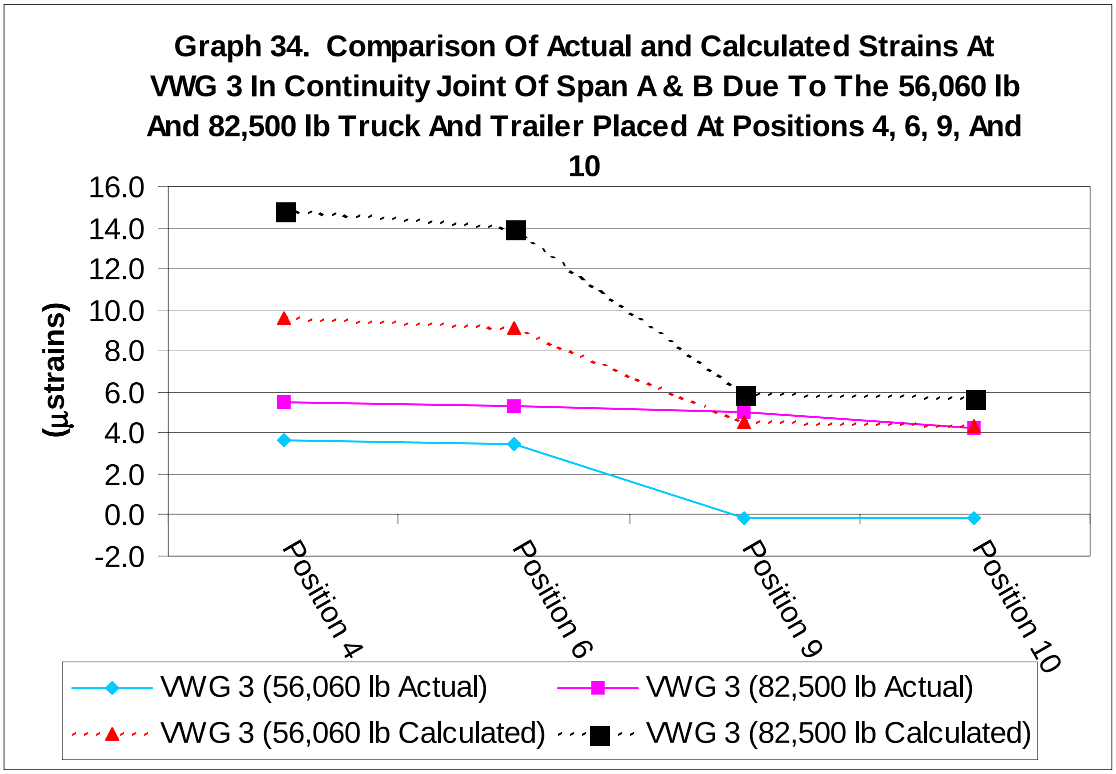
Graph 34. Comparison Of Actual and Calculated Strains At VWG 3 In Continuity Joint Of Span A & B Due To The 56,060 lb And 82,500 lb Truck And Trailer Placed At Positions 4, 6, 9, And 10
(µstrains)
16.0
14.0
12.0
10.0
8.0
6.0
4.0
2.0
0.0
-2.0
Position 4
Position 6
Position 9
Position 10
VWG 3 (56,060 lb Actual)
VWG 3 (82,500 lb Actual)
VWG 3 (56,060 lb Calculated)
VWG 3 (82,500 lb Calculated)

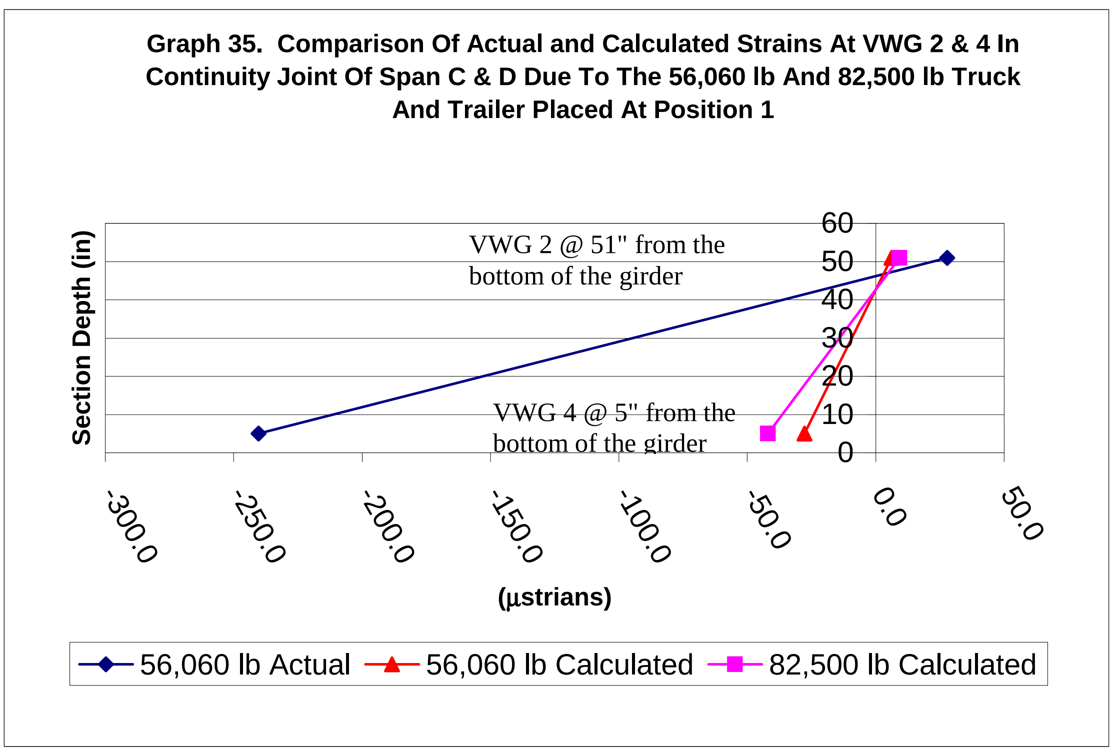
Graph 35. Comparison Of Actual and Calculated Strains At VWG 2 & 4 In Continuity Joint Of Span C & D Due To The 56,060 lb And 82,500 lb Truck And Trailer Placed At Position 1
Section Depth (in)
VWG 2 @ 51" from the bottom of the girder
VWG 4 @ 5" from the bottom of the girder
60
50
40
30
20
10
0
-300.0
-250.0
-200.0
-150.0
-100.0
-50.0
0.0
50.0
(µstrians)
56,060 lb Actual
56,060 lb Calculated
82,500 lb Calculated

Graph 36. Comparison Of Actual and Calculated Strains At VWG 2 & 4 In Continuity Joint Of Span C & D Due To The 56,060 lb And 82,500 lb Truck And Trailer Placed At Position 3

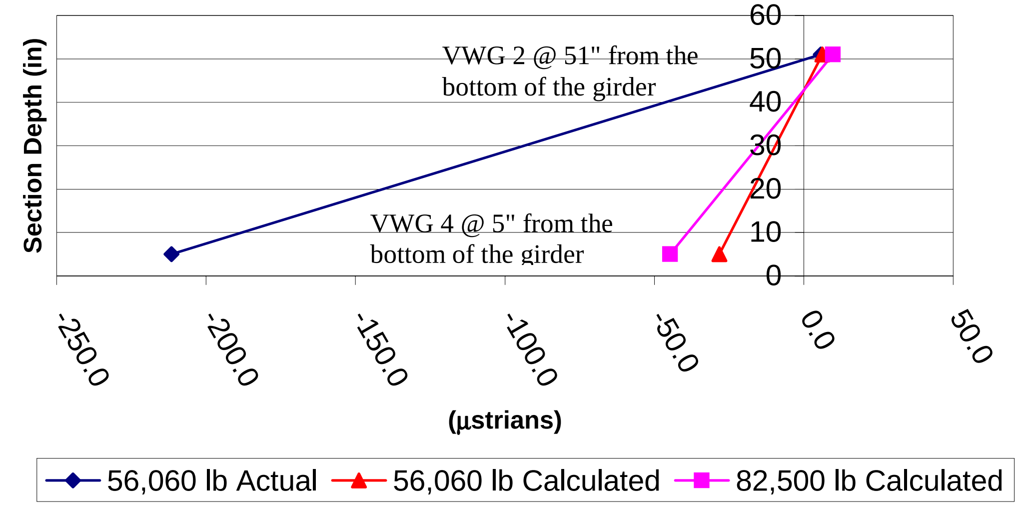

Graph 37. Comparison Of Actual and Calculated Strains At VWG 2 & 4 In Continuity Joint Of Span C & D Due To The 56,060 lb And 82,500 lb Truck And Trailer Placed At Position 7

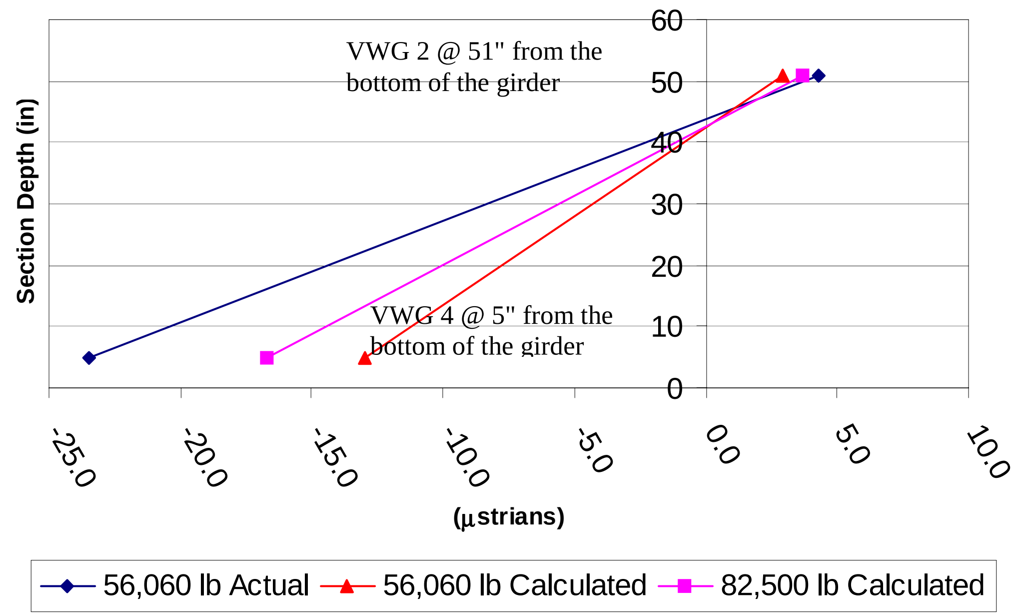

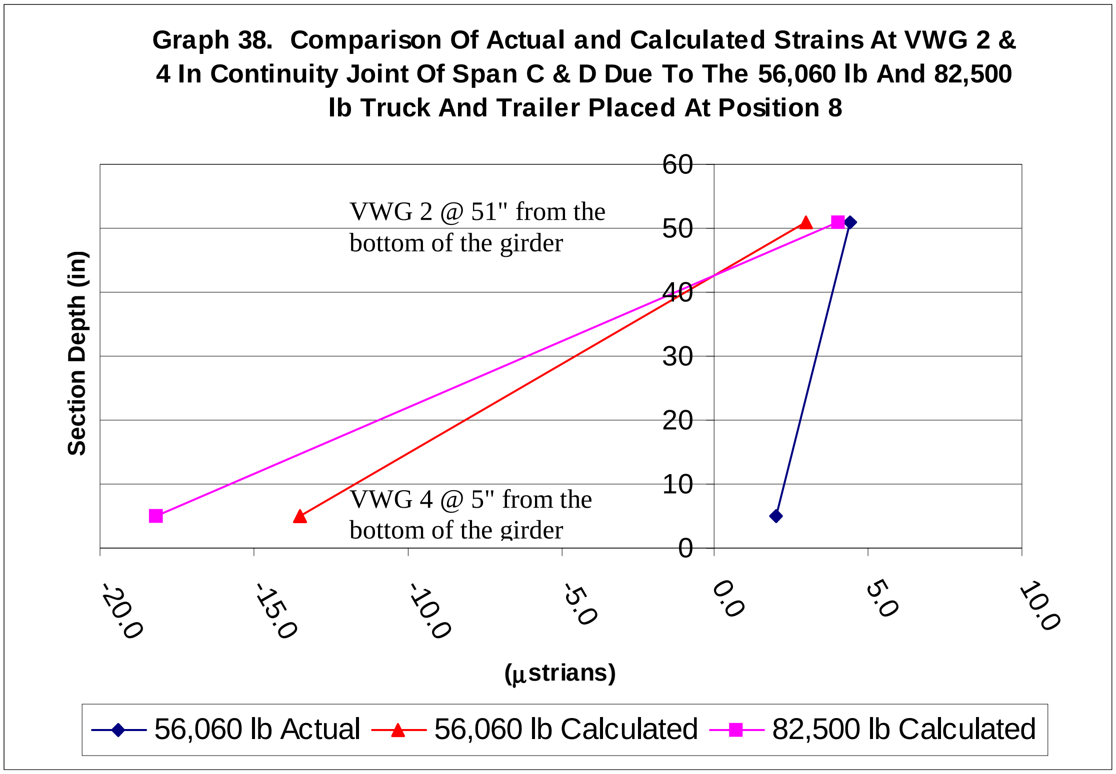
Graph 38. Comparison Of Actual and Calculated Strains At VWG 2 & 4 In Continuity Joint Of Span C & D Due To The 56,060 lb And 82,500 lb Truck And Trailer Placed At Position 8
VWG 2 @ 51" from the bottom of the girder
VWG 4 @ 5" from the bottom of the girder
Section Depth (in)
60
50
40
30
20
10
0
-20.0
-15.0
-10.0
-5.0
0.0
5.0
10.0
(µstrians)
56,060 lb Actual
56,060 lb Calculated
82,500 lb Calculated

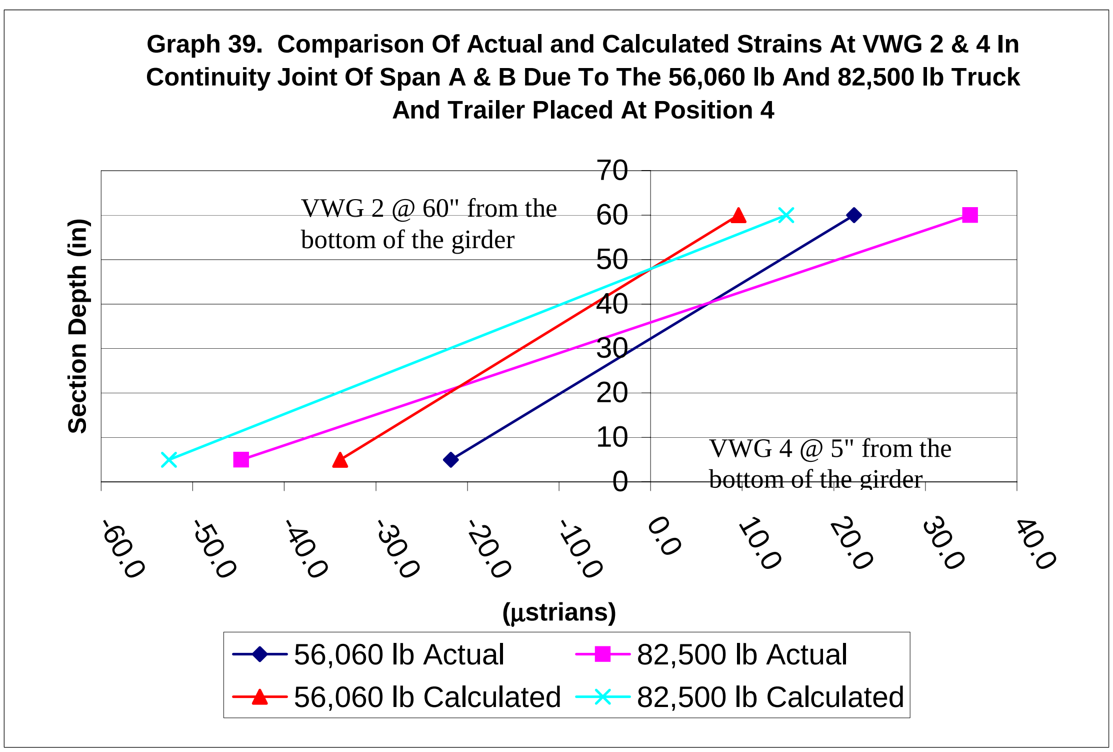
Graph 39. Comparison Of Actual and Calculated Strains At VWG 2 & 4 In Continuity Joint Of Span A & B Due To The 56,060 lb And 82,500 lb Truck And Trailer Placed At Position 4
VWG 2 @ 60" from the bottom of the girder
VWG 4 @ 5" from the bottom of the girder
Section Depth (in)
70
60
50
40
30
20
10
0
-60.0
-50.0
-40.0
-30.0
-20.0
-10.0
0.0
10.0
20.0
30.0
40.0
(µstrians)
56,060 lb Actual
82,500 lb Actual
56,060 lb Calculated
82,500 lb Calculated

Graph 40. Comparison Of Actual and Calculated Strains At VWG 2 & 4 In Continuity Joint Of Span A & B Due To The 56,060 lb And 82,500 lb Truck And Trailer Placed At Position 6

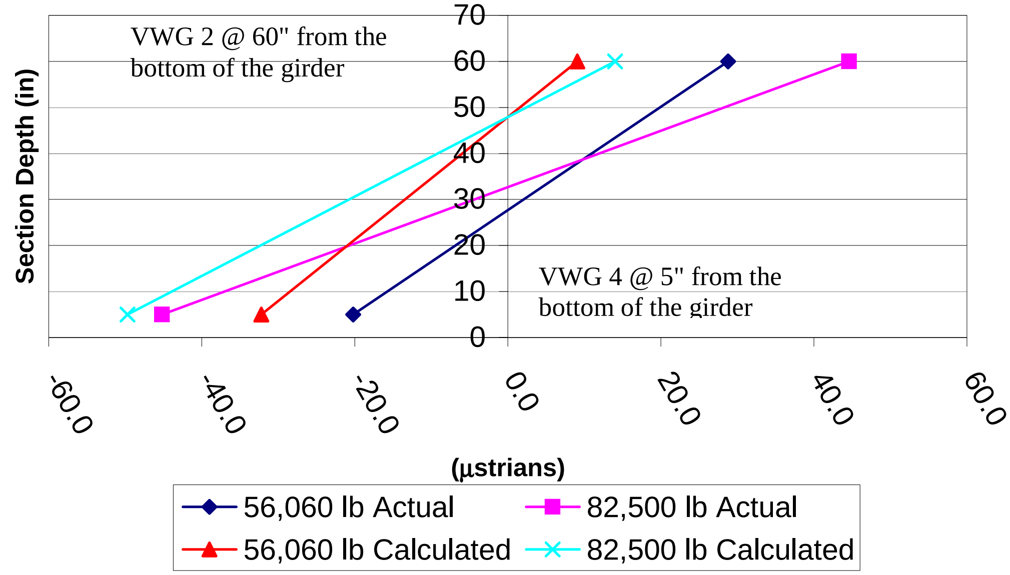

Graph 41. Comparison Of Actual and Calculated Strains At VWG 2 & 4 In Continuity Joint Of Span A & B Due To The 56,060 lb And 82,500 lb Truck And Trailer Placed At Position 9

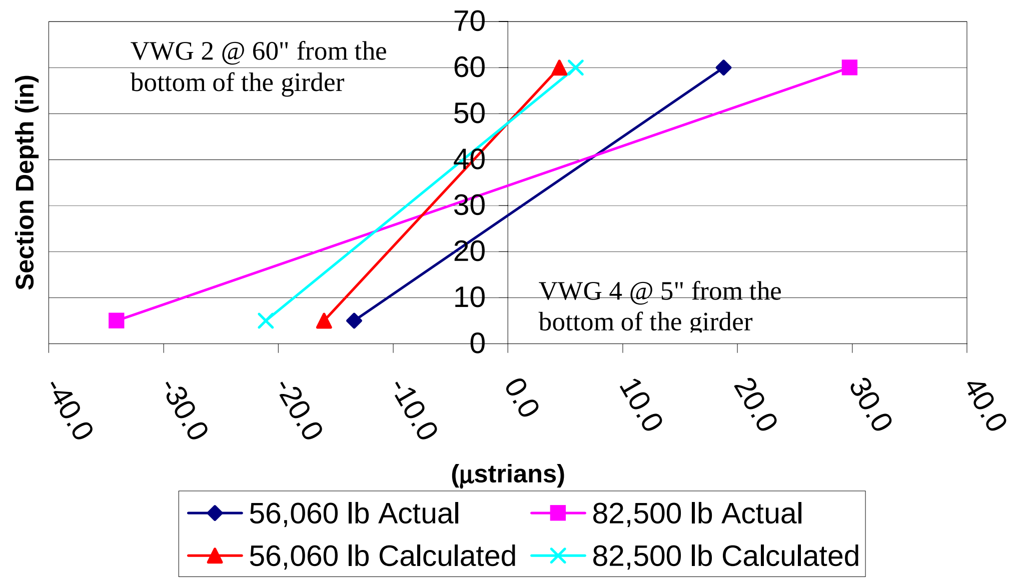

Graph 42. Comparison Of Actual and Calculated Strains At VWG 2 & 4 In Continuity Joint Of Span A & B Due To The 56,060 lb And 82,500 lb Truck And Trailer Placed At Position 10

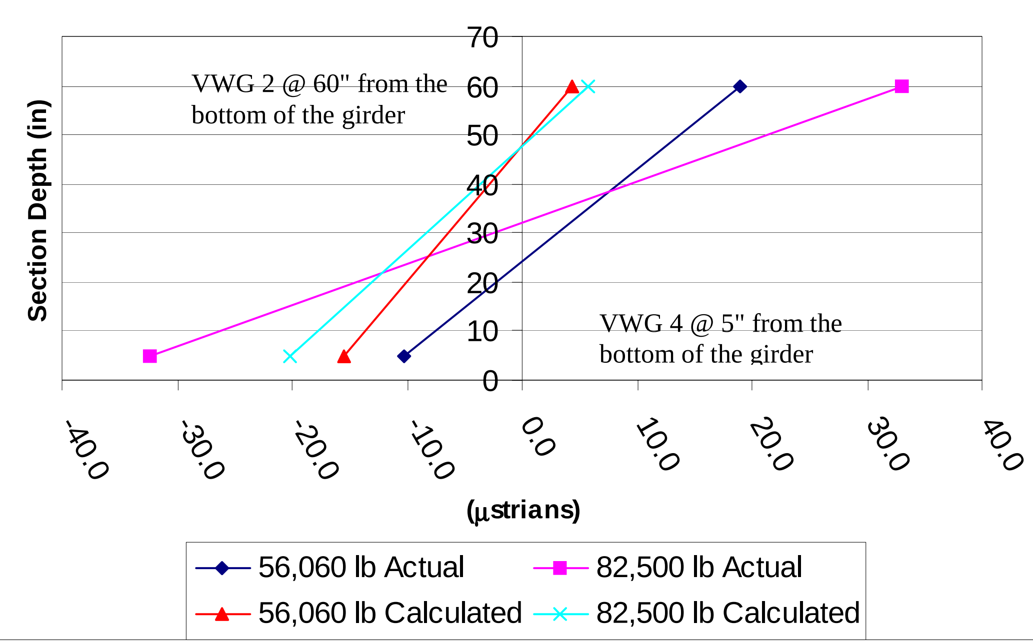

Graph 43. Comparison Of Actual and Calculated Deflection At String Potentiometer Attached At Mid-Span Of Span D Due To The 56,060 lb Truck And Trailer Placed At Positions 1, 3, 7, And 8

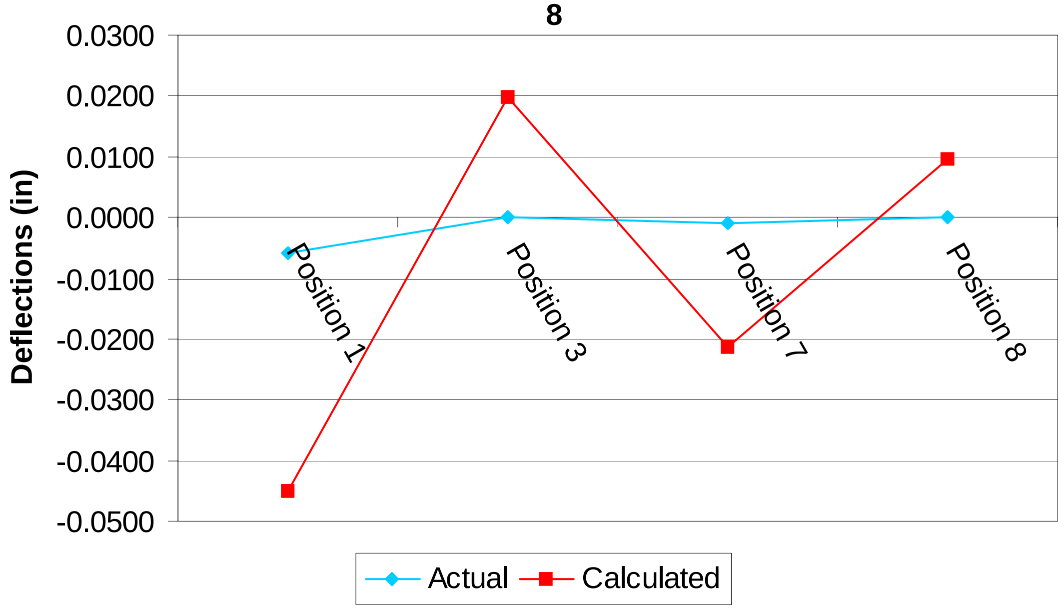

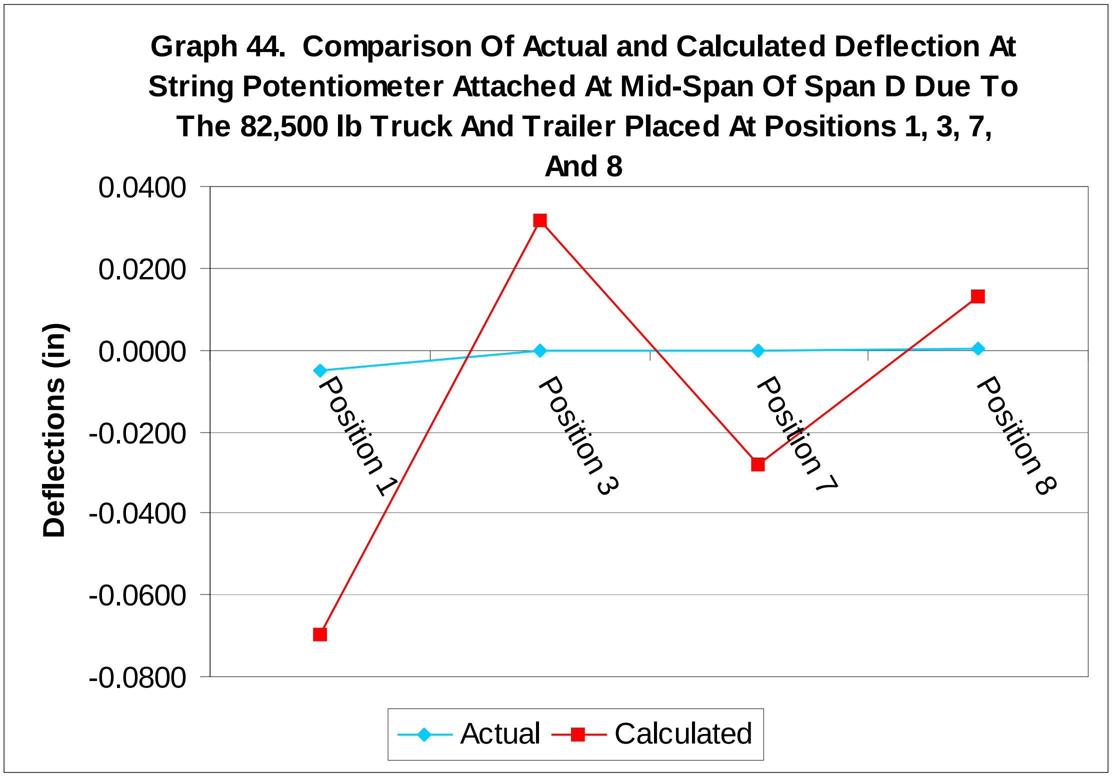
Graph 44. Comparison Of Actual and Calculated Deflection At String Potentiometer Attached At Mid-Span Of Span D Due To The 82,500 lb Truck And Trailer Placed At Positions 1, 3, 7, And 8
0.0400
0.0200
0.0000
-0.0200
-0.0400
-0.0600
-0.0800
Deflections (in)
Position 1
Position 3
Position 7
Position 8
Actual
Calculated

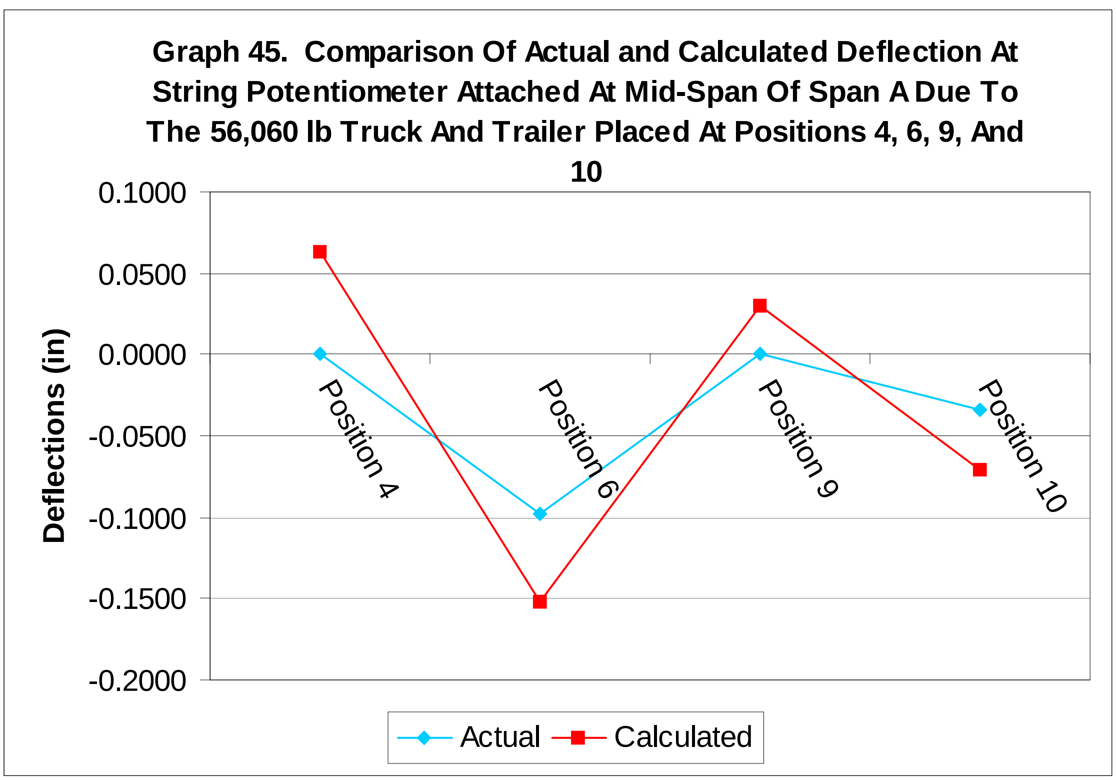
Graph 45. Comparison Of Actual and Calculated Deflection At String Potentiometer Attached At Mid-Span Of Span A Due To The 56,060 lb Truck And Trailer Placed At Positions 4, 6, 9, And 10
0.1000
0.0500
0.0000
-0.0500
-0.1000
-0.1500
-0.2000
Deflections (in)
Position 4
Position 6
Position 9
Position 10
Actual
Calculated

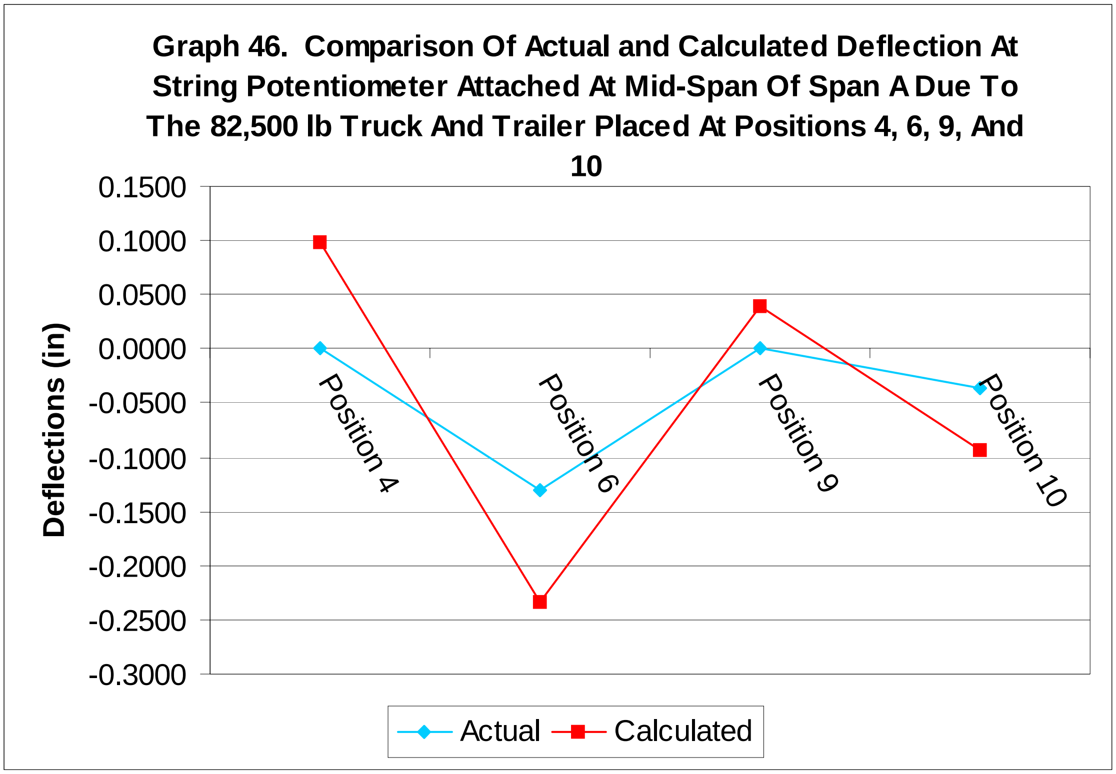

Graph 46. Comparison Of Actual and Calculated Deflection At String Potentiometer Attached At Mid-Span Of Span A Due To The 82,500 lb Truck And Trailer Placed At Positions 4, 6, 9, And 10
Deflections (in)
0.1500
0.1000
0.0500
0.0000
-0.0500
-0.1000
-0.1500
-0.2000
-0.2500
-0.3000
Position 4
Position 6
Position 9
Position 10
Actual
Calculated

Appendix C

Initial Stain Readings

Table 7 displays the initial strain readings of the internal VWGs embedded in the girders of girder-line 4 of the bridge described earlier in section 3.2.

Table 7. Initial Strain Readings for the Internal VWGs embedded in the Girders

VWG's for Span A4				
Date	VWG 8 L (μstrains)	VWG 9 L (μstrains)	VWG 10 L (μstrains)	
10/5/00	3364.0	3373.4	3374.0	
10/6/00	2696.2	2665.4	2689.8	
10/28/01	2292.6	2252.1	2239.8	<-- Before Deck Casting
VWG's for Span B4				
Date	VWG 5 L (μstrains)	VWG 6 L (μstrains)	VWG 7 L (μstrains)	
10/5/00	2880.2	3300.0	3293.0	
10/6/00	2132.0	2588.0	2579.2	
10/28/01	1705.5	2186.8	2172.2	<-- Before Deck Casting
VWG's for Span C4				
Date	VWG 8 L (μstrains)	VWG 9 L (μstrains)	VWG 10 L (μstrains)	
10/3/00	2466.0	2456.4	2581.2	
10/4/00	2277.0	2192.8	2230.0	
10/14/01	1288.2	1592.6	1694.3	<-- Before Deck Casting
VWG's for Span D4				
Date	VWG 5 L (μstrains)	VWG 6 L (μstrains)	VWG 7 L (μstrains)	
10/3/00	2120.2	2444.0	2533.0	
10/4/00	2022.0	2325.8	2383.0	
10/14/01	1483.7	1459.6	1460.3	<-- Before Deck Casting

Table 8 displays the initial strain readings of the internal VWGs embedded in the bridge deck and the girder joints of the bridge described earlier in section 3.3.

Table 8. Initial Strain Readings For The Internal VWGs Embedded In The Bridge Deck And Girder Joints					
VWG's for Span A4 and B4 Placed in Bridge Deck and Girder Joint					
Date	VWG 1 L (μstrains)	VWG 2 L (μstrains)	VWG 3 L (μstrains)	VWG 4 L (μstrains)	
10/28/01	2082.8	2195.8	1786.1	2846.2	<-- Before Deck Casting
VWG's for Span C4 and D4 Placed in Bridge Deck and Girder Joint					
Date	VWG 1 L (μstrains)	VWG 2 L (μstrains)	VWG 3 L (μstrains)	VWG 4 L (μstrains)	
10/14/01	3158.7	3175.7	2908.4	2022.5	<-- Before Deck Casting

Table 9 displays the initial strain readings of the internal VWGs embedded in the 6”x12” cylinder specimens and the 3’x3’ slab specimen described earlier in section 4.3.

Table 9. Strain Readings For The Internal VWGs Embedded In The 6" x 12" Cylinder And 3'x3' Slab Specimen			
VWG's for Cylinders Specimens			
Date	Cylinder for Spans AB L (μstrains)	Cylinder for Spans CD L (μstrains)	
10/26/01	--	2827.8	<-- Initial Readings Recorded for Cylinder CD
10/31/01	2569.1	2584.7	<-- Initial Readings Recorded for Cylinder AB
11/2/01	2751.1	2534.5	
11/8/01	2776.5	--	
7/23/01	2666.0	2470.0	
VWG's for 3'x3' Slab Specimen			
Date	VWG 37 L (μstrains)	VWG 38 L (μstrains)	
10/31/01	4304.9	2369.0	<-- Initial Readings Recorded for VWG 37 and VWG 38 of the 3'x3' Slab Specimen
11/2/01	3869.5	2372.9	
11/8/01	3886.9	2386.8	

Modulus Of Elasticity

Graphs 47 –50 represent the stress-strain relationship of the concrete specimens described in section 4.2, where the modulus of elasticity was extracted from the slope of the stress-strain relationship. The modulus of elasticity is reported along with the compressive strength in each specimen's graphs.

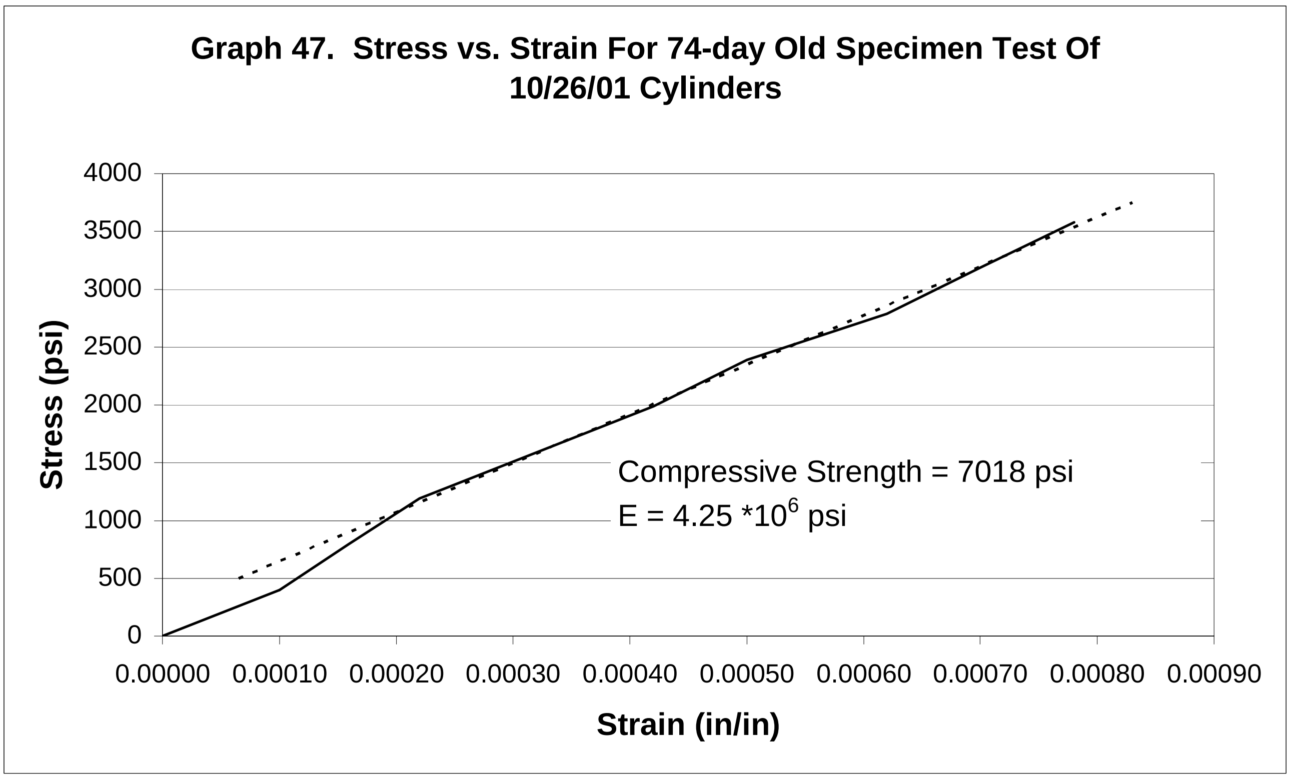

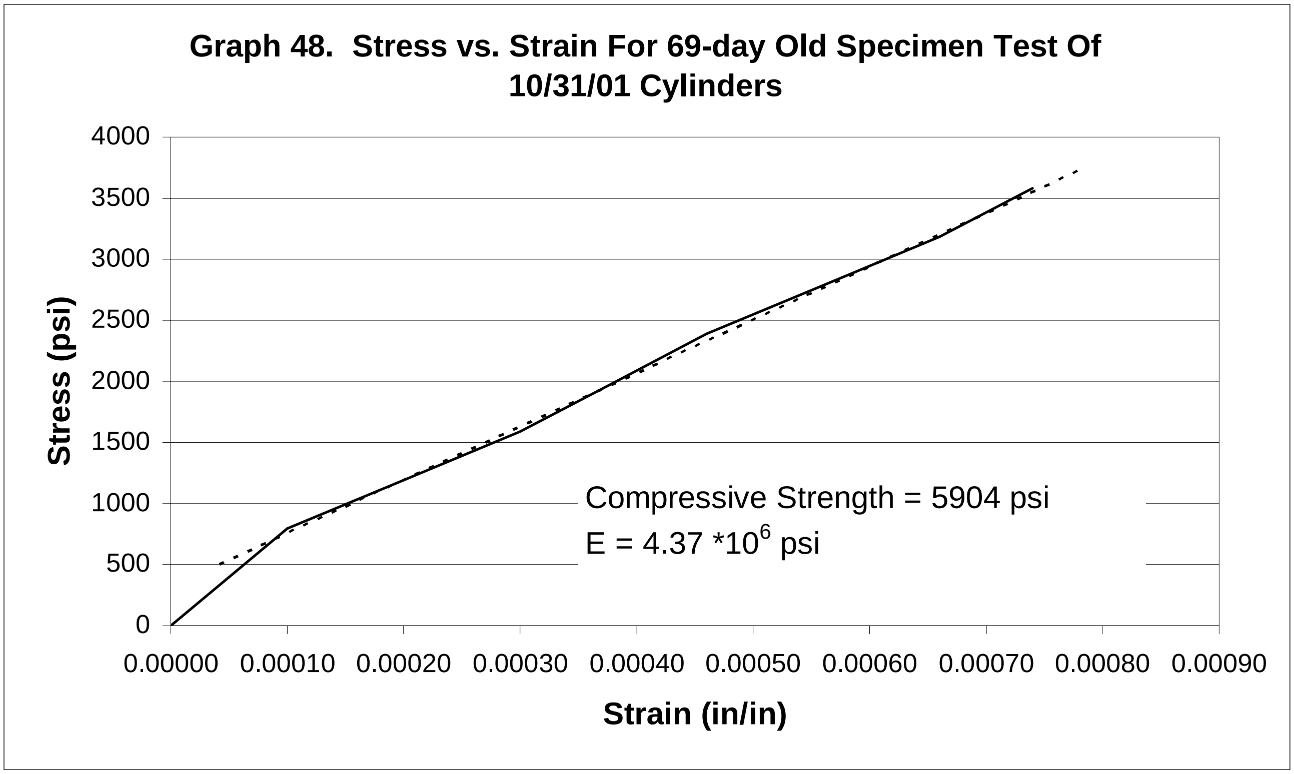
Graph 48. Stress vs. Strain For 69-day Old Specimen Test Of 10/31/01 Cylinders
4000
3500
3000
2500
2000
1500
1000
500
0
Stress (psi)
Compressive Strength = 5904 psi
E = 4.37 *10^6 psi
0.00000
0.00010
0.00020
0.00030
0.00040
0.00050
0.00060
0.00070
0.00080
0.00090
Strain (in/in)

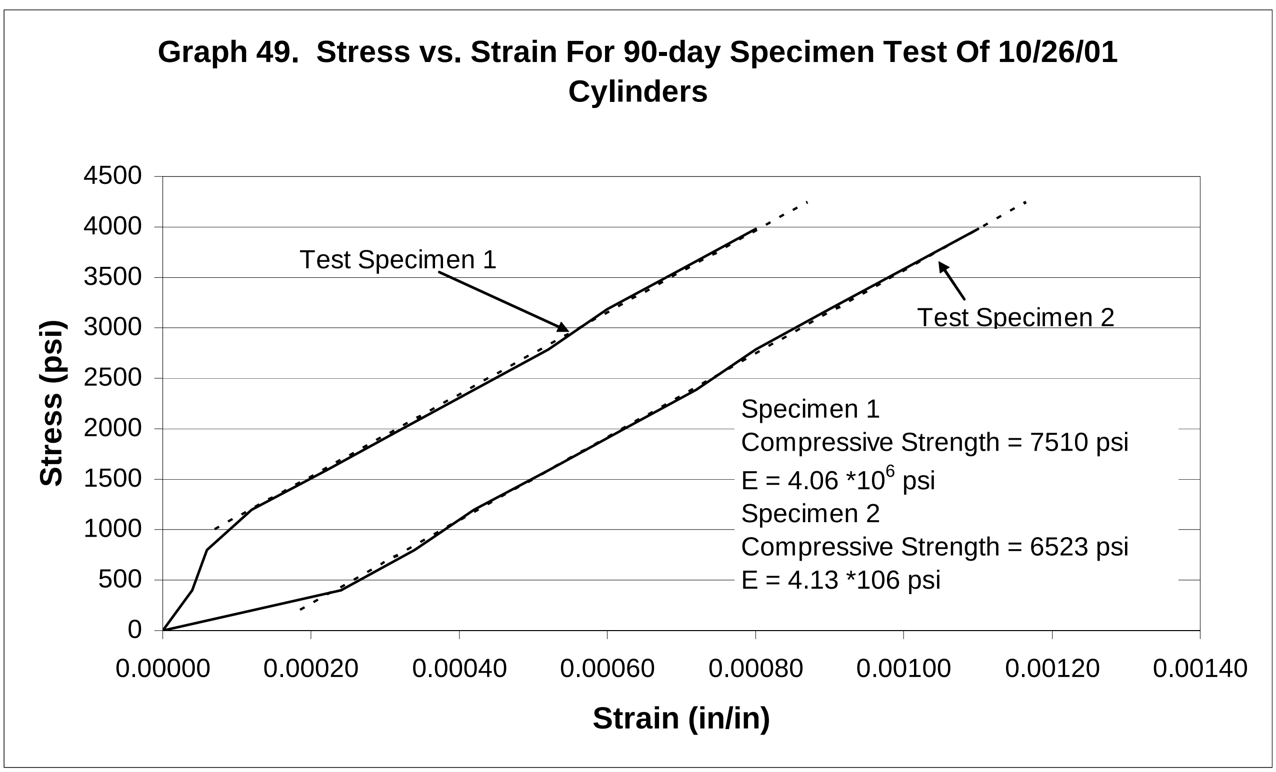
Graph 49. Stress vs. Strain For 90-day Specimen Test Of 10/26/01 Cylinders
4500
4000
3500
3000
2500
2000
1500
1000
500
0
Stress (psi)
Test Specimen 1
Test Specimen 2
Specimen 1
Compressive Strength = 7510 psi
E = 4.06 *10^6 psi
Specimen 2
Compressive Strength = 6523 psi
E = 4.13 *106 psi
0.00000
0.00020
0.00040
0.00060
0.00080
0.00100
0.00120
0.00140
Strain (in/in)

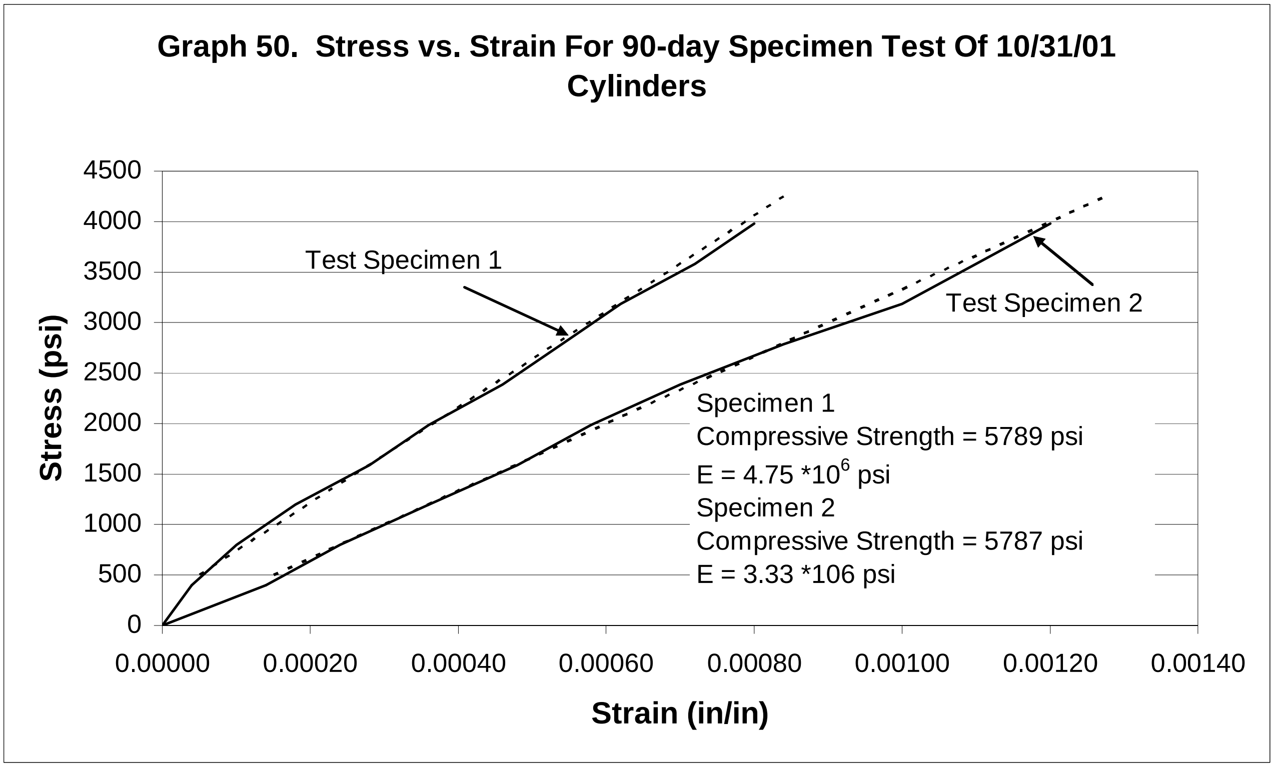
Graph 50. Stress vs. Strain For 90-day Specimen Test Of 10/31/01 Cylinders
Stress (psi)
4500
4000
3500
3000
2500
2000
1500
1000
500
0
0.00000
0.00020
0.00040
0.00060
0.00080
0.00100
0.00120
0.00140
Strain (in/in)
Test Specimen 1
Test Specimen 2
Specimen 1
Compressive Strength = 5789 psi
E = 4.75 *10^6 psi
Specimen 2
Compressive Strength = 5787 psi
E = 3.33 *106 psi

Appendix D: In-Service Behavior

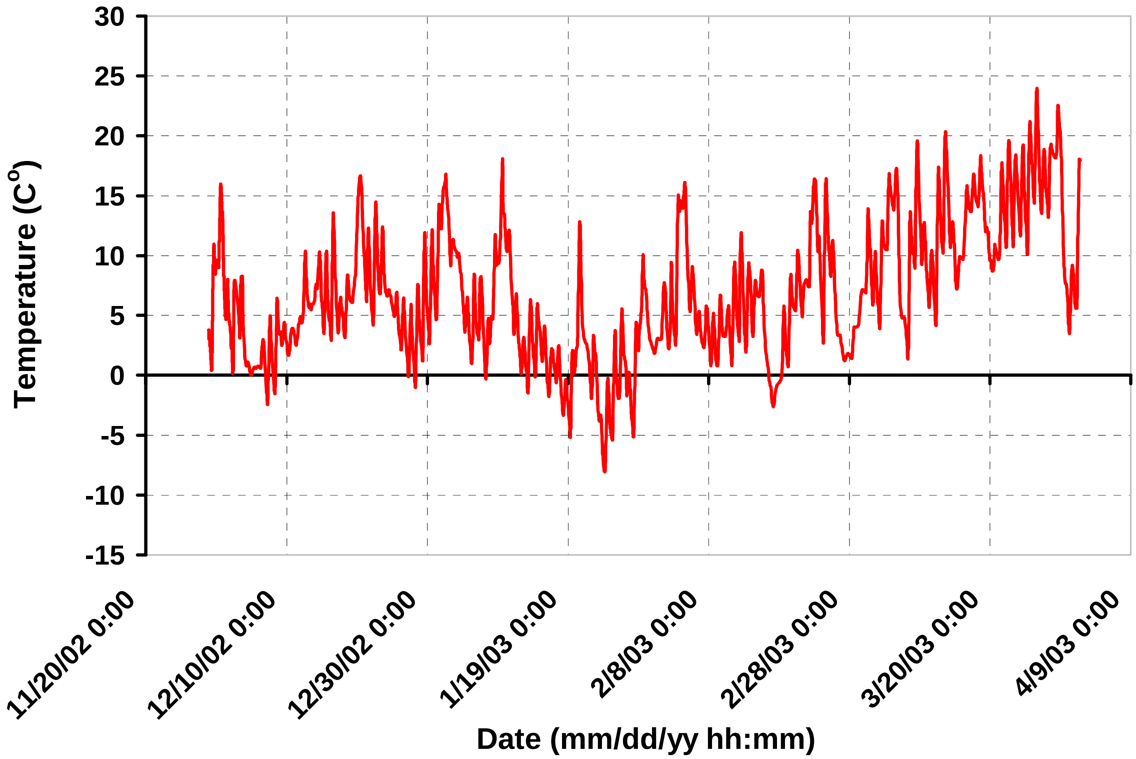

Graph 51. Temperature Readings for Thermocouple-1 in Span-D

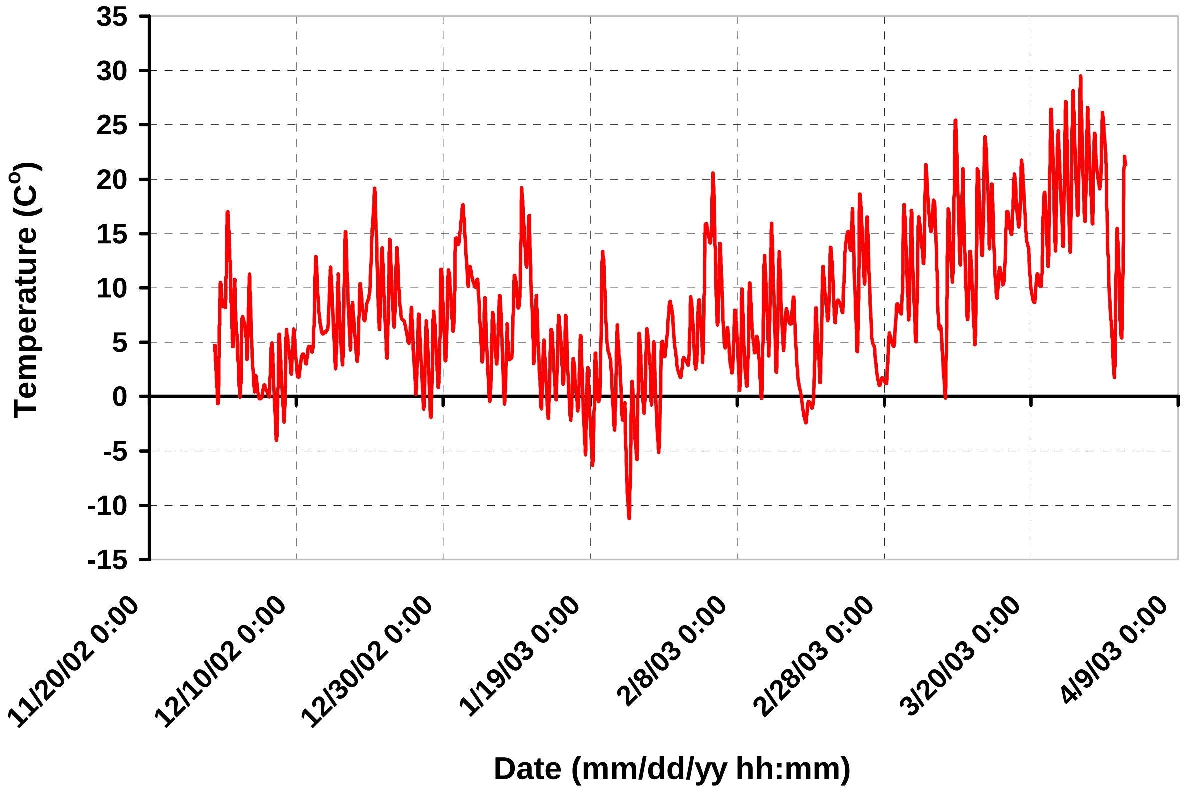

Graph 52. Temperature Readings for Thermocouple-2 in Span-D

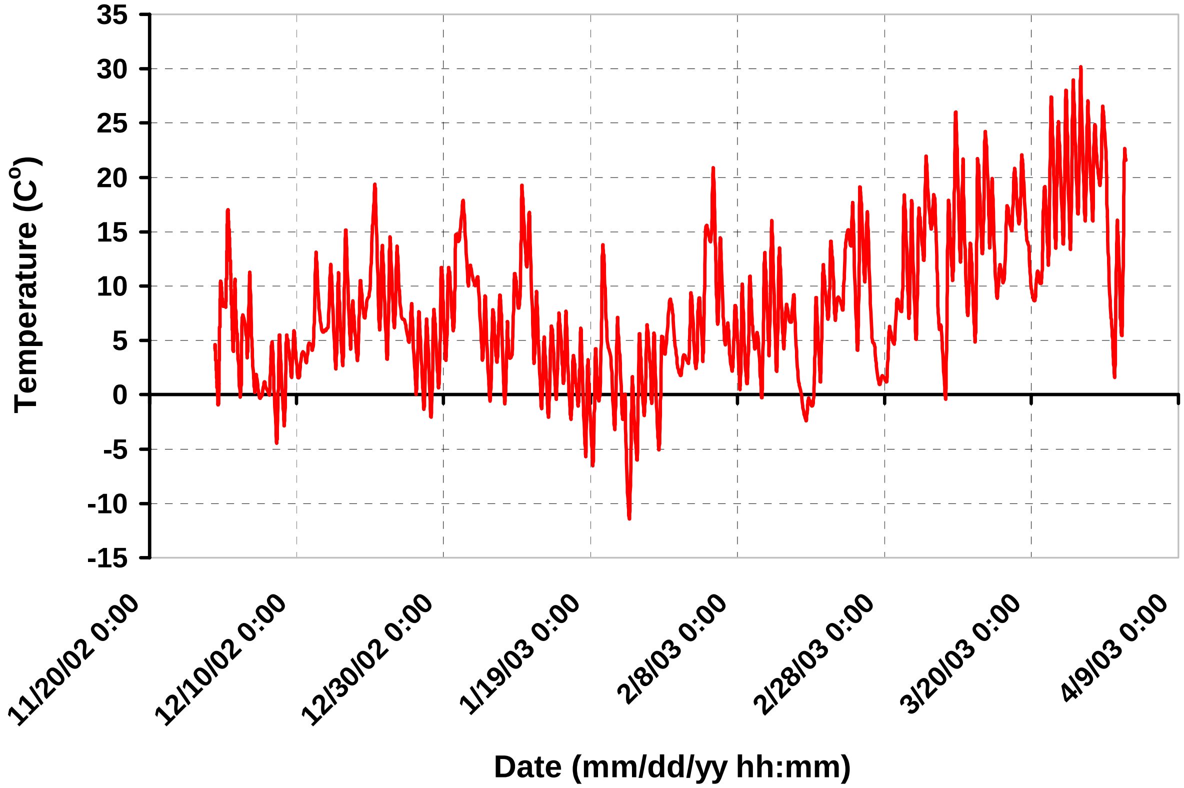

Graph 53. Temperature Readings for Thermocouple-3 in Span-D

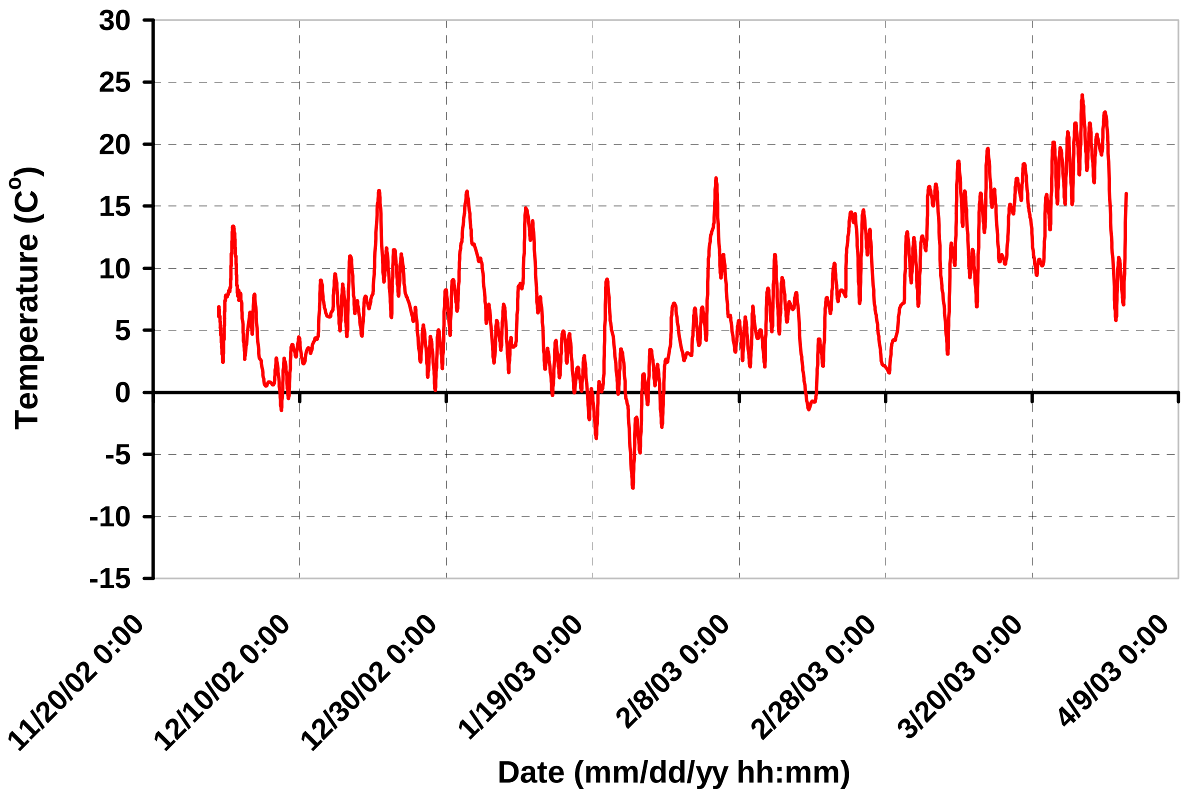

Graph 54. Temperature Readings for Thermocouple-4 in Span-D

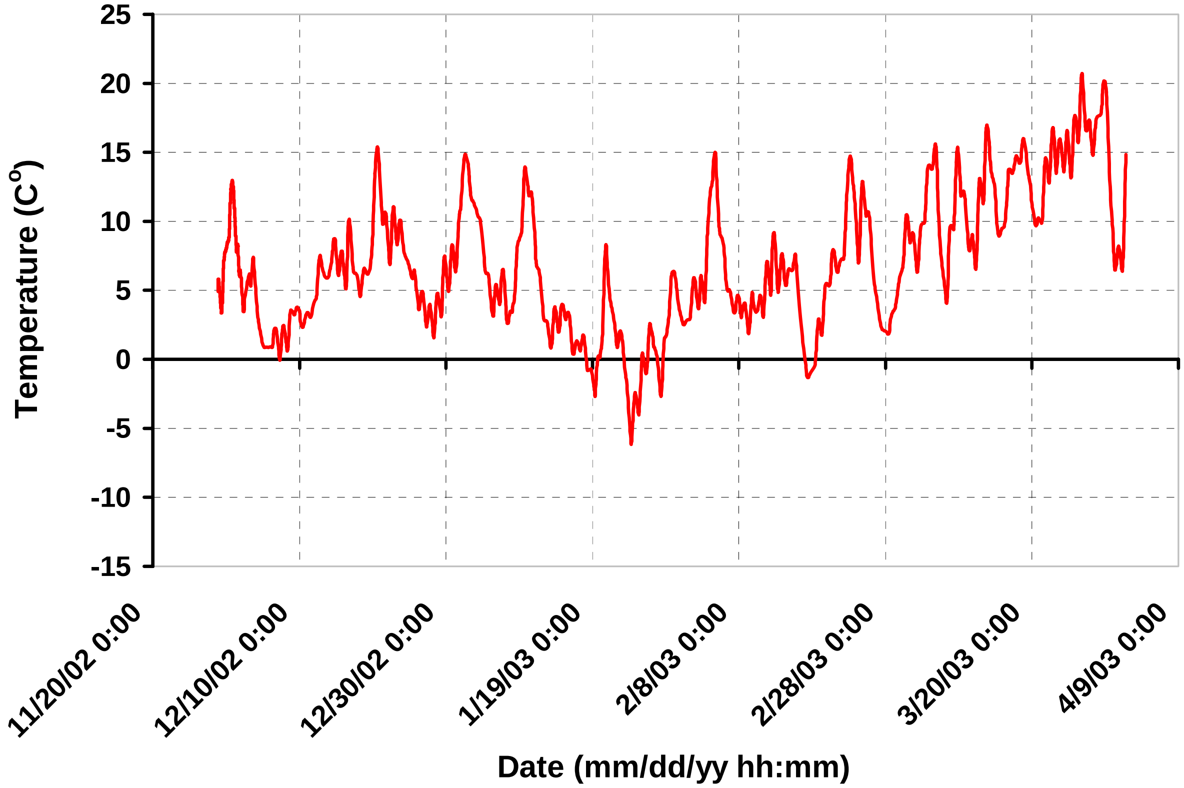

Graph 55. Temperature Readings for Thermocouple-5 in Span-D

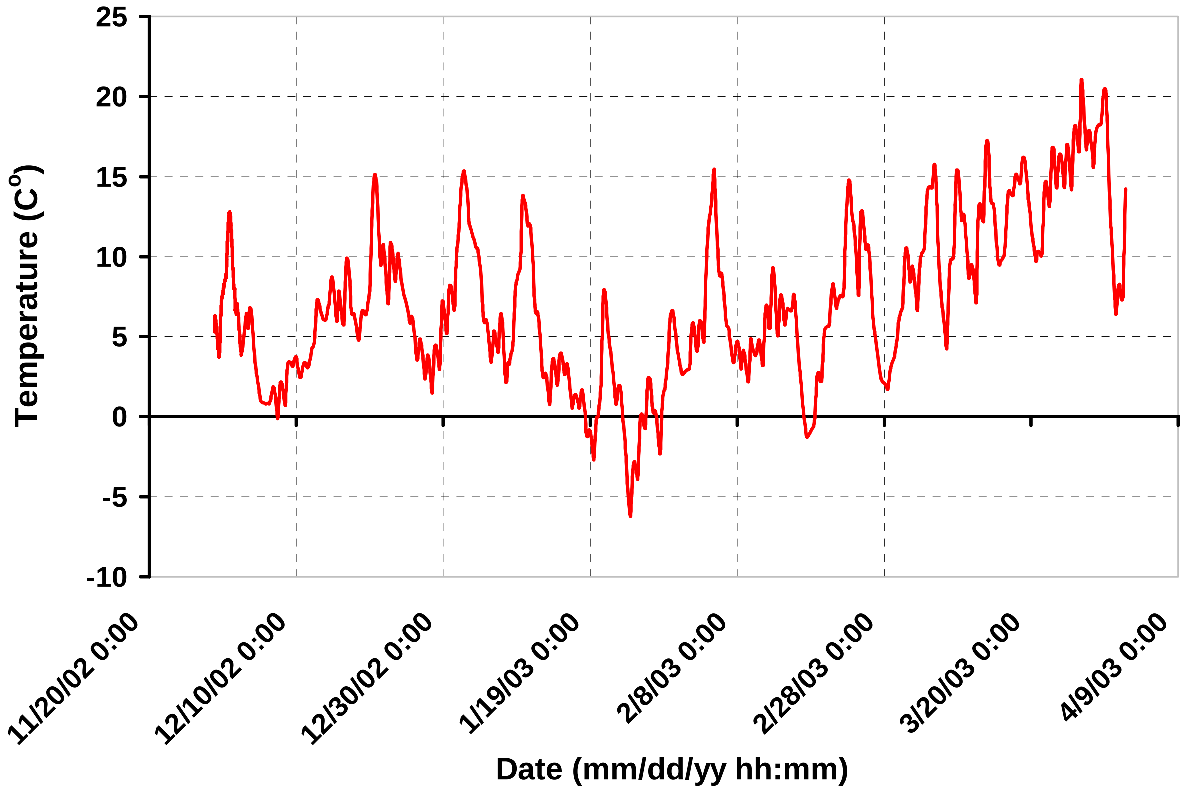

Graph 56. Temperature Readings for Thermocouple-6 in Span-C

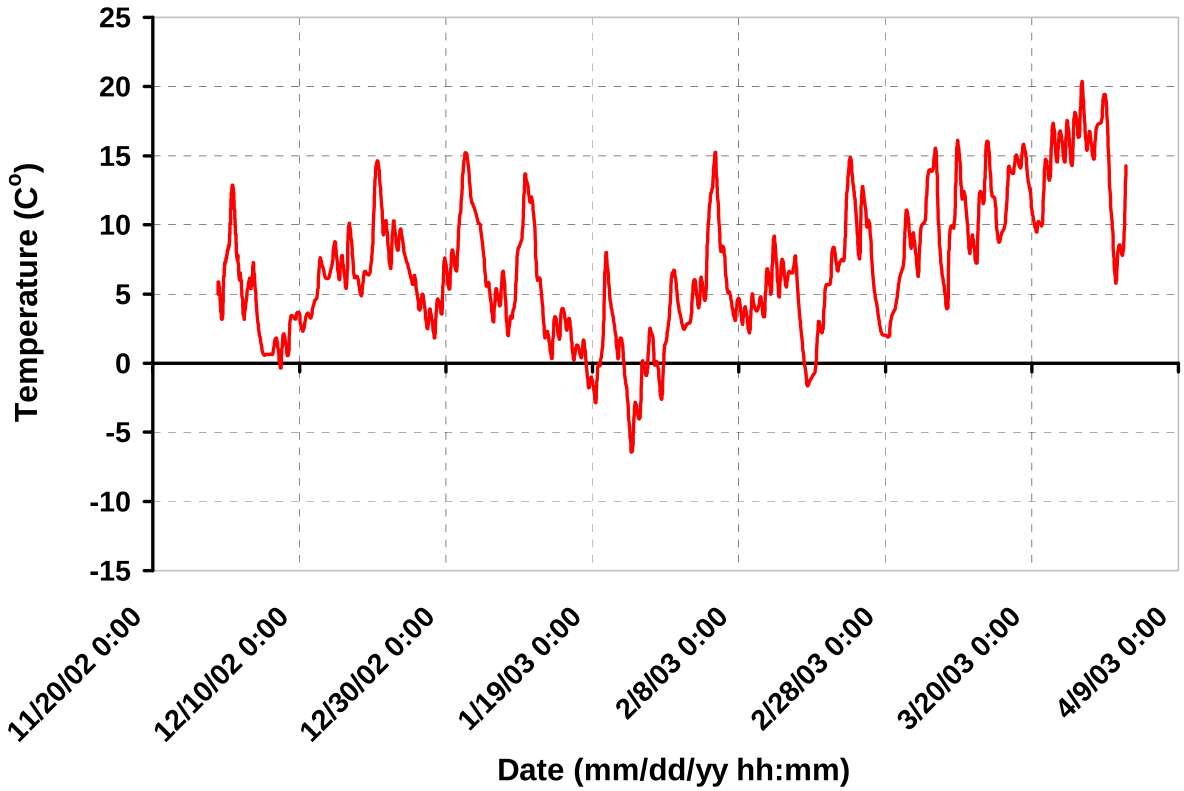

Graph 57. Temperature Readings for Thermocouple-8 in Span-C

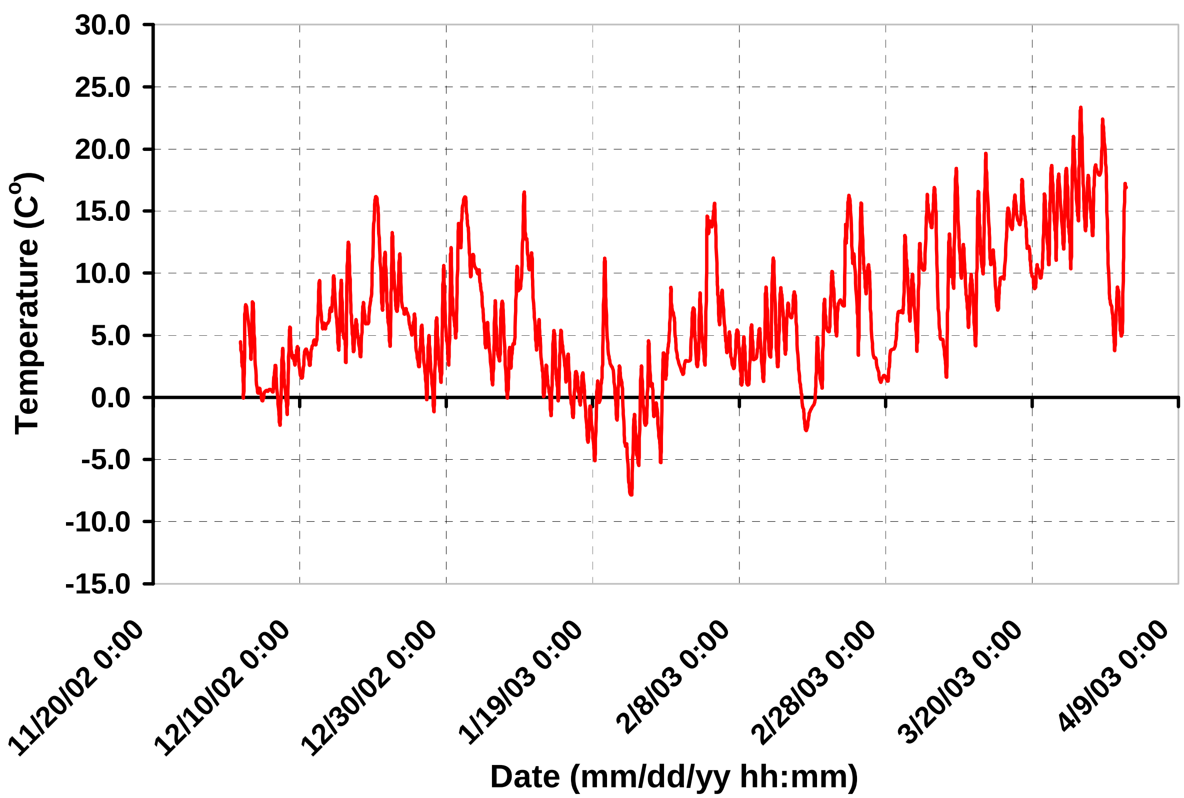

Graph 58. Temperature Readings for Thermocouple-1 in Span-A

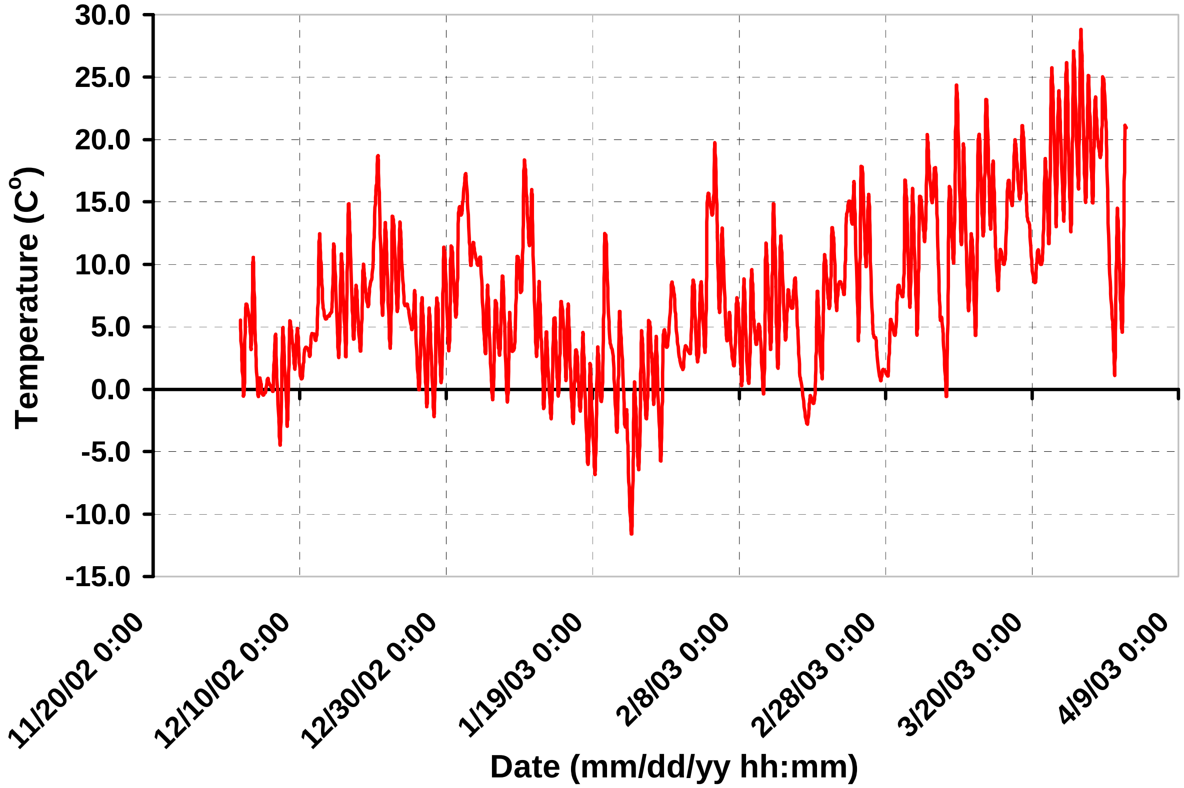

Graph 59. Temperature Readings for Thermocouple-2 in Span-A

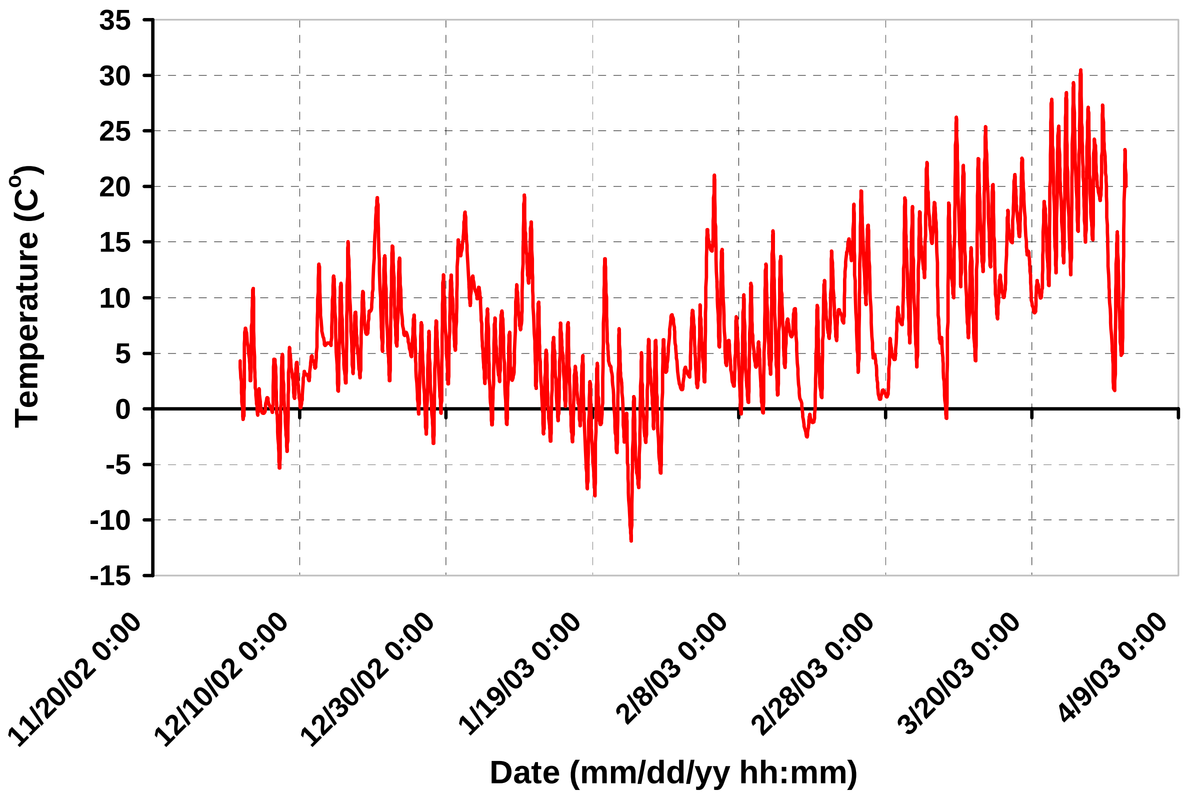

Graph 60. Temperature Readings for Thermocouple-3 in Span-B

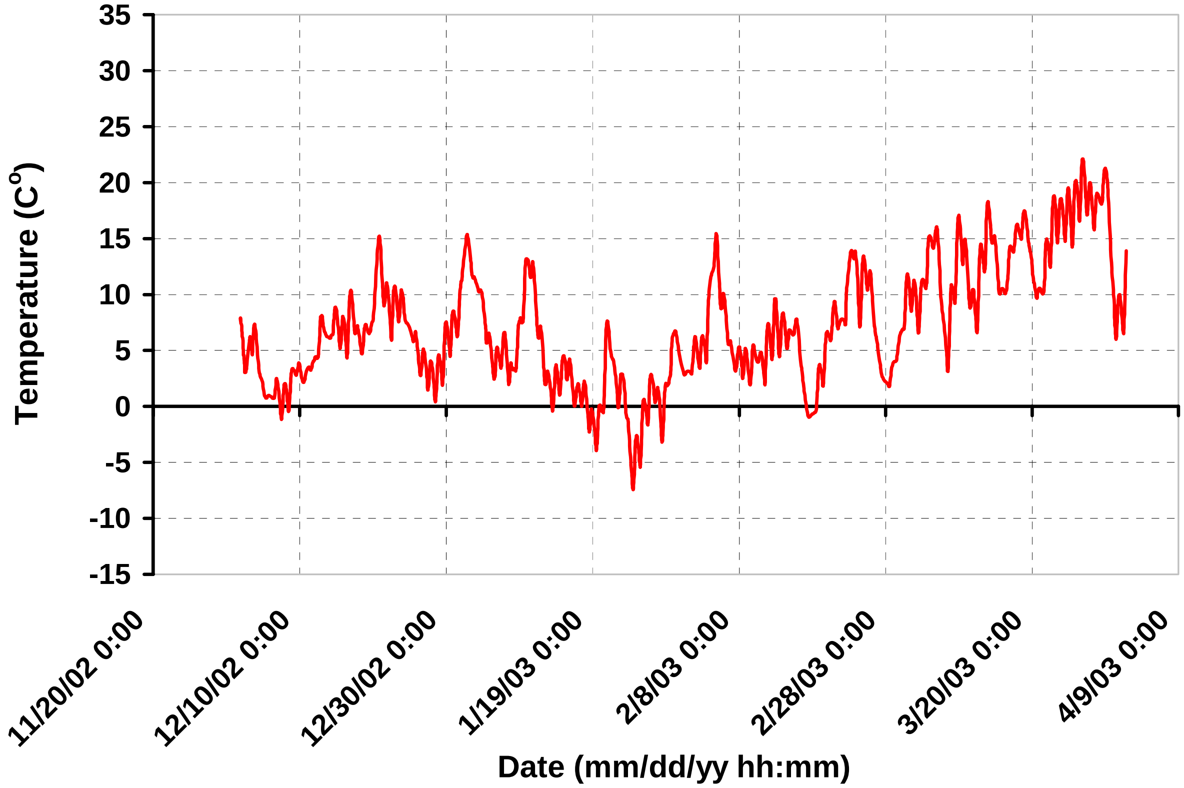

Graph 61. Temperature Readings for Thermocouple-4 in Span-B

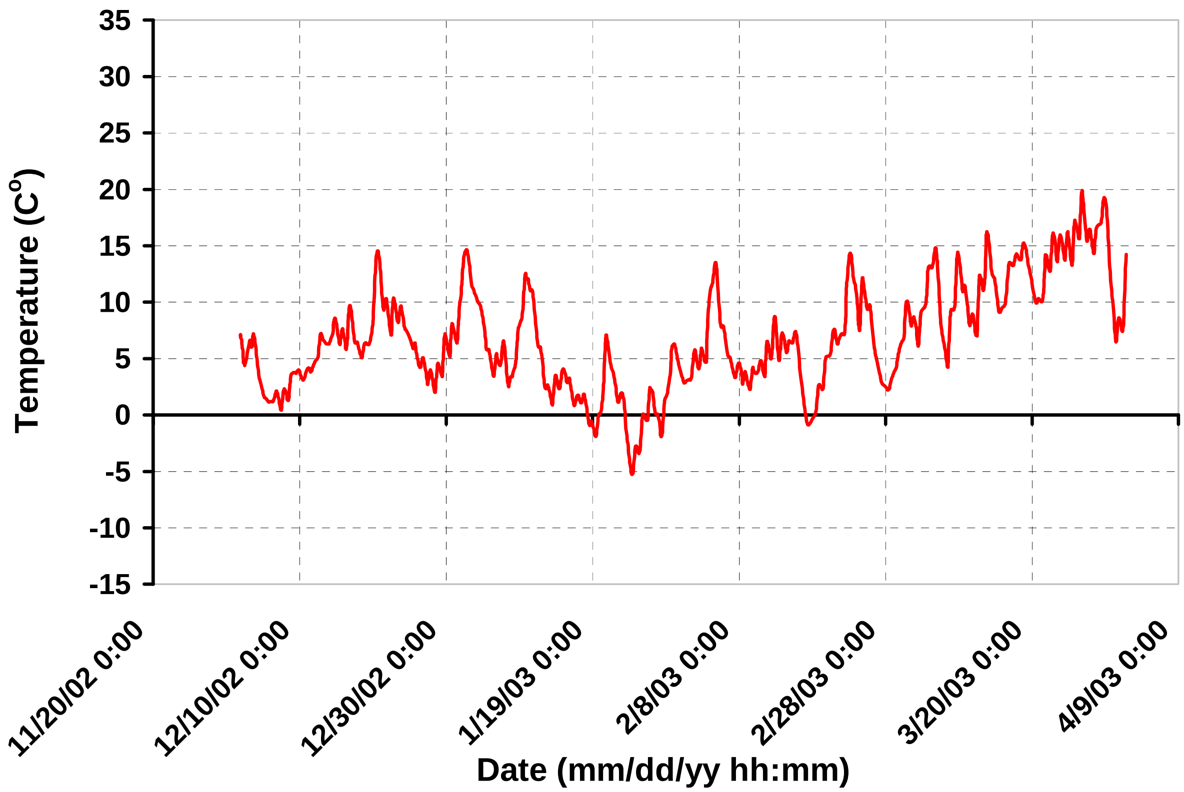

Graph 62. Temperature Readings for Thermocouple-5 in Span-B

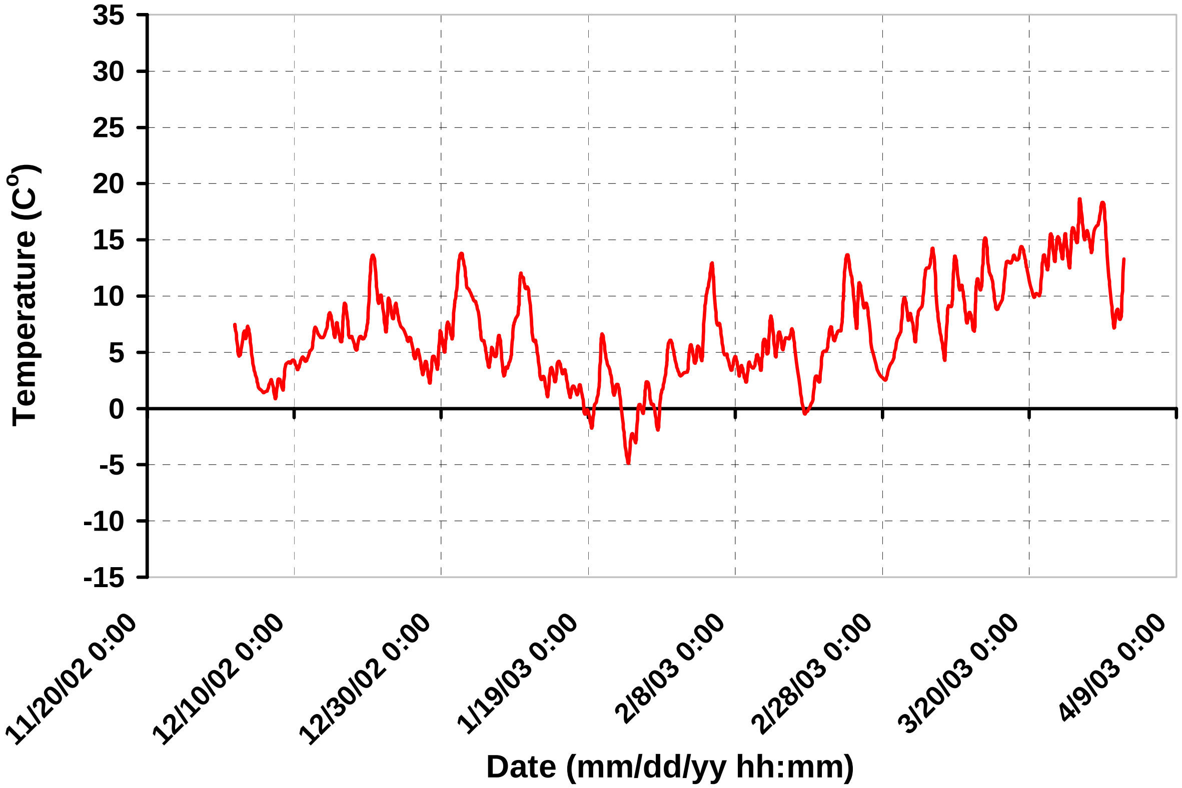

Graph 63. Temperature Readings for Thermocouple-6 in Span-A

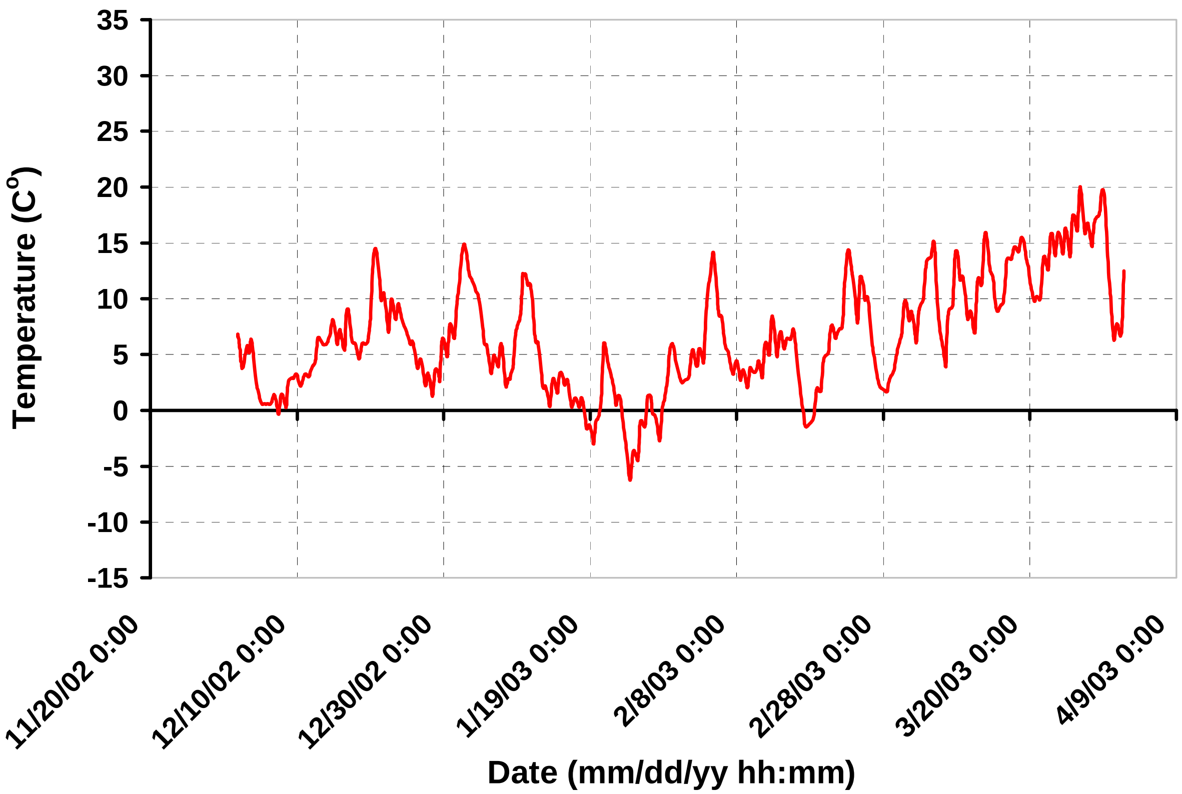

Graph 64. Temperature Readings for Thermocouple-8 in Span-A

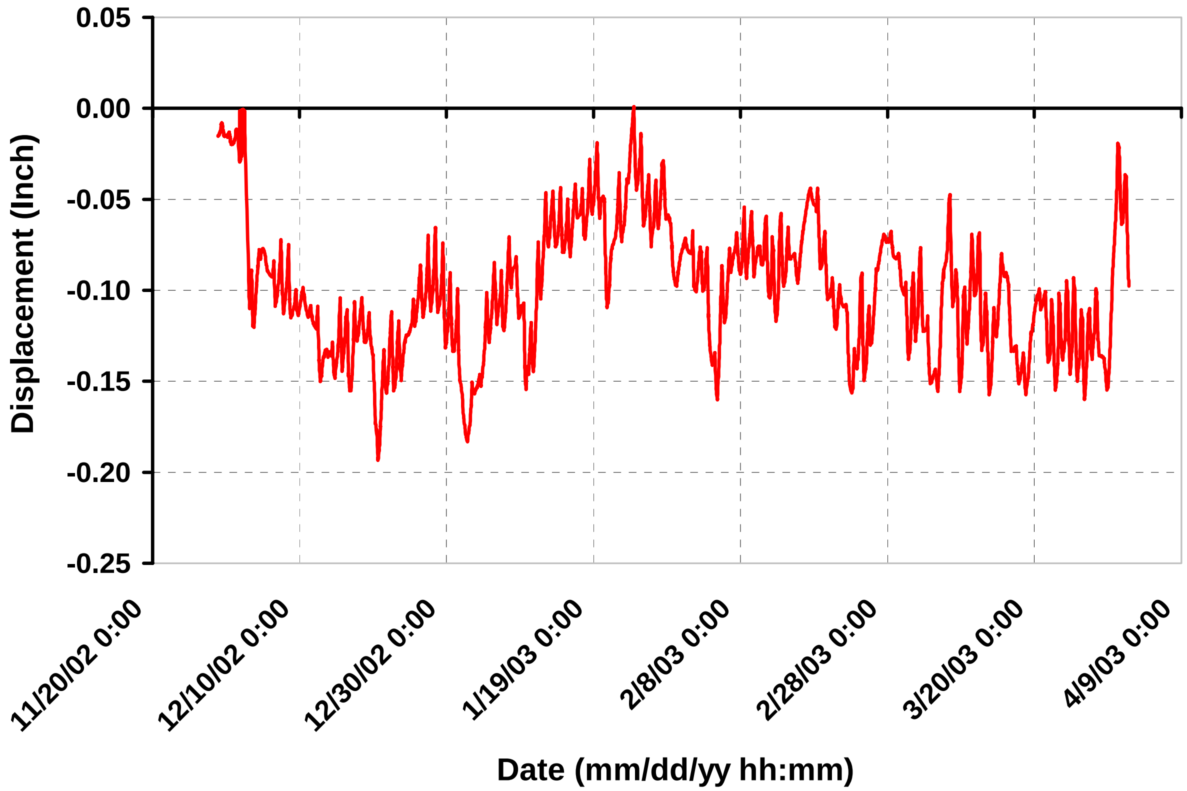

Graph 65. Girder-D End Displacement at the North Abutment

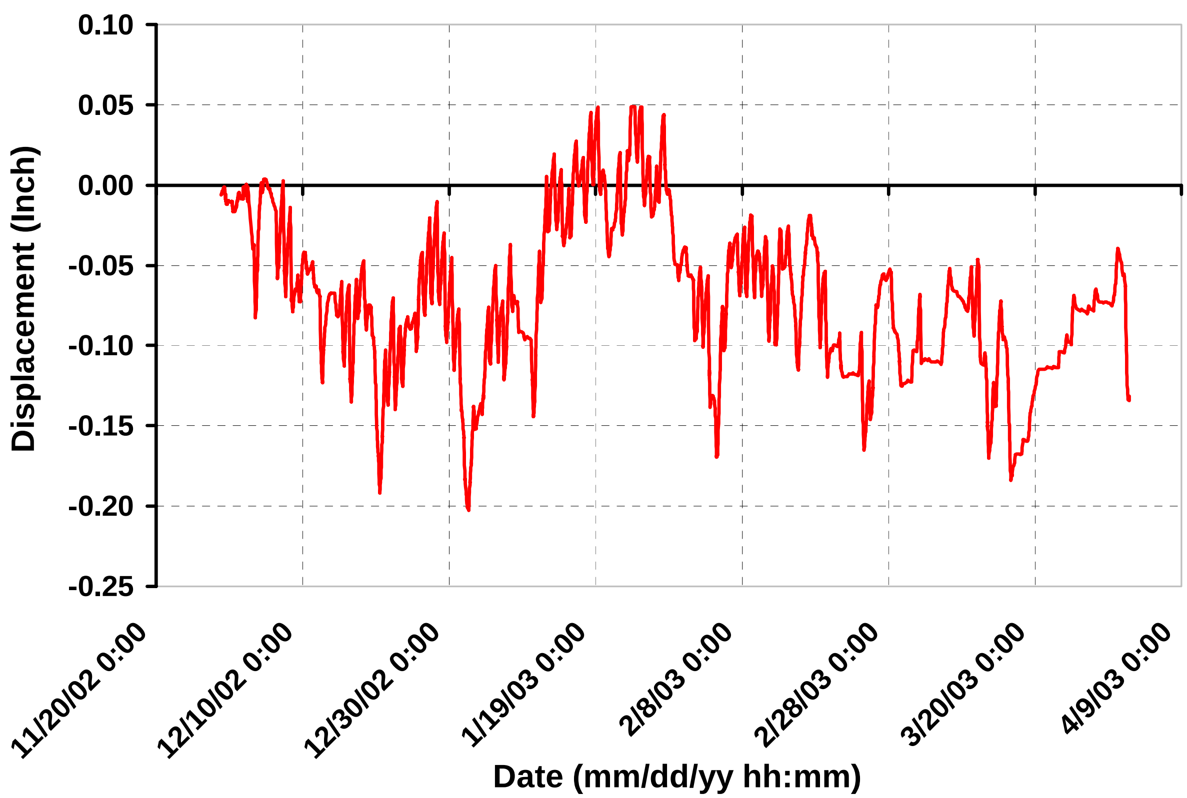

Graph 66. Girder-C End Displacement at the Expansion Joint

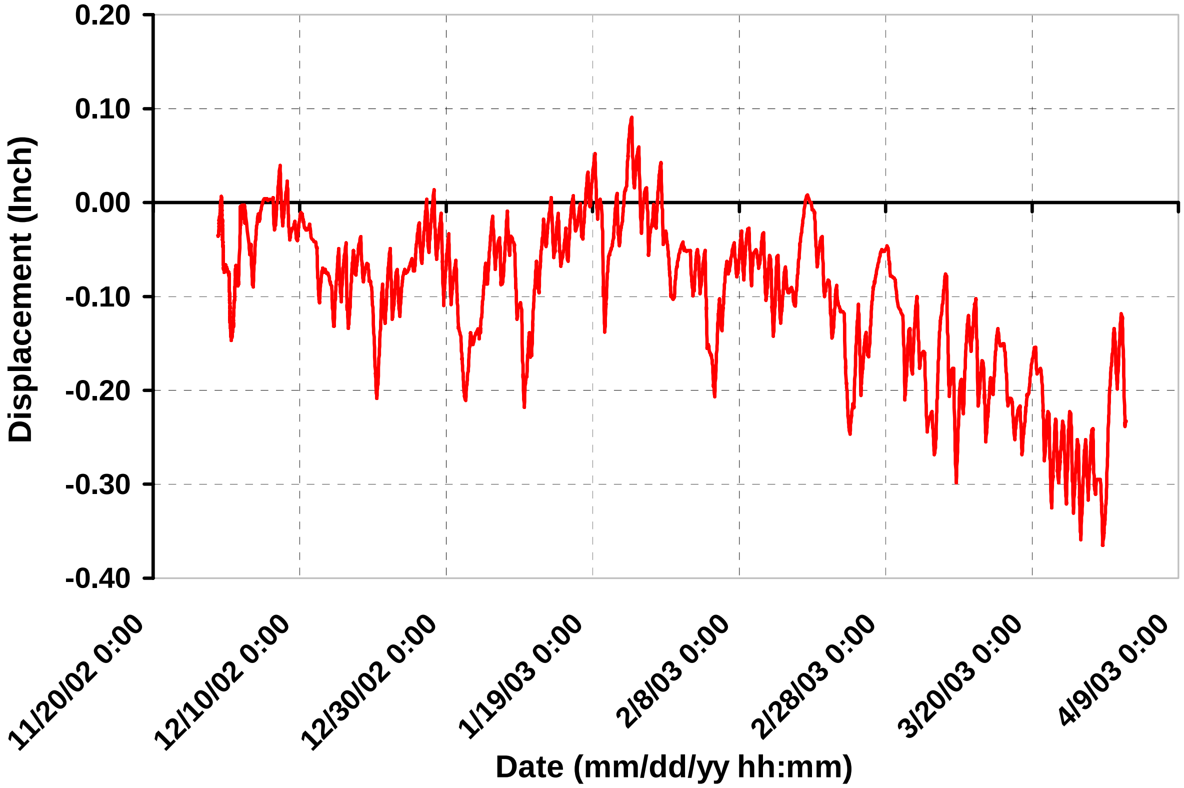

Graph 67. Girder-B End Displacements at the Expansion Joint

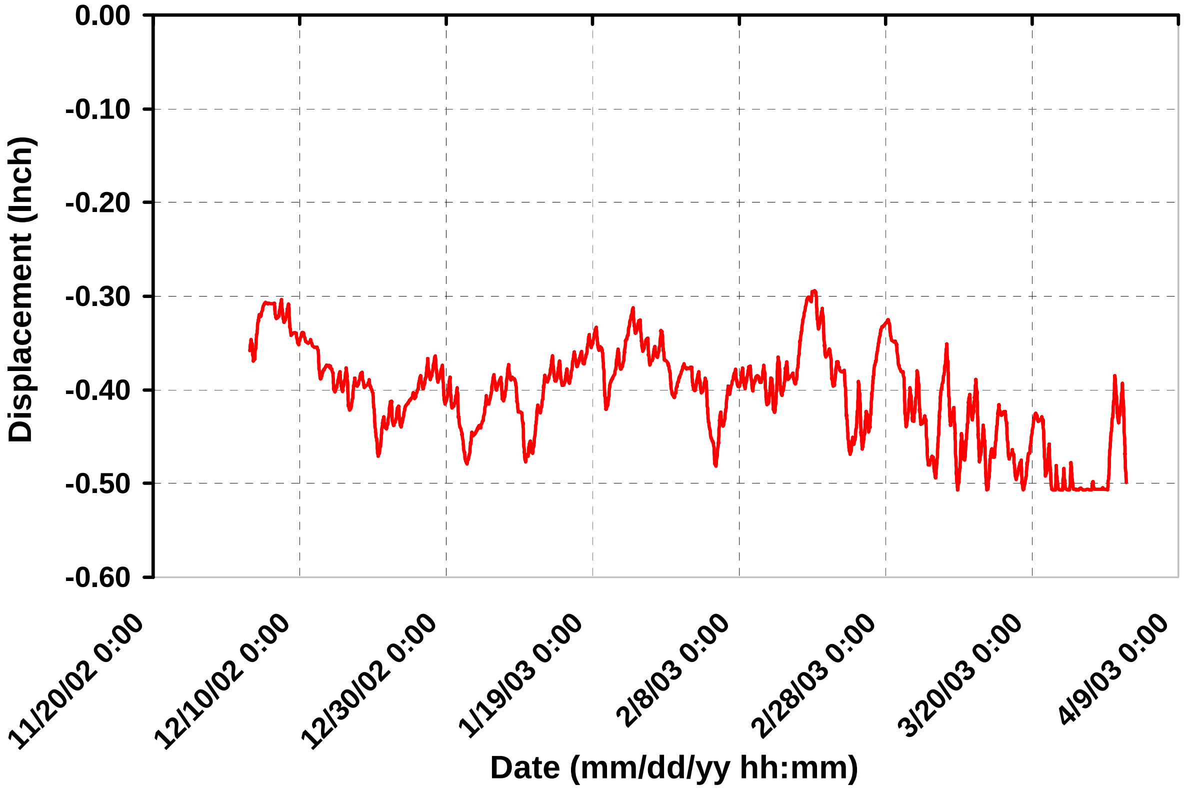

Graph 68. Girder-A End Displacements at the South Abutment